Fall 12-14-2011

Characterization of Structure and Function of SECA Domains

Ying-Ju Huang
GSU

CHARACTERIZATION OF STRUCTURE AND FUNCTION OF SECA DOMAINS

by

YING-JU HUANG

Under the Direction of Phang C. Tai

ABSTRACT

SecA is a central component of the general secretion system that is essential for growth and virulence of bacteria. A series of fluorescein analogs were tested against ATPase activities of *Escherichia coli* SecA. Rose Bengal (RB) and Erythrosin B are potent inhibitors abolishing the activities of three forms of SecA ATPase with IC_{50} in μM range. Both inhibit SecA intrinsic ATPase with two mechanisms depending on ATP concentrations, indicating they influence the two non-identical nucleotide binding sites differently. RB shows different inhibitory effects against three forms of SecA ATPase activities, suggesting that the inhibition is related to the conformation of SecA. RB with IC_{50} at sub-μM level is the most potent inhibitor of SecA ATPases and SecA-dependent protein translocation to date. The fluorescein analogs inhibit intrinsic ATPase of *Bacillus subtilis* SecA similarly, and also exhibit antibacterial effects in *E. coli* and *B. subtilis.* Our findings in-

dicate the value of fluorescein analogs as probes for mechanistic studies of SecA and the potential development of new SecA-targeted antimicrobial agents.

A series of SecA derivatives with truncated C-terminus within the first long α-helix of the helix-bundle extending the ATPase catalytic domain of N68 was analyzed. These SecA variants interact with lipids, and those containing the C-terminal portion of the long α-helix starting at residues #639 form the ring-like structure in liposomes, indicating the critical domains for forming the protein-conducting channel. The presence and length of the C-domain influence the response to RB of NBDII mutants and C-terminal truncates of SecA. Thus this region may interact with the inhibitors and is involved in the structure and regulation of SecA ATPase activity.

B. subtilis SecA was analyzed for interspecies comparison. Despite sharing high homology, this SecA homolog cannot complement *E. coli* mutants with SecA defect. Phospholipids do not stimulate ATPase activities of *B. subtilis* SecA, but induce its conformational changes, leading to the lipid-specific domains and ring-like structures similar to *E. coli* SecA. These pore-ring structures may represent part of the protein-conducting channels. Therefore, the potential structural roles of SecA in the protein translocation machinery may be universal in both Gram-negative and Gram-positive bacteria.

INDEX WORDS: SecA, ATPase, Inhibitor, Fluorescein dyes, Protein conduction channel, Gram-positive bacteria

CHARACTERIZATION OF STRUCTURE AND FUNCTION OF SECA DOMAINS

by

YING-JU HUANG

A Dissertation Submitted in Partial Fulfillment of the Requirements for the Degree of

Doctor of Philosophy

in the College of Arts and Sciences

Georgia State University

2011

CHARACTERIZATION OF STRUCTURE AND FUNCTION OF SECA DOMAINS

by

YING-JU HUANG

Committee Chair: Phang C. Tai

Committee: Parjit Kaur

Chung-Dar Lu

Zehava Eichenbaum

Electronic Version Approved:

Office of Graduate Studies

College of Arts and Sciences

Georgia State University

December 2011

DEDICATION

For Neko, with the memories we share.

ACKNOWLEDGEMENTS

I would like to thank my advisor, Dr. Phang C. Tai, for his mentorship during my graduate studies at Georgia State University. I am grateful to my committee members, Dr. Parjit Kaur, Dr. Chung-Dar Lu, and Dr. Zehava Eichenbaum, for their suggestions regarding my project. I also thank the former and current Tai Lab members for their friendship and help, Ping Jiang for DNA sequencing, and Hui Zhao for AFM in the Biology Core Facility. Special thanks go out to my mentees, Yang Lu and Qian Liu, for their assistance with the experiments.

Finally, and most importantly, I want to thank my family, for their unconditional love and support. Thank you to my parents, sisters, and in-laws for your encouragement. For my husband and my son, without you, I could not go this far.

TABLE OF CONTENTS

LIST OF TABLES

LIST OF FIGURES

1 INTRODUCTION

Protein secretion in bacteria. In all organisms, the translocation of proteins into various cellular and extra-cellular compartments is important to maintain normal physiological functions. In bacteria, more than one-third of the proteins are located in or outside the cellular cytoplasmic membrane. These secreted proteins are involved in stress sensing/response, signal transduction, nutrients uptake, communication with the environment or other cells, microbe-host attachment, adhesion on specific surfaces, virulence of pathogen, and other essential processes (Chitlaru, Gat et al. 2006; Zhou, Theunissen et al. 2010). 13.2% of *Escherichia coli* genome is allotted to various transporters, indicating the importance of protein transport systems to the life cycles (Serres, Goswami et al. 2004). Sixteen systems involved in protein export and secretion have been identified in bacteria (Economou, Christie et al. 2006). These systems can be divided into two categories – Sec-dependent and Sec-independent.

Sec-pathway mediates the transport of proteins inserted into or across the cytoplasmic membrane. In Gram-positive bacteria, these proteins will be retained in the cell wall or released into medium after fold into the native conformation (van Wely, Swaving et al. 2001). SecA-dependent systems operate a two-step process in Gram-negative bacteria. In step one, proteins pass the inner membrane and reach the pariplasmic space. Then in step two, other secretion systems are utilized to direct proteins into or through the outer membrane. These systems include the type II secretion system (T2SS), some of the type IV secretion system (T4SS) related to toxin secretion (Rambow-Larsen and Weiss 2004),

autosecretion (T5SS), chaperon-usher for pili, and two-partner secretion (TPS) (Economou, Christie et al. 2006).

Sec-independent pathways include the type I secretion system (T1SS, ATP-binding cassette (ABC) transporters), type III secretion system (T3SS), some T4SS related to conjugation system, newly discovered type VI secretion system (T6SS) in some Gram-negative bacteria, and Esc (originally called ESAT-6 (Pallen 2002)) in Gram-positive bacteria (Economou, Christie et al. 2006). The twin arginine translocation (Tat) system mediates the delivery of fully folded proteins with specialized N-terminal signal peptides carrying the consensus sequence of twin-arginine motif across the cytoplasmic membrane (de Leeuw, Granjon et al. 2002). In Gram-negative bacteria, these proteins are further transported across the outer membrane through T2SS (Voulhoux, Ball et al. 2001).

Components and the current model of Sec-pathway. Sec-pathway is responsible for the transport of the majority of exported proteins. Proteins destined to this route carry N-terminal signal sequences, composed of a positive-charged N-terminus, a hydrophobic core of 8-12 residues, and a hydrophilic C-terminus with the consensus sequence for signal peptidases (Tjalsma, Antelmann et al. 2004; Papanikou, Karamanou et al. 2007). Preproteins are recognized by signal-recognition particle (SRP) or Sec system specific chaperone (SecB) and directed to the translocase by docking FtsY or SecA, respectively (Papanikou, Karamanou et al. 2007).

There are a series of proteins involved in the Sec translocation apparatus. The current model for Sec-pathway (Wickner and Leonard 1996) illustrates that the core channel for protein translocation is formed by heterotrimeric SecYEG complex (Akimaru, Matsuyama et al. 1991; Nishiyama, Mizushima et al. 1992; Hanada, Nishiyama et al.

1994). SecYEG is the homolog of Sec61 channel complex in the endoplasmic reticulum (van Wely, Swaving et al. 2001; van der Sluis and Driessen 2006). The proposed translocation channel is composed of oligomers of SecY complex, and the pore is formed by one copy of SecY (Osborne and Rapoport 2007). In this structure, the pore is blocked by a short helix, termed plug, which can be moved upon the interaction with signal peptides to open the channel (Van den Berg, Clemons et al. 2004; Osborne, Rapoport et al. 2005). The peripheral protein SecA hydrolyzes ATP to provide the energy required for the movement of preproteins across the plasma membrane (Eichler and Wickner 1997). Integral membrane protein complex, SecDFYajC, can stabilize the SecYEG complex and increase the efficiency of protein secretion but is not the essential component of the system (Economou, Pogliano et al. 1995; Driessen and Nouwen 2008). Membrane protein YidC is involved in the insertion of membrane proteins (Samuelson, Chen et al. 2000; Chen, Xie et al. 2002). SecB is a molecular chaperone that rapidly binds to precursor proteins to maintain their unfolded status and then targets them to SecA for translocation (Fekkes and Driessen 1999). There is no SecB homolog found in Gram-positive bacteria (van der Sluis and Driessen 2006), and CsaA is a chaperone proposed for preprotein-SecA targeting in Gram-positive bacteria (Muller, Ozegowski et al. 2000).

The quaternary structure of SecA. SecA can form oligomers, and its quaternary structure may be related to allosteric control and physiological function. SecA is found in solution as dimers and undergoes equilibrium between monomer and dimer depending on temperature, concentration, and ionic strength (Akita, Shinkai et al. 1991; Driessen 1993; Woodbury, Hardy et al. 2002; Ding, Hunt et al. 2003). Both monomer and dimer structures have been illustrated by X-ray crystallography of various SecA proteins (Sardis and

Economou 2010). However, in which status SecA functions in membranes during the protein translocation is still controversial. Some reports conclude that monomer is the active form of SecA because acidic phospholipids, a synthetic signal peptide (Or, Navon et al. 2002), and SecYEG (Alami, Dalal et al. 2007) trigger the dissociation of SecA dimer. Contradictory results show signal peptides induce SecA oligomerization and membrane insertion (Benach, Chou et al. 2003; Shin, Kim et al. 2006). The inactive SecA monomeric mutant (Jilaveanu, Zito et al. 2005) and active cross-linked SecA dimers (de Keyzer, van der Sluis et al. 2005; Jilaveanu and Oliver 2006) lead to the conclusion of dimer as the active form. We have also shown that SecA functions in membrane as dimer *in vivo* and *in vitro*, and the dissociation into monomer is not essential for protein translocation (Wang, Na et al. 2008). With the same approach, genetically constructed SecA trimer show similar activity and structures *in vitro* as the tandem dimer (Wang and Tai, unpublished data), raising the possibility that SecA may exist in higher order status (such as hexamers) in membranes. Thus the quaternary oligomeric state of functional SecA still remains unclear, and more work is needed to resolve this puzzle.

Domains of SecA. Soluble SecA consists of two separable domains, the N-terminal 68 kDa fragment (N68) and the C-terminal 34 kDa regulatory domain (C34). N68 holds high ATPase activity equivalent to the translocation ATPase which is down-regulated by IRA1 in C34 (Karamanou, Vrontou et al. 1999). N68 catalytic domain contains several subdomains of SecA: two nucleotide-binding domains (NBDI and NBDII) and preprotein cross-linking domain (PPXD). NBDI is composed of the conserved Walker A and B motifs and is responsible for the high affinity binding and hydrolysis of ATP (Mitchell and Oliver 1993; Sianidis, Karamanou et al. 2001). NBDII comprises a consensus sequence

of Walker A and a putative Walker B motif (Mitchell and Oliver 1993). There is no experimental demonstration of nucleotide binding to NBDII. Instead, NBDII binds to NBDI and plays the role as intramolecular regulator of the hydrolysis of ATP (IRA2) (Nakatogawa, Mori et al. 2000). N68 contains conserved DEAD superfamily II motifs in NBDI and IRA2 and represents a DEAD motor (Sianidis, Karamanou et al. 2001). SecA interacts with preproteins at PPXD which is inside NBDI but composes a separate domain in the tertiary structure (Hunt, Weinkauf et al. 2002; Papanikou, Karamanou et al. 2005).

C-34 can be divided into three structural subdomains: the α-helical scaffold domain (HSD), the α-helical wing domain (HWD), and the C-terminal domain (CTD) (Hunt, Weinkauf et al. 2002). HSD is composed by the bundle of three α-helixes. The first long α-helix (amino acid #621-668) extends through the whole length of SecA, with one side interacting with NBDI and NBDII (IRA2) and the other side interacting with the other protomer in the homodimer. The second and third α-helixes form the helix-loop-helix (HLH) structure in which the IRA1 is located (Karamanou, Vrontou et al. 1999). The third helix interacts with PPXD, keeping IRA1 at the opposite side of NBDI and IRA2. HSD is suggested to be a global conformational template, binding to the subdomains to ensure their relative positions of each other. HWD is inserted between the first and second α-helixes of HSD and is weakly linked to other parts of SecA. CTD is not well conserved in SecA and is not essential for its function (Kakeshtia, Kageyama et al. 2010). The extreme C-terminal region of CTD is involved in SecB and lipid binding (Breukink, Nouwen et al. 1995), and is connected to the rest of C-34 by C-terminal linker peptide (CTL). CTD has dynamic structure and is not observed in the crystal structure (Hunt,

Weinkauf et al. 2002; Sharma, Arockiasamy et al. 2003). These major structural domains are summarized in Figure 1.1.

SecA is the major component of the bacterial Sec-system that is found both in the cytoplasm and the membrane (Cabelli, Dolan et al. 1991). SecA ATPase functions as a molecular motor that hydrolyzes ATP to provide the essential energy for the Sec-dependent protein translocation. The intrinsic ATPase activity of SecA is relatively low, while the membrane ATPase could be stimulated by anionic phospholipids or membranes. Binding to SecYEG complex and precursor proteins further fully activates the ATPase activity referred to as SecA translocation ATPase (Lill, Dowhan et al. 1990; Wang, Miller et al. 2000). As a central component of Sec-system, SecA interacts with almost all other components involved in protein translocation through different regions. Besides the domains already mentioned above, several binding sites for other proteins and ligands have been identified. Both C-terminus and N-terminus of SecA are involved in SecB binding (Fekkes, de Wit et al. 1999; Randall and Henzl 2010). N-terminal part (residues 221-227) of PPXD is essential for signal peptide binding while the C-terminal part (residues 267-340) may be the binding site for mature domain of preproteins (Kimura, Akita et al. 1991; Vrontou and Economou 2004). SecA interacts with the cytoplasmic membrane by low-affinity binding with anionic phospholipids, and high-affinity binding with SecYEG (Hartl, Lecker et al. 1990; Lill, Dowhan et al. 1990). SecA interacts with SecYEG complex through contact with SecY. Both the C-terminal region (Snyders, Ramamurthy et al. 1997) and the N-terminal catalytic domain of SecA (Dapic and Oliver 2000; Vrontou, Karamanou et al. 2004) show interaction with SecY. In addition, the first 8 residues of the N-terminus of SecA can bind to SecG (Mori, Sugiyama et

al. 1998). Therefore, the interaction of SecA and SecYEG may involve multiple areas of contact.

SecA as target for new antibiotics. Because of the improper use and overconsumption of antibiotics, drug-resistant bacteria strains have emerged and spread with increased rapidity (Chen, Chopra et al. 2009). This emergence has created a demand for new antibacterial agents, especially those agents with alternative mechanisms that will avoid cross-resistance with existing antibiotics (Payne 2008). Protein secretion systems have been proposed as new antibiotic targets as a consequence of the importance for bacterial cell growth and virulence (Stephens and Shapiro 1997). The general secretion (Sec)-pathway mediates the majority of protein transportation and is highly conserved in bacteria (van Wely, Swaving et al. 2001; Driessen and Nouwen 2008). Among the components of the Sec-system, SecA is of particular interest because of the following reasons: (1) SecA is essential for both Gram-positive and Gram-negative bacteria, including a variety of pathogens (Segers and Anne 2011). (2) Unlike SecYEG, which is homologous to the Sec61 channel complex in the endoplasmic reticulum in yeast and mammalian, there is no structurally-similar human counterpart of SecA (Manting and Driessen 2000; Pohlschroder, Hartmann et al. 2005; van der Sluis and Driessen 2006). (3) Several putative ligand-binding sites have been found in EcSecA and can serve as potential drug targets (Segers and Anne 2011). (4) Potential inhibitors can be screened through rapid functional assays of SecA ATPase activity. With all these features, SecA is an ideal target for the development of new antibacterial drugs.

Azide is a well-known SecA inhibitor used as a molecular tool to probe the Sec-system (Knott and Robinson 1994), but it only inhibits the translocation ATPase, not in-

trinsic or membrane ATPase (Oliver, Cabelli et al. 1990; Nakane, Takamatsu et al. 1995). However, azide also inhibits many other enzymes in mammalian cells, such as cytochrome oxidase (Berndt, Callaway et al. 2001) and superoxide dismutase (Marklund 1984). The general cytotoxicity in host cells and the simple structure with less potential for further optimizing make azide a less-favored candidate. Antibacterial activities are found from natural SecA inhibitors. Only translocation ATPase is repressed by CJ21058, but the effects on the intrinsic and membrane ATPase are unknown (Sugie, Inagaki et al. 2002). The effect against SecA function is not reported in the study of pannomycin (Parish, de la Cruz et al. 2009). There is still a need to search for SecA inhibitors with a correlation between their ability to inhibit SecA and the antimicrobial activities. The obtained SecA inhibitors should provide a new perspective for pharmaceutical application and help us gain insight into the molecular mechanism of SecA-dependent protein translocation.

SecA as protein conducting channels. Although the model of SecYEG complex as the protein conducting channel in the cytoplasmic membrane is widely accepted, there is controversy over the necessity of SecYEG for protein translocation. Membranes depleted of SecY and SecE are still active in translocation of some precursor proteins, suggesting these two proteins are not essential for the transportation of all proteins (Watanabe, Nicchitta et al. 1990; Watanabe and Blobel 1993; Yang, Lian et al. 1997; Yang, Yu et al. 1997). On the other hand, the membrane-integral form of SecA and two lipid-specific domains have been identified (Chen, Xu et al. 1996). Pore-like structures of EcSecA in lipids detected by electronic microscopy (EM) and atomic force microscopy (AFM) reveal the ability of SecA itself to form the channel-like structure, which is independent of

ATP or on-going protein translocation (Wang, Chen et al. 2003). Electro-physiological data show EcSecA, but not SecYEG, is the major contributor for channel activity, providing more evidence that SecA can form the protein-conducting channel (Lin, dissertation, 2006) (Hsieh, Zhang et al. 2011). Therefore, we are testing the hypothesis that in addition to catalyzing ATP hydrolysis, certain domains of SecA play an important structural role in the translocation machinery, constructing part of the protein-conduction channels.

SecA in Gram-positive bacteria. Because of the difference of cellular structure, secreted proteins in Gram-positive bacteria only need to cross a single membrane to reach the extra-cellular environment. Gram-positive bacteria (*e.g.*, *Bacillus* species) have the ability to secrete a large amount of protein into the extra-cellular medium; therefore, they are often used in industry for commercial production of secreted proteins. The genome sequence analysis implies that the protein secretion systems of Gram-positive and Gram-negative bacteria are quite similar because they share the major components (van Wely, Swaving et al. 2001). The availability of the X-ray crystallography and domain analysis of *B. subtilis* SecA enhances our understanding of its structure and function (Hunt, Weinkauf et al. 2002). The research in our lab centers on the structure and function of SecA, using *E. coli* as the model system. Currently, we are expanding our interest to other bacteria. In particular, SecA from *B. subtilis* (BsSecA) and *S. pyogenes* (SpSecA) are used in this study as models of Gram-positive bacteria.

Here we explore the structure and function of SecA with multiple approaches. This dissertation includes three parts: (1) Screening and analysis of SecA inhibitors as potential antibacterial agents; (2) The structural and functional analysis of the first α-helix of

C-terminal domain of EcSecA; and (3) A comparative study of Gram-positive SecA. This study will help us to elucidate the role of SecA in protein-translocation systems.

a

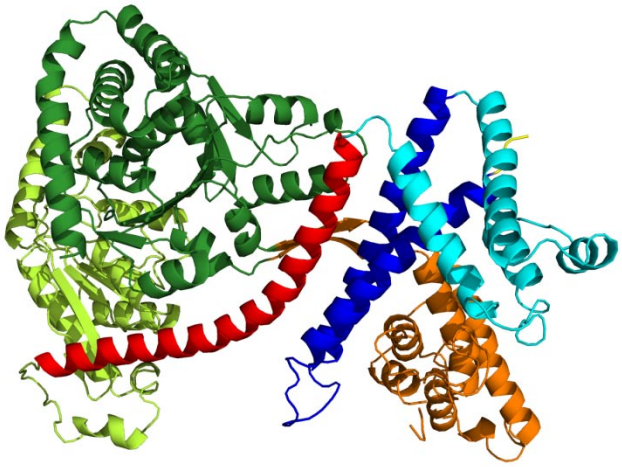

b

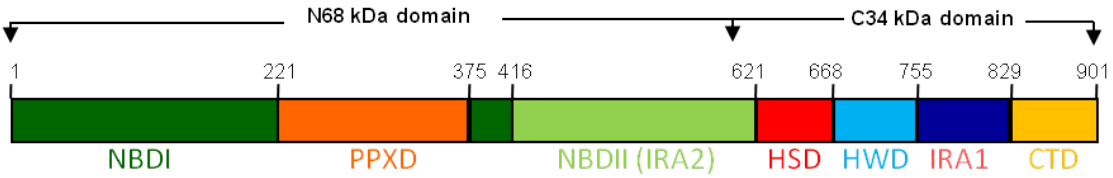

Figure 1.1. Structure of SecA. (a) The structure of one protomer of the homodimer of EcSecA (Protein Data Bank (PDB) number 2FSF) (Papanikolau, Papadovasilaki et al. 2007); (b) Positions of the subdomains. The boundaries are labeled with the residue numbers. NBD: nucleotide binding domain; PPXD: preprotein cross-linking domain; IRA: intramolecular regulator of the hydrolysis of ATP; HSD: α-helical scaffold domain; HWD: α-helical wing domain; CTD: C-terminal domain.

2 Fluorescein analogs inhibit SecA ATPase: the first sub-μM inhibitor for bacterial protein translocation

Part of this chapter is in a manuscript submitted for publication by

Ying-Ju Huang, Hongyun Wang, Fen-Biao Gao, Minyong Li, Hsiuchin Yang, Binghe Wang, and Phang C. Tai.

2.1 Abstract

SecA is a central component of the general secretion system that is essential for bacterial growth. A series of fluorescein analogs were tested against the ATPase activity using the SecA catalytic domain. Rose Bengal (RB) and Erythrosin B (EB) were found to be potent inhibitors with IC_{50} values of 0.5 μM and 2 μM, respectively, while azide, a well-known SecA inhibitor which has no effect up to 10 mM. RB and EB inhibit the catalytic SecA ATPase more than the F_1F_0-proton ATPase. RB and EB also inhibit the SecA intrinsic ATPase activity with IC_{50} of 20-30 μM. Kinetics study reveals that the SecA intrinsic ATPase is affected by these fluorescein analogs competitively at low ATP concentrations and non-competitively at high ATP concentrations. The membrane and translocation ATPases are inhibited non-competitively by RB, with IC_{50} of about 4 μM and 1μM, respectively. In contrast, the inhibition by EB for all 3 forms of SecA ATPase remains constant with IC_{50} about 20-30 μM. The *in vitro* translocation of proOmpA precursors into membrane vesicles is strongly inhibited by RB with IC_{50} of about 0.25 μM, making RB so far the most potent inhibitor of SecA ATPases and SecA-dependent protein translocation. These compounds also exhibit antibacterial effects. Our findings show the value of fluorescein analogs as probes for mechanistic studies of SecA functions, and for the potential development of new antimicrobial agents with SecA as the target.

2.2 Introduction

In all growing cells, the translocation of proteins into various cellular and extracellular compartments is essential to maintain normal physiological functions. In bacteria, more than 30% of the proteins are located in or outside the cellular cytoplasmic mem-

brane. The general secretion (Sec)-pathway mediates the transport of most unfolded proteins across or inserted into the cytoplasmic membrane before these proteins reach their final destinations in the cytoplasmic membrane, periplasmic space or outer membrane (Papanikou, Karamanou et al. 2007). The bacterial Sec-pathway consists of a series of membrane proteins including SecY, SecE, and SecG that constitute an oligomeric complex, which is homologous to the Sec61 channel complex in the endoplasmic reticulum (Mori and Ito 2001; Driessen and Nouwen 2008). SecA is the major component of the bacterial Sec-system that is found both in the cytoplasm and the membrane (Cabelli, Dolan et al. 1991), and functions as an ATPase that provides the essential energy for the Sec-dependent protein translocation. The intrinsic ATPase activity of SecA is relatively low, while the membrane ATPase could be stimulated by anionic phospholipids. Binding to SecYEG complex and precursor proteins further fully activates the ATPase activity referred to as SecA translocation ATPase (Lill, Dowhan et al. 1990; Wang, Miller et al. 2000).

Inhibitors can be useful tools for probing the conformational changes of SecA during protein translocation. Azide is a well-known SecA inhibitor (Knott and Robinson 1994; Nakane, Takamatsu et al. 1995). However, azide inhibits only the translocation ATPase but not the intrinsic and membrane ATPases of SecA (Oliver, Cabelli et al. 1990; Nakane, Takamatsu et al. 1995). It has been reported that a natural fungal fermentation product CJ21058 also inhibits the translocation ATPase, though the effect on the intrinsic or membrane ATPase of SecA has not been reported (Sugie, Inagaki et al. 2002). More recently, a secondary metabolite (pannomycin) from fungi with similar structure was isolated by the antisense-based screening against SecA (Parish, de la Cruz et al. 2009). This

compound only shows weak antibacterial activity with MIC in the mM range, and the inhibitory effect against SecA function was not reported. By virtual screening and optimizing, we recently found several thiouracil-based compounds capable of inhibiting the intrinsic SecA ATPase (IC_{50} 20-60 μM) (Li, Huang et al. 2008). A subsequent study synthesized a series of thiazolo[4,5-*d*]pyrimidine derivatives with the most potent compound having an IC_{50} value of 135 μM against EcSecA intrinsic ATPase, but showed minor effect on the translocation ATPase (Jang, De Jonghe et al.). It has also been reported that some halogenated fluorescein analogs could influence the activity of phosphatase as non-hydrolyzable nucleotide analogs (Mignaco, Lupi et al. 1996). In this work, the effects of several fluorescein analogs were tested against SecA ATPase activity. Rose Bengal and Erythrosine B show strong inhibitory effects on the three forms of SecA ATPase activity and the *in vitro* protein translocation, as well as exhibit antimicrobial effects.

2.3 Material and methods

Bacterial strains, medium, and chemicals. *Escherichia coli* K-12 strain MC4100 (Casadaban 1976), NR698 (MC4100 *imp*4213), a leaky mutant with increased outer membrane permeability (Ruiz, Falcone et al. 2005) from T. Slhavy, and BA13 (MC4100 *secA13(am) supF(ts)*) (Cabelli, Chen et al. 1988) from D. Oliver and *Bacillus subtilis* strain 168 (lab stock) were used in this study. Luria-Bertani (LB) liquid and solid (1.5% agar) media with 0.2% glucose were used for bacterial growth. Fluorescein analogs were purchased from Sigma-Aldrich Corp (St. Louis, MO) and were dissolved in water (for Rose Bengal, Erythrosin B, and fluorescein) or 100% DMSO (for diiodofluorescein, Ecosin Y, and dinitrofluorescein).

Determination of bacteriostatic and bactericidal concentrations of fluorescein analogs. *Plate assay*: 0.5 mL culture of bacterial cells (exponential phase, OD_{600}=0.5) was mixed with 4 mL of LB with 0.2% of glucose and 0.75% soft agar and then was poured into petri dishes. After the soft agar solidified, 1 μL of the potential inhibitors was spotted on the surface of the culture. Bacteriostatic effect was judged by the appearance of a clear zone of growth inhibition after overnight incubation at 37°C. *Liquid culture assay*: Bacterial cells of exponential phase (OD_{600} about 0.5-0.8) were diluted to OD_{600}=0.05 with LB with 0.2% of glucose. 90 μL of diluted culture was incubated at 37 °C, at 1,000 rpm (Eppendorf Thermomixer R, Brinkmann Instruments, Inc.) in the presence of 10 μL of inhibitors or equal volume of water as control. After 14 hours of incubation, cell growth was determined by OD_{600}. Inhibition of cell growth (or bacteriostatic effect) was illustrated by decreasing OD. *Bactericidal effect assay*: 40 μL inhibitors were added into 360 μL of bacteria cultures (exponential phase, OD_{600}=0.5) while the same volume of water was used as control. After one hour treatment at 37°C, cultures were spread on LB plate after serial dilutions, and the colony forming unit (CFU) of survival cells were enumerated after overnight incubation at 37°C. Inhibitory effect (or bactericidal effect) was illustrated by the decreasing of the log value of CFU. All assays were done at least in triplicate, and the results were presented as line or bar graphs with standard error of the means.

Preparations of various SecA proteins, F_1F_0-ATPase, proOmpA, and membrane vesicles. The N-terminal catalytic domain of SecA from *E. coli* (EcN68) was overexpressed from pIMBB28 (Karamanou, Vrontou et al. 1999) obtained from A. Economou. EcN68 was used for the early screening because it has higher intrinsic activity and

is more sensitive to inhibitors. The full-length SecA from *E. coli* (EcSecA) and *B. subtilis* (BsSecA) were over-expressed from plasmids pT7-SecA (Cabelli, Chen et al. 1988) and pT7div (McNicholas, Rajapandi et al. 1995) respectively, both obtained from D. Oliver. SecA proteins were purified as described (Chen, Xu et al. 1996; Chen, Brown et al. 1998). F_1F_0-ATPase enriched membrane of *E. coli* strain KY7485 (Kanazawa, Miki et al. 1979) obtained from W. Brusilow was prepared as described (Foster and Fillingame 1979). F_1F_0-ATPase was partially purified by sucrose gradient fractionation and then re-constituted into liposomes by dialysis. The purification of proOmpA was described without radioactive labeling (Chen, Xu et al. 1996). SecA-depleted BA13 membrane vesicles were prepared as described (Tai, Tian et al. 1991), and washed with 6 M urea to reduce endogenous ATPase activity.

***In vitro* ATPase activity assay.** ATPase activity assays were performed as described (Lill, Dowhan et al. 1990) with minor modifications. For intrinsic and membrane ATPase assay, 50 µL reaction mixtures contained 1.8 µg EcN68, or 1.5 µg EcSecA unless specified otherwise, 20 µg ovalbumin, 1.2 mM ATP, 50 mM Tris-HCl (pH7.6), 20 mM KCl, 20 mM NH_4Cl, 2mM $Mg(OAc)_2$, 1 mM DTT, and (for membrane ATPase) 3 µg urea-washed *E. coli* BA13 membrane. For translocation ATPase assay, reaction mixtures contained 1 µg proOmpA in addition to membranes. For proton ATPase activity, reconstituted-liposomes containing partially purified F_1F_0-proton ATPase were assayed in the same condition as the intrinsic ATPase. All reactions were carried out at 40°C for an appropriate time in the linear ranges of the activity assay that was determined by the release of inorganic phosphate detected by the photometric method (Lanzetta, Alvarez et al. 1979) with the absorption measured at 660 nm (SmartSpec Plus, Bio-Rad Laboratories,

Inc.). The inhibitory effects were illustrated by the percentage (%) of remaining ATPase activity as compared to the controls in the absence of potential inhibitors. All assays were performed at least in triplicate, and the results were presented as line graphs with standard error of the mean.

***In vitro* protein translocation assay.** Protein translocation assay was carried out as previously described using ^{35}S-labeled proOmpA as a marker (Wang, Na et al. 2008). The protease-resistant translocated proteins were analyzed by SDS-PAGE, autoradiographed, and quantified by a densitometer (GS-800 Calibrated Densitometer, Bio-Rad, Hercules, CA).

Molecular simulation of docking complexes. For simulating the binding profiles of DI, EB, RB and CJ-21058, their structures were docked into the ATP site of EcSecA using the DOCK 6 program (Ewing, Makino et al. 2001; Moustakas, Lang et al. 2006). Residues within a radius of 6 Å around the center of ATP were defined as the active site to construct a grid. The active site included residues Gly80, Met81, Arg82, His83, Phe84, Gln87, Arg103, Thr104, Gly105, Glu106, Gly107, Lys108, Thr109, Leu110, Arg138, Asp209, Glu210, Arg509 and Gln578. The subsequent computational work was conducted as described previously (Li and Wang 2006; Li and Wang 2007). Briefly, the docked complexes were solvated by using the TIP3P water model (Jorgensen, Chandrasekhar et al. 1983), and then subjected to 500 steps of molecular mechanics minimization and molecular dynamics simulations at 300 K for 1.5 ns using the SANDER module in AMBER 8 program (Case, Cheatham et al. 2005).

2.4 Results

Fluorescein analogs as ATPase inhibitors.

A series of commercially available fluorescein analogs were screened against the *in vitro* intrinsic ATPase of SecA. For measuring higher intrinsic ATPase activity, we used the N-terminal catalytic domain of EcSecA (EcN68) without the C-terminal domain possessing the unregulated ATPase activity (Karamanou, Vrontou et al. 1999; Karamanou, Sianidis et al. 2005). The inhibitory effect of the potential SecA inhibitors is illustrated (Figure 2.1) and the IC_{50} values of fluorescein analogs with significant inhibitory effects are summarized in Table 1. Among the screened compounds, RB and EB are the most effective, with IC_{50} of 0.5 μM and 2 μM, respectively (Figure 2.2). Since RB and EB are known to inhibit some ATPases from animal tissues (Morris, Silbergeld et al. 1982; Silbergeld, Anderson et al. 1982; Fricke 1985), we tested whether these compounds inhibit other *E. coli* ATPases such as F_1F_0-ATPase. The IC_{50} values of RB and EB for F_1F_0-ATPase are about 10 μM and 30 μM, respectively (Figure 2.2). The data indicate that RB and EB may be general ATPase inhibitors. However, they are more effective on the catalytic SecA ATPase. RB has been reported to inhibit some ATPases by photo-oxidation (Watson and Haynes 1982; Glaser, Cadenas et al. 1988). We found that RB shows similar inhibitory effects of SecA ATPase in normal room illumination and in dark conditions (Figure 2.3), suggesting that photo-oxidation is probably not related to the inhibition of SecA under the conditions used.

RB and EB show different inhibitory effects on three forms of EcSecA ATPase activity.

Since the ATPase activity of the catalytic domain of SecA could be inhibited by these fluorescein analogs, we examined the inhibitory effects on the ATPase activity of full-length SecA. RB and EB strongly inhibit the intrinsic ATPase activity of EcSecA, with IC_{50} of about 20-30 μM. We further investigated the inhibitory effects of RB and EB on the membrane and translocation ATPases of EcSecA. The data show that RB and EB inhibit all three forms of EcSecA ATPase activities (Figure 2.4 a-c). EB shows similar inhibitory effects to all three forms of ATPase activity with IC_{50} of about 10-20 μM (Figure 2.4 a-c, Table 2.2); interestingly, RB shows significantly different potencies depending on the form of ATPase tested. While the inhibition of the intrinsic ATPase by RB is similar to EB, the membrane ATPase is more sensitive to RB with IC_{50} of 4 μM, and the translocation ATPase is the most sensitive with IC_{50} of 0.9 μM (Table 2.2). The lipid-stimulated ATPase activity is also inhibited by RB and EB (Figure 2.4d).

Since RB shows different inhibitory effects on three forms of SecA ATPase, we determined their kinetic parameters to elucidate the mechanism of inhibition. Data were fit by nonlinear regression analysis to determine the apparent Michaelis-Menten constants (Table 2.3). The sigmoid Michaelis-Menten plot of intrinsic ATPase indicates that there may be two inhibition sites (Figure 2.5a). Double reciprocal plots clearly demonstrate two inhibitory mechanisms in different concentration ranges of the substrate (Figure 2.5b and c). At low ATP concentrations (below 0.6 mM), RB acts as a competitive inhibitor against the intrinsic ATPase with an apparent K_i of 22.44±3.33 μM, increased K_m and about constant V_{max} (Table 2.3). At high ATP concentrations (above 1mM), RB acts as a non-competitive inhibitor with an apparent K_i of 57.11±3.37 μM, constant $K_{m,}$ and decreased V_{max} (Table 2.3). The inhibition of the SecA membrane ATPase by RB exhibits a

"mixed-mechanism." It has both competitive and non-competitive inhibition characters but more toward the later, resulting in an average K_i of 1.42±0.22 μM, slightly increased $K_{m,}$ and decreased V_{max} (Figure 2.6 and Table 2.3). On the other hand, RB inhibits the translocation ATPase of SecA only non-competitively in a broad range of ATP concentrations with K_i of 0.43±0.02 μM, constant K_m, and decreased V_{max} (Figure 2.7 and Table 2.3).

Similarly, the inhibition of EB on the intrinsic ATPase activity of SecA also shows differential effects of various ATP concentrations. Thus at low ATP concentrations, EB inhibits the SecA ATPase competitively with K_i of 4.06 ± 0.32 μM, while at high ATP concentrations, it inhibits SecA ATPase non-competitively with K_i of 34.29 ± 8.08 μM (Figure 2.8). These data indicate that RB and EB affect the intrinsic SecA ATPase in a similar manner. Since different forms of SecA show similar sensitivities to EB but drastically different ones to RB, it would be interesting to compare the inhibitory mechanisms of these two inhibitors against the translocation ATPase. Unlike RB inhibits the translocation ATPase non-competitively (Figure 2.7), EB shows an obvious mixed-mechanism of competitive and non-competitive inhibition with average K_i of 1.17 ± 0.24 μM (Figure 2.9). These data reveal the difference between these two structure-alike inhibitors.

RB and EB also inhibit ATPase activities of BsSecA.

Gram-positive *Bacillus subtilis* SecA (BsSecA) has high homology (51% identity) to EcSecA, and has much higher intrinsic ATPase activity. We determined the inhibition profile of RB and EB on BsSecA. As expected, both RB and EB show inhibitory effects

on BsSecA intrinsic ATPase activities, with RB as a stronger inhibitor (Figure 2.10). Different forms of BsSecA ATPase with *E coli* membrane and OmpA precursor have similar sensitivities for RB and EB, with IC_{50} of 10-20 μM and 40-70 μM, respectively (Table 2.2). The inhibitory mechanism of RB against the intrinsic ATPase of BsSecA also shows the similar two-site inhibition: at low ATP concentrations (below 0.6 mM), RB acts as a competitive inhibitor against the BsSecA intrinsic ATPase with an apparent K_i of 4.97 ± 1.07 μM. At high ATP concentrations (above 1 mM), RB acts as a non-competitive inhibitor with an apparent K_i of 7.99± 0.69 μM (Figure 2.11). This phenomenon indicates that the inhibitory mechanisms of RB against the intrinsic ATPase of BsSecA and EcSecA are similar.

RB and EB inhibit the protein translocation *in vitro*.

The translocation ATPase activity of SecA is essential for the translocation of precursor proteins *in vitro* (Oliver, Cabelli et al. 1990; Sianidis, Karamanou et al. 2001). Since the translocation ATPase of EcSecA is significantly affected by RB and EB (Table 2), we further investigated the effects of RB and EB on the SecA-dependent protein translocation *in vitro*. We found that the *in vitro* translocation of precursor proOmpA into membrane vesicles is severely inhibited by RB and EB (Figure 2.12). Interestingly, the protein translocation is about three to four folds more sensitive to RB and EB than the translocation ATPase. Consistent with the result of translocation ATPase, RB shows stronger inhibitory effect (with IC_{50} of 0.25 μM) than EB (with IC_{50} of 4 μM).

RB is bactericidal on both Gram-positive and Gram-negative bacteria.

It has been reported that RB can inhibit the growth and kill *Staphylococcus aureus* in dark, while kills various bacteria through photo-oxidation (Banks, Board et al. 1985; Rasooly and Weisz 2002; Kim, Park et al. 2008; Waite and Yousef 2009). Since SecA is an essential protein for bacterial growth, we next examined the antimicrobial effect of these SecA inhibitors. The fluorescein analogs that inhibit EcN68 ATPase *in vitro* were subjected to the following study. These compounds inhibit the growth of both Gram-positive and Gram-negative bacteria in plate assay (Table 2.4). Gram-negative bacteria *E. coli* MC4100 is very resistant to the fluorescein analogs possibly because of the outer-membrane barrier but its permeable leaky mutant NR698 (Ruiz, Falcone et al. 2005) shows similar sensitivity to Gram-positive *B. subtilis*. Among the tested fluorescein analogs, diiodofluorescein (DI), Ecosin Y (EY), and dinitrofluorescein (DN) show the MIC at mM level, while RB and EB have stronger inhibition with MIC at low μM level. RB also inhibits the growth of both Gram-positive and Gram-negative bacteria in liquid culture. The growth of *E. coli* NR698 and *B. subtilis* 168 can be completely inhibited at low concentration level (50-75 μM) (Figure 2.13). RB shows the same potency of bacteriostatic activity with or without 0.2% glucose in the media, suggesting that F_1F_0-proton ATPase indeed is not the primary target of the inhibition. The bactericidal effects of RB and EB were also tested. After one-hour treatment on exponential-phase cells, the CFU was determined after overnight incubation. The leaky mutant NR698 is very sensitive to RB. With 100 μM of RB, cell survival decreases about 10 log units (Figure 2.14a). Without the barrier of outer membrane, RB shows strong bactericidal effect on *B. subtilis* in a concentration dependent manner (Figure 2.14b). Cell density does not drop in the pres-

ence of 100 μM RB up to 90 min (Figure 2.15), indicating that the bactericidal effects of RB on both bacteria are not caused by cell lysis.

The structures of RB and EB fit in the SecA ATP pocket.

Earlier studies show that fluorescein analogs bind to enzymes containing nucleotide binding sites with high affinity (Jacobsberg, Kantrowitz et al. 1975; Yip and Rudolph 1976; Morris, Silbergeld et al. 1982). In order to examine the binding profile between SecA and fluorescein analogs, *in silico* modeling was conducted by molecular simulation. The structures of RB, EB, and DI were docked into the ATP site of EcSecA. RB and EB show very similar binding profiles, while DI shows a different conformation because of the lack of the diiodo-moiety (Figure 2.16). For comparison, the binding mode of CJ-21058, a natural product SecA inhibitor, was also examined. RB and CJ-21058 seemed to occupy the same position and with the same orientations.

2.5 Discussion

In the present study, we have found that several fluorescein-related analogs can inhibit the ATPase activity of SecA, the SecA-dependent *in vitro* protein translocation, and the growth of cells with bactericidal effects. Among these, RB is the most potent and show different inhibitory mechanisms for the SecA ATPases.

It has been previously reported that some ATPases from animal tissues could be inhibited by RB and EB mediated photo-oxidation (Watson and Haynes 1982; Glaser, Cadenas et al. 1988). The singlet oxygen attacks the essential amino acid residues and causes structural and functional degradation of enzymes. Photo-oxidation has been re-

ported to be the primary mechanism for RB and some halogenated fluoresceins working as the photosensitizer in antimicrobial actions (Banks, Board et al. 1985; Rasooly and Weisz 2002; Kim, Park et al. 2008; Waite and Yousef 2009). In our studies, all assays have been performed under the condition of normal room illumination without special light excitation. Moreover, reactions with or without light show no difference in IC_{50}. Thus the inhibitory effects against the three forms of SecA ATPase activities or cell growth are not likely due to photo-oxidation. Other earlier reports also show that RB, EB, and DI can inhibit the ion-pump related ATPases from animal tissue without photo-oxidation (Morris, Silbergeld et al. 1982; Silbergeld, Anderson et al. 1982; Fricke 1985). Non-photooxidation antibacterial activities of halogenated fluoresceins are also reported, but the mechanism is not clear (Banks, Board et al. 1985; Rasooly and Weisz 2002; Kim, Park et al. 2008; Waite and Yousef 2009). Prior studies demonstrate that the fluorescein derivatives influence the enzymes as the non-hydrolyzable nucleotide analogs (Mignaco, Lupi et al. 1996; Linnertz, Kost et al. 1998; Linnertz, Urbanova et al. 1998; Tanfani, Linnertz et al. 2000). Here we demonstrate the inhibitory effects of these fluorescein analogs on SecA ATPase and *E. coli* F_1F_0-ATPase. The results here indicate that fluorescein analogs are general ATPase inhibitors but may be more specific for SecA because the catalytic ATPase of SecA is more sensitive, and the antibacterial activity is observed in the presence of glucose that minimizes the effects on F_1F_0-proton ATPase. Taken together, the results suggest that SecA may be the target of fluorescein analogs and the inhibition of ATPase and translocation may contribute to the antibacterial effects.

A striking feature of RB and EB is that these two inhibitors influence the intrinsic ATPase of SecA in a competitive manner at low ATP concentrations and a non-

competitive manner at high ATP concentrations. One possible interpretation of these findings is that RB and EB affect two non-identical nucleotide binding sites on SecA. Two nucleotide binding sites (NBDs) have been identified in SecA through sequence alignment and biochemical studies (Mitchell and Oliver 1993; Economou, Pogliano et al. 1995; van der Wolk, Boorsma et al. 1997; Karamanou, Vrontou et al. 1999; Nakatogawa, Mori et al. 2000). NBDI binds to ATP with high-affinity and is considered as the catalytic site; however, there is no direct evidence of binding, and less is known about the low-affinity site (NBDII). In this study, kinetics analysis suggests that RB and EB apparently prefer to bind to the high-affinity site; therefore, competitive inhibition is observed at low ATP concentrations. It is also interesting to note that the high-affinity site has a lower V_{max} while the low-affinity site has a 2.5 times higher V_{max}. A possible interpretation of the results presented above is that high concentration of ATP may be a signal for increasing the ATPase activity of SecA and NBDII may serve as the sensor. At high ATP concentrations, RB and EB inhibit the activity arisen from the low-affinity site non-competitively. Some fluorescein-related pseudo ATP analogs have been shown to be useful probes for biochemical study of the two ATP binding sites of P-type ATPase (Linnertz, Kost et al. 1998; Linnertz, Urbanova et al. 1998; Tanfani, Linnertz et al. 2000). RB and EB inhibit the two ATP binding sites differently, and this result suggests that these fluorescein analogs may be a useful tool for unraveling the functional significance of the two nucleotide binding sites of SecA.

Interestingly, the inhibitory mechanisms of RB against the membrane and translocation ATPases of EcSecA are different from the intrinsic ATPase. RB inhibits the membrane ATPase by a “mixed-mechanism” between competitive and non-competitive man-

ners (but more toward the later), and the translocation ATPase by a non-competitive manner in a broad range of ATP concentrations. It is likely that binding to the membrane and precursor proteins dramatically changes the conformation of EcSecA and causes the alteration of inhibition profiles. RB has various inhibitory effects on three forms of EcSecA ATPase activities, with IC_{50} values range from translocation ATPase (0.9 μM) < membrane ATPase (5 μM) < intrinsic ATPase (25 μM). The significant differences of the sensitivities of three forms of ATPase of EcSecA also indicate that conformational changes of SecA in the interaction with membranes and precursors may influence the accessibility of the enzyme to inhibitors. RB and EB share the fluorescein-based chemical structure, and these two compounds show similar binding profiles in the computer modeling. Even with these similarities, EB shows similar inhibitory effects on the three forms of ATPase of EcSecA. One possible explanation is that RB and EB are docked into the intrinsic EcSecA conformation which may be very different from the changed SecA conformation induced by the presence of membrane and precursor. Thus, the modeling could not reveal the dissimilar binding profiles between RB and EB with EcSecA in the presence of membrane and/or precursor proteins. The BsSecA ATPases are also inhibited by RB and EB. RB showed stronger inhibitory effect on the intrinsic ATPase of BsSecA than EcSecA. However, the intrinsic, membrane and translocation ATPases show similar sensitivities to the same inhibitor. These data raise the possibility that the conformational changes of BsSecA for the membrane and translocation ATPases are different since the heterogeneous components (Ec membrane and precursors proOmpA) are used in the assay.

The translocation ATPase activity of SecA is essential for the SecA-dependent *in vitro* translocation. Azide inhibits the translocation ATPase of SecA and the transport of precursor proteins across the inner membrane vesicles *in vitro* (Oliver, Cabelli et al. 1990). SecA mutants that lose stimulated translocation ATPase show defect of preprotein translocation *in vitro* (Sianidis, Karamanou et al. 2001). The *in vitro* translocation of precursor protein proOmpA into membrane vesicles is also inhibited by RB and EB. The *in vitro* translocation is even more sensitive to RB and EB than the translocation ATPase of EcSecA. This difference is also reported for azide and but the *in vitro* protein translocation and the cell growth show similar sensitivities (Oliver, Cabelli et al. 1990). In the case of RB and EB, *in vivo* growth is significantly less sensitive than *in vitro* protein translocation. This may due to the different membrane permeability of inhibitors. Azide is a small inorganic molecule while RB and EB are much bigger organic molecules with lower permeability across bacterial membranes. In fact, the outer membrane leaky mutant shows stronger inhibitory effects than its parent.

In recent years, antibiotic-resistant strains have become a serious problem because of the overuse of antibacterial medicine. There is an urgent need for development of novel antibacterial agents. Protein secretion system is essential for bacterial viability and virulence; therefore, it has been considered as an ideal target for pharmaceutical interests (Stephens and Shapiro 1997). The majority of secreted and membrane proteins is mediated by the Sec pathway. This fact makes the components of the Sec system potentially valuable for antibiotic targeting (Economou 2001). SecA is the central element of the Sec pathway and is highly conserved in bacteria and is involved in the major route of bacterial protein translocation that is essential for the growth and virulence of bacterial cells.

More importantly, SecA has no human counterpart, making it a good target for development of new antibiotics (Stephens and Shapiro 1997). Thus SecA has the potential to be the target of a new class of antimicrobial drugs, and SecA inhibitors have the potential to be new antibacterial agents. Up to now, there are very few inhibitors against SecA have been studied. Sodium azide is the most well-known SecA ATPase inhibitor; however, the intrinsic ATPase of SecA was not inhibited by sodium azide up to 10 mM. The inhibitory effect of azide against translocation ATPase of SecA and *in vitro* protein translocation are relatively high, with IC_{50} at low mM ranges (Oliver, Cabelli et al. 1990). On the other hand, RB inhibits the translocation ATPase and protein translocation very efficiently, with sub-μM IC_{50} which is several thousand times more effective than azide. The IC_{50} of natural compound from fungi (CJ21058) against translocation ATPase of SecA is 38.7 μM (Sugie, Inagaki et al. 2002). The organic thiouracil-based compounds that we recently found by virtual screening and following optimizing inhibit the intrinsic ATPase of SecA with IC_{50} of 20-60 μM (Li, Huang et al. 2008; Chen, Huang et al. 2010), which may be further optimized. While this manuscript is in preparation, a few inhibitors against the intrinsic ATPase of SecA of *Candidatus Liberibacter asiaticus* with low IC_{50} (around 2-5 μM) have been shown by structure-based screening (Akula, Zheng et al.), but the effects on other forms of ATPase and the protein translocation were not reported. It is worthwhile to mention here that RB and EB are the first inhibitors against all three forms of SecA ATPase with low μM concentration level, and RB inhibits protein translocation at sub-μM range. The inhibitory effects on enzyme activity and bacterial growth may lead to some useful antimicrobial strategies. The fluorescein analogs used in this study are hydroxyxanthenes. Xanthene derivatives are well known and used as additive food

dyes for some time. Although some xanthenes dyes have safety concern, there are still ten of them certifiable as regulated by FDA for food, drug, or cosmetic use (Waite and Yousef 2009). Rose Bengal was reportedly in phase II trials in a study for treatment of metastatic melanoma (Thompson, Hersey et al. 2008; Foote, Burmeister et al. 2010). Erythrosine B (FD&C Red No. 3) is at present the only xanthenes derivative with approval for food use (US 2011). These fluorescein analogs have several advantages as SecA inhibitors: the convenience of commercialized availability, the high solubility in water, the known chemical structure for further modification, and with relatively low or no toxicity for food and drug use.

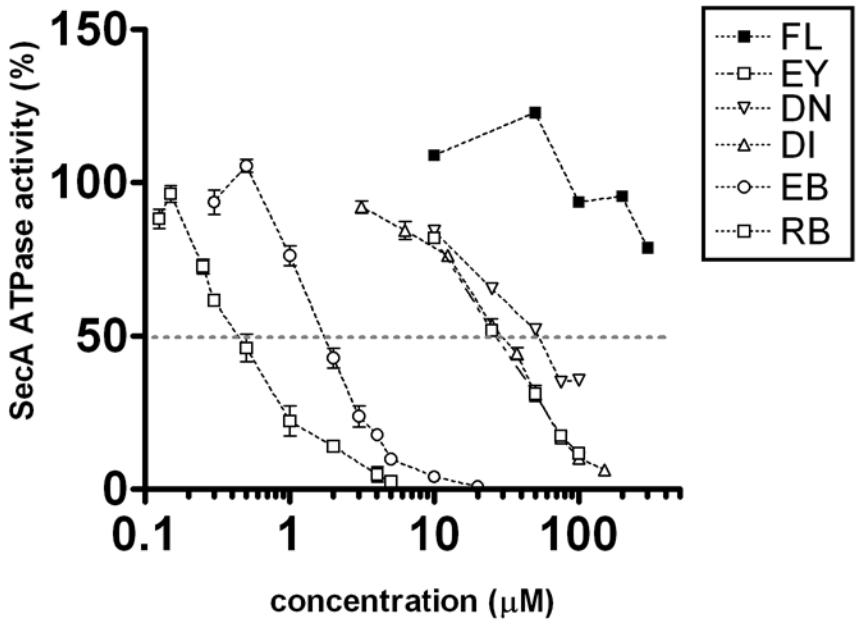

Figure 2.1. The inhibitory effect of fluorescein analogs against ATPase of EcN68. ATPase activity of the catalytic domain of SecA (EcN68) was assayed with different concentrations of fluorescein analogs. The inhibitory effects were illustrated by the percentage (%) of remaining ATPase activity as compared to the controls in the absence of inhibitors.

Table 2.1. Screening of fluorescein analogs

Chemical*	IC_{50}
Rose Bengal (RB)	0.5 μM
Erythrosin B (EB)	2 μM
Diiodofluorescein (DI)	30 μM
Ecosin Y (EY)	25 μM
Dinitrofluorescein (DN)	50 μM
Sodium azide	>10 mM

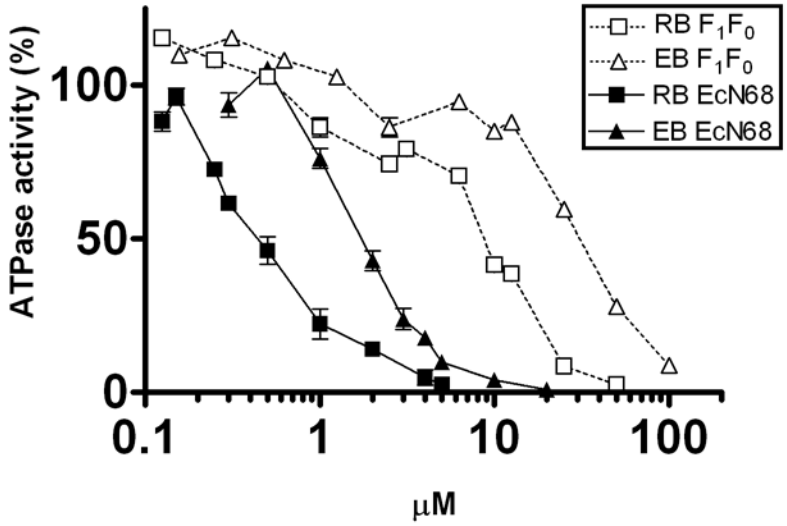

Figure 2.2. The inhibitory effect of RB and EB against different ATPases. ATPase activities of the catalytic domain of SecA (EcN68) and the F_1F_0-proton ATPase were assayed with different concentrations of RB and EB. The inhibitory effects were illustrated by the percentage (%) of remaining ATPase activity as compared to the controls in the absence of inhibitors.

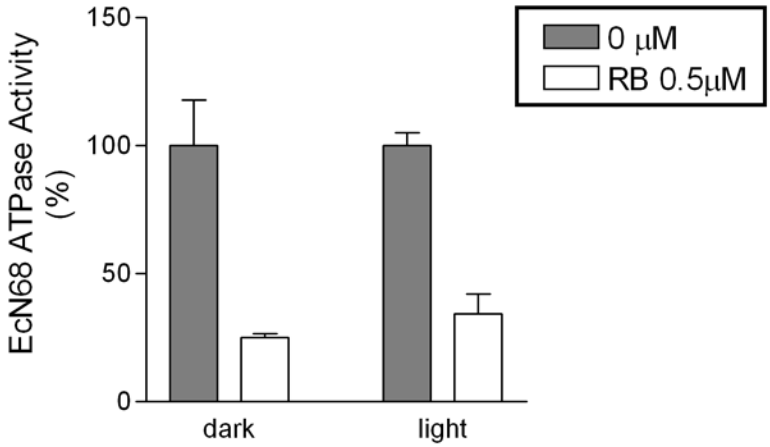

Figure 2.3. The lack of light effect on the inhibitory effect of RB. ATPase activity of EcN68 was assayed with 0.5 μM RB at normal room illumination and in dark condition.

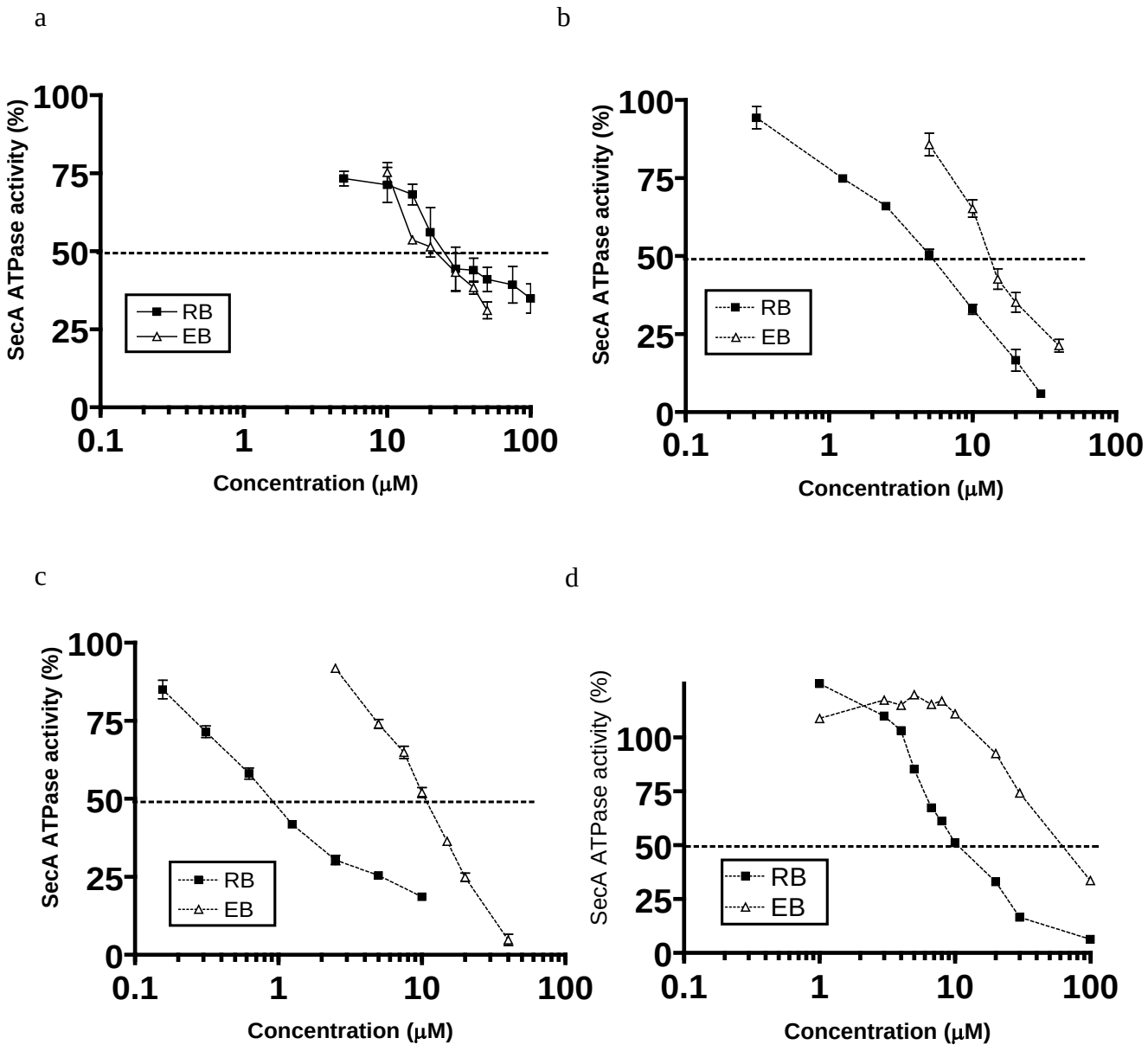

Figure 2.4. The inhibitory effects of RB and EB against different forms of ATPase of EcSecA. (a) intrinsic, (b) membrane, and (c) translocation ATPase; (d) with lipid. The inhibitory effects were illustrated by the percentage (%) of remaining ATPase activity as compared to the controls in the absence of inhibitors. The values of IC_{50} were summarized in Table 2.2.

Table 2.2. IC_{50} of RB and EB against different forms of ATPases of SecA

ATPase \ Inhibitor		RB (μM)	EБ (μM)
Ec	Intrinsic	25	21
	Lipid	10	50
	Membrane	5	12
	Translocation	0.9	10
Bs	Intrinsic	7	70
	Membrane	15	50
	Translocation	22	33

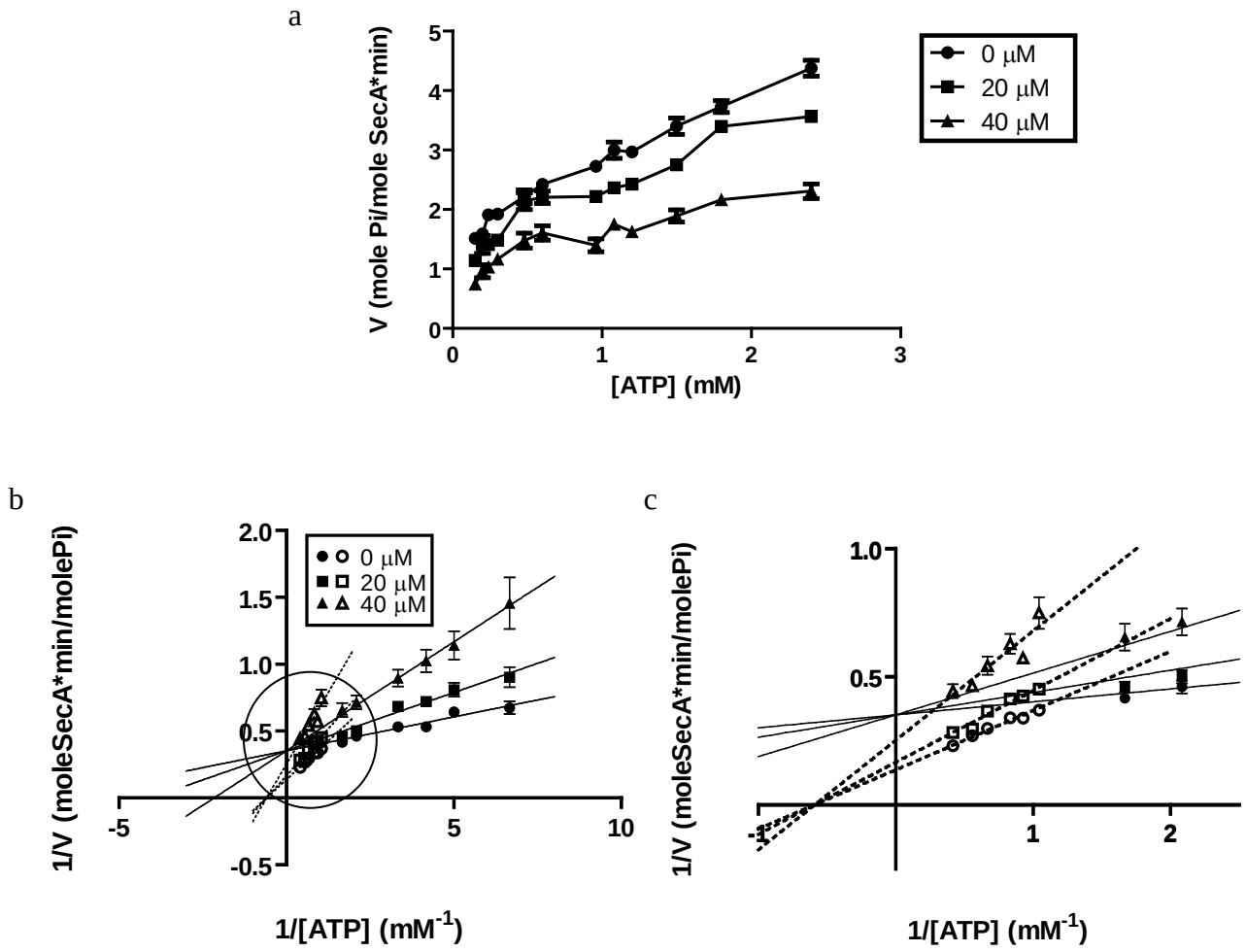

Figure 2.5. Kinetics study of the inhibitory mechanisms of RB against the intrinsic ATPase of EcSecA. (a): Michaelis-Menten plot; (b and c): Lineweaver-Burk plots. The assays were carried out as described in Materials and Methods per 50 µL reaction with 5 µg of EcSecA, in the presence of various concentrations of RB and ATP (0.15-2.4 mM). (b): Competitive inhibition at low ATP concentrations (<0.6 mM, filled symbols), and non-competitive fashion at high ATP concentrations (>1 mM, open symbols) of the intrinsic ATPase by RB; (c): enlarged circle area of (b).

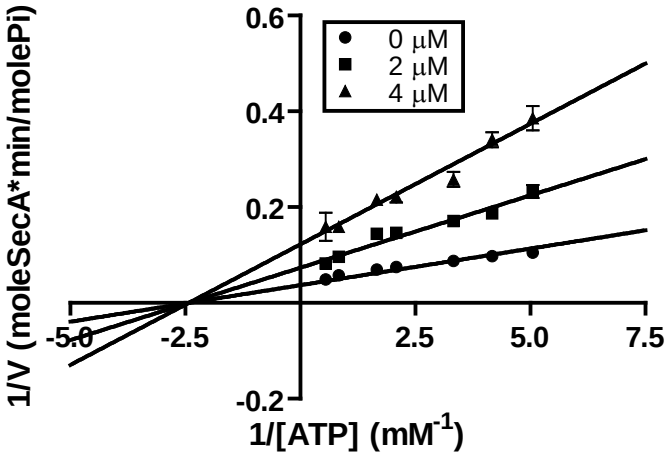

Figure 2.6. Lineweaver-Burk plot of the inhibitory mechanism of RB against the membrane ATPase of EcSecA. The assays were carried out as described in Materials and Methods per 50 µL reaction with 1.5 µg of EcSecA and 3 µg of BA13 membrane, in the presence of various concentrations of RB and ATP (0.198-1.8 mM). RB inhibits the EcSecA membrane ATPase by a mixed-competitive and non-competitive manner.

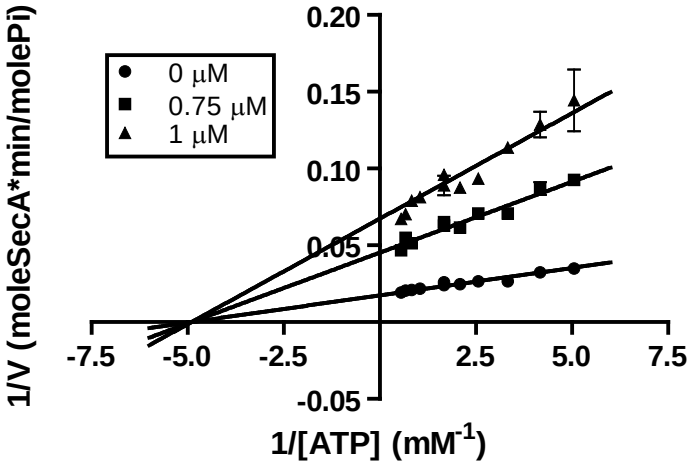

Figure 2.7. Lineweaver-Burk plot of the inhibitory mechanism of RB against the translocation ATPase of EcSecA. The assays were carried out as described in Materials and Methods per 50 µL reaction with 0.5 µg of EcSecA, 1 µg of BA13 membrane, and 1 µg proOmpA, in the presence of various concentrations of RB and ATP (0.198-1.8 mM). RB inhibits SecA translocation ATPase by a non-competitive manner.

Table 2.3. Apparent Michaelis-Menten constants for the three forms of ATPase of EcSecA* in the presence of RB.

			RB concentration		
			0 μM	20 μM	40 μM
intrinsic	High [ATP]	V_{max}†	7.37	6.08	3.99
		K_m (mM)	1.68±0.21	1.68±0.21	1.68±0.21
	Low [ATP]	V_{max}†	3.07±0.16	3.07±0.16	3.07±0.16
		K_m (mM)	0.14	0.25	0.46
			0 μM	2 μM	4 μM
membrane		V_{max}†	26.95	13.61	8.18
		K_m (mM)	0.31±0.03	0.31±0.03	0.31±0.03
			0 μM	0.75 μM	1 μM
translocation		V_{max}†	57.27	23.42	15.06
		K_m (mM)	0.18±0.01	0.18±0.01	0.18±0.01

*Experimental conditions were as Figure 2.5-2.7. The values of K_m and V_{max} were determined by nonlinear regression analysis by Prism 5 (GraphPad Software, La Jolla, CA).

†Unit: molePi·moleSecA^{-1}min^{-1}

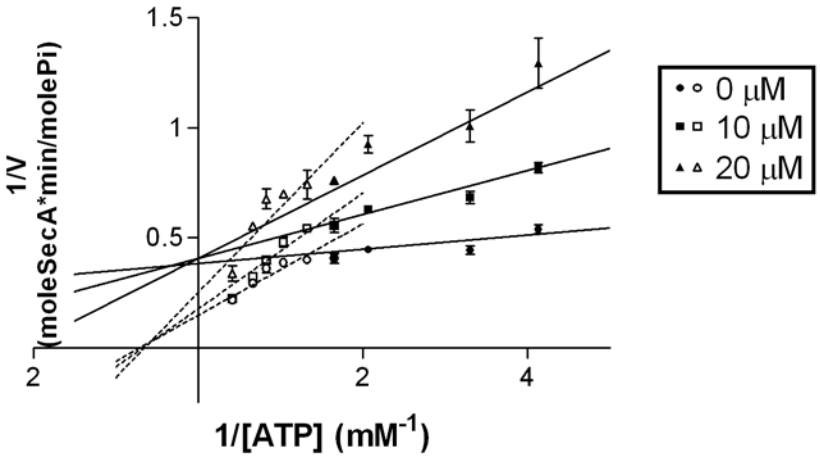

Figure 2.8. Lineweaver-Burk plot of the inhibitory mechanism of EB against the intrinsic ATPase of EcSecA. Competitive inhibition at low ATP concentrations (< 0.6 mM, filled symbols), and non-competitive inhibition at high ATP concentrations (> 1 mM, open symbols) for intrinsic ATPase activity of EcSecA by EB. The assays were carried out as described in Materials and Methods with 5 μg of EcSecA, in the presence of various concentrations of inhibitors and ATP (For clarity, data below 0.24 mM are not shown).

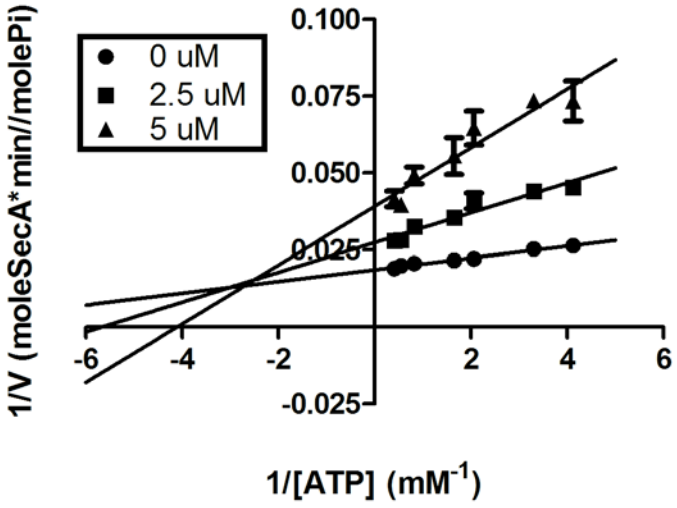

Figure 2.9. The Lineweaver-Burk plot of the inhibitory mechanism of EB against the translocation ATPase of EcSecA. Mixed-mechanism of competitive and non-competitive inhibition in a board range of ATP concentrations for translocation ATPase activity of EcSecA. The assays were carried out as described in Materials and Methods per 50 μL reaction with 0.5 μg of EcSecA, 1 μg of BA13 membrane, and 1 μg proOmpA, in the presence of various concentrations of EB and ATP (0.24-2.42 mM).

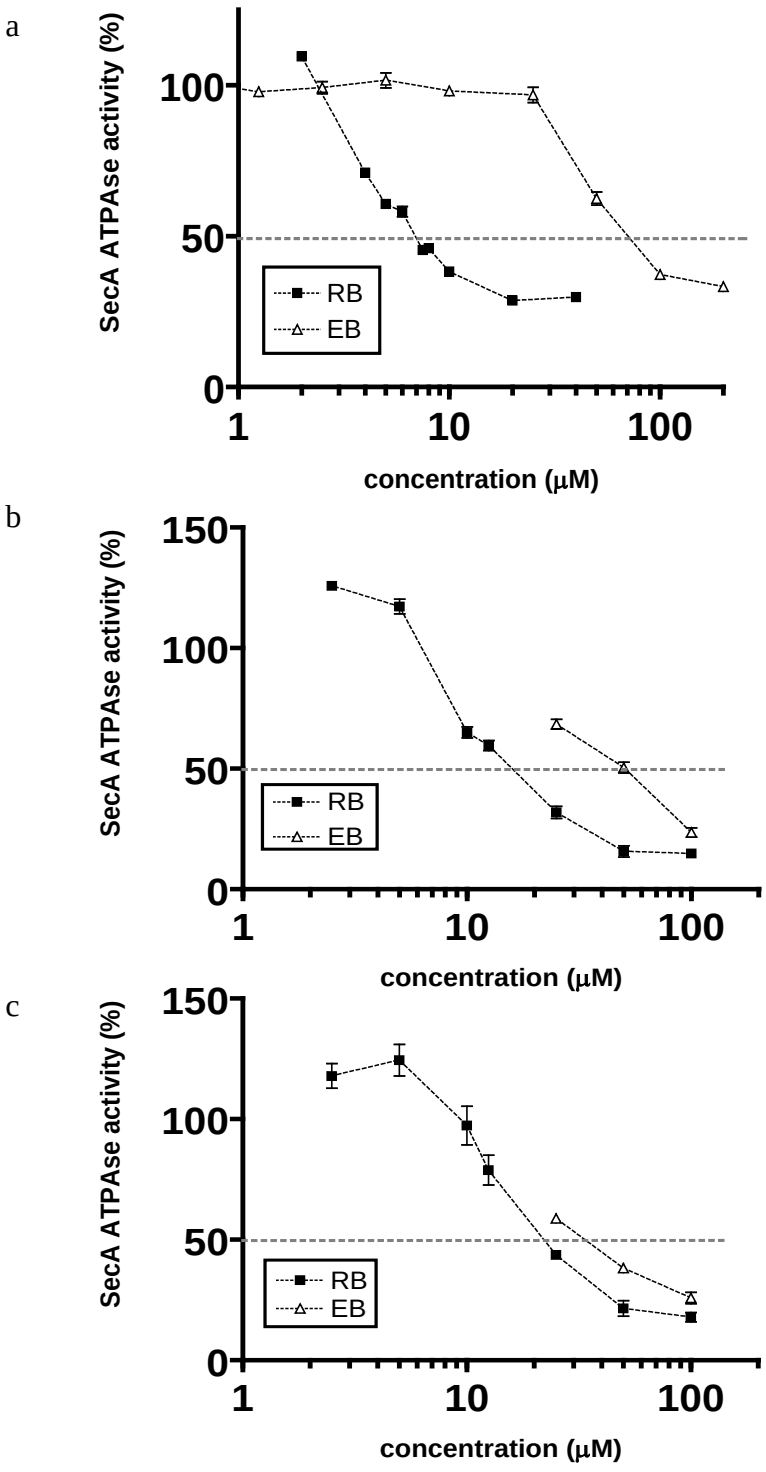

Figure 2.10. The inhibitory effects of RB and EB against three forms of ATPase of BsSecA. (a) intrinsic, (b) membrane, and (c) translocation ATPase. The inhibitory effects were illustrated by the percentage (%) of remaining ATPase activity as compared to the controls in the absence of inhibitors. The values of IC_{50} were summarized in Table 2.2.

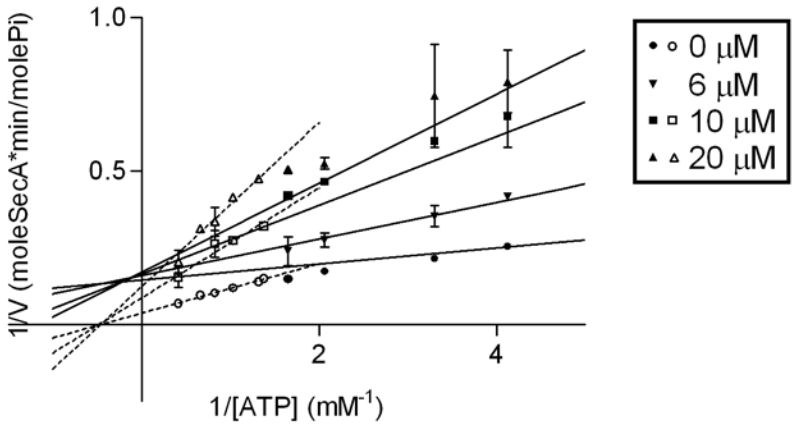

Figure 2.11. Lineweaver-Burk plot of the inhibitory mechanism of RB against the intrinsic ATPase of BsSecA. Competitive inhibition at low ATP concentrations (< 0.6 mM, filled symbols), and non-competitive inhibition at high ATP concentrations (> 1 mM, open symbols) for intrinsic ATPase activity of BsSecA by RB. The assays were carried out as described in Materials and Methods with 3.75 μg of BsSecA, in the presence of various concentrations of inhibitors and ATP (For clarity, data below 0.24 mM are not shown).

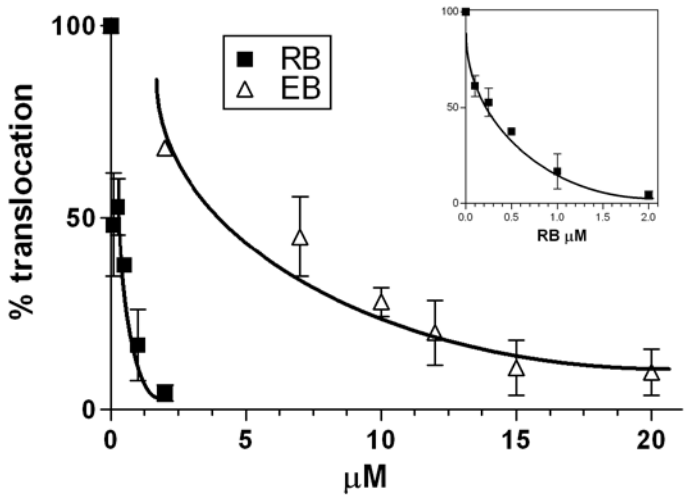

Figure 2.12. The inhibitory effects of RB and EB against the SecA-dependent *in vitro* translocation of proOmpA. The translocation of proOmpA precursors into membrane vesicles was assayed in the presence of RB and EB. The insert is the expanded presentation for RB. The inhibitory effects were illustrated by the percentage (%) of translocated proteins as compared to the controls in the absence of inhibitors. The results were presented as line graphs with standard error of the mean. This work was carried out by H. Wang.

Table 2.4. MIC† of fluorescein analogs on growth of microbes of plate assay

Chemical* \ Bacteria	*E. coli* MC4100	*E. coli* NR698	*B. subtilis* 168
Rose Bengal (RB)	>1 mM	3.1 μM	3.1 μM
Erythrosin B (EB)	>10 mM	250-500 μM	250-500 μM
Diiodofluorescein (DI)	>3 mM	200-500 μM	1 mM
Ecosin Y (EY)	NA	1-2.5 mM	2.5 mM
Dinitrofluorescein (DN)	NA	10-20 mM	10 mM

†Minimal inhibition concentrations (MIC) were determined by the concentration of inhibitors showing a clear zone after overnight incubation as compared to the surrounding area.

*Fluorescein analogs were applied to the bacteria cells as described in Material and Methods.

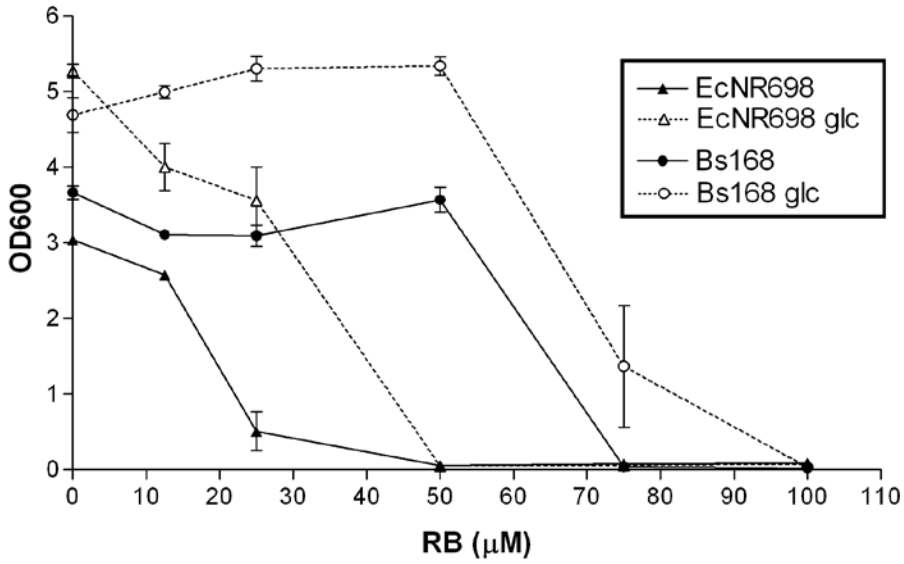

Figure 2.13. The bacteriostatic effect of RB against Gram-negative and Gram-positive bacteria in liquid culture. Cells of exponential phase of permeability leaky mutant *E. coli* NR698 and *B. subtilis* 168 were treated with RB with and without 0.2% glucose in the media. The bacteriostatic activities are illustrated by the decrease of OD600 after 14 hour growth with various concentrations of inhibitors.

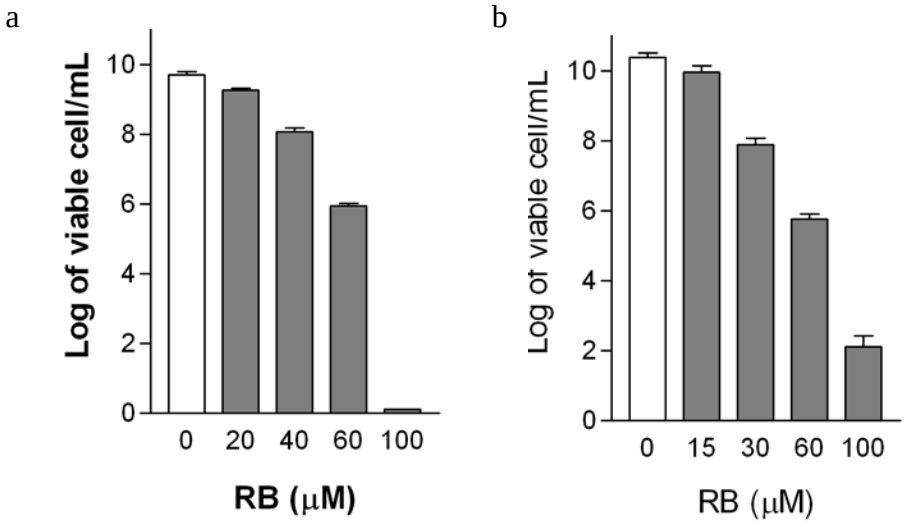

Figure 2.14. The bactericidal effect of RB on Gram-positive and Gram-negative bacteria. The bactericidal activities are illustrated by the number of survived cells as CFU after one hour treatment with various concentrations of inhibitors (gray bar) as compared to the controls (white bar) in the absence of inhibitors. (a) Permeability leaky mutant *E. coli* NR698; (b) *B. subtilis* 168.

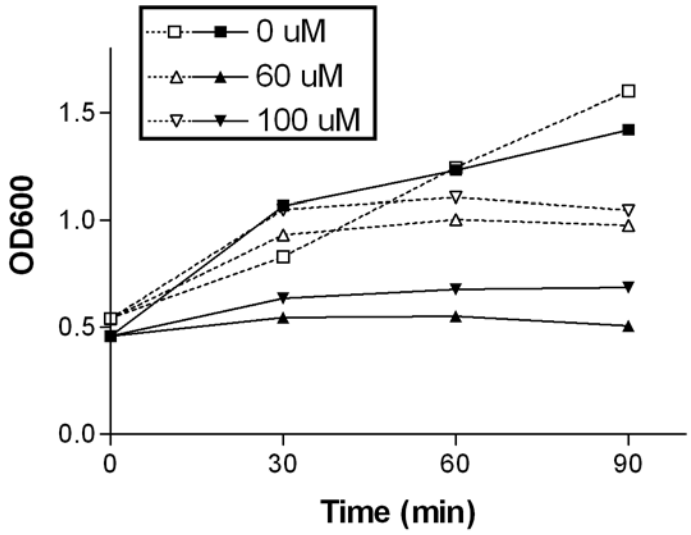

Figure 2.15. Cell density of Gram-positive and Gram-negative bacteria during RB treatment. Bacterial cells were treated with RB as the same condition as Figure 2.13 and the cell density was monitored in time course up to 30 min after the standard bactericidal assay. Open symbol: permeability leaky mutant *E. coli* NR698; closed symbol: *B. subtilis* 168.

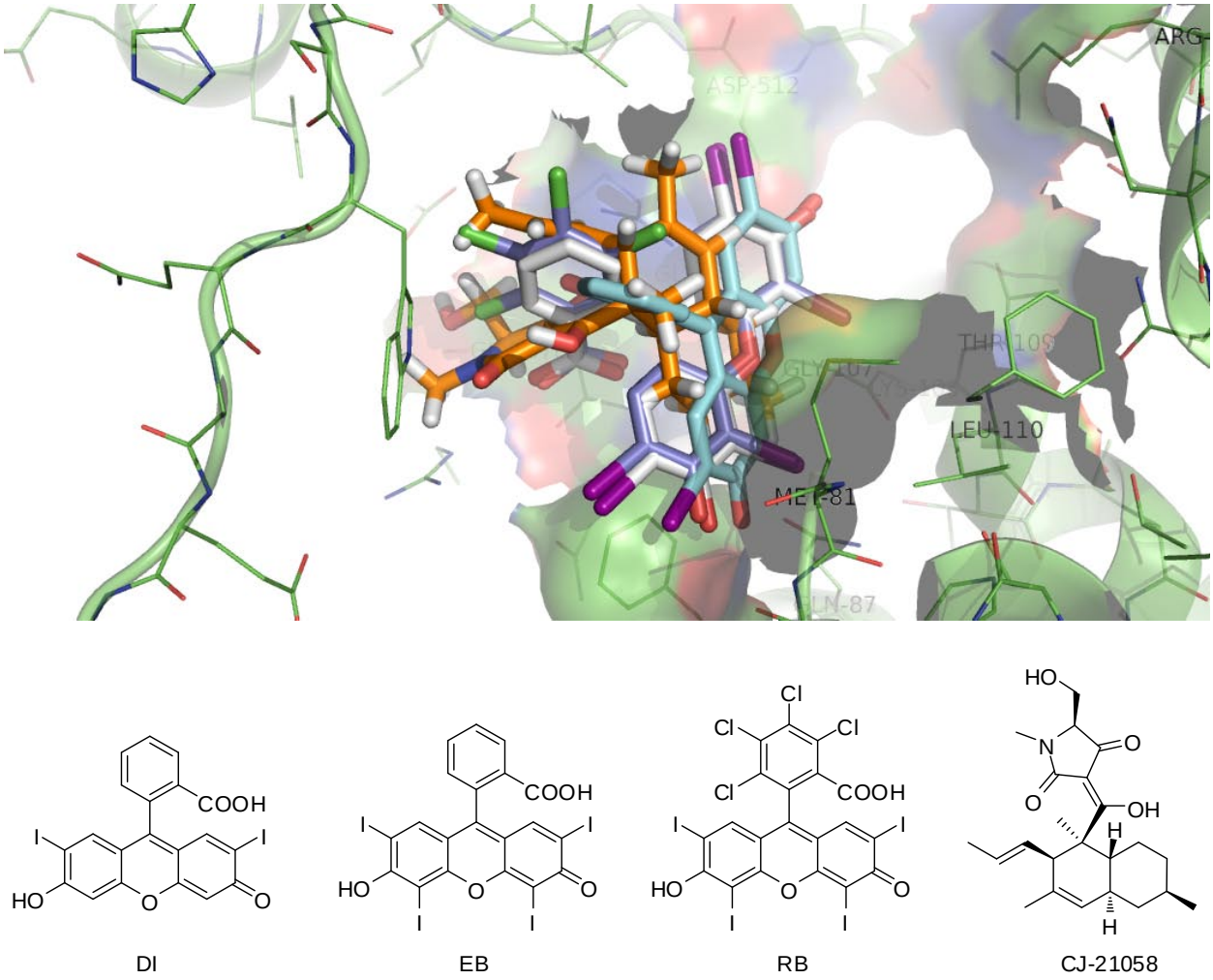

Figure 2.16. The chemical structures and docking conformations of DI (light blue), EB (grey), RB (heavy blue) and CJ-21058 (orange) around EcSecA ATP-site. This figure is provided by M. Li.

3 The structural and functional analysis of the C-terminal regulatory domain of EcSecA

3.1 Abstract

SecA plays an essential role in the Sec-dependent protein translocation in *Escherichia coli*. Molecular modeling and experimental results indicate that the interaction among the three α-helixes in HSD of the C-terminal regulatory domain may be important for its structure and function. A series of SecA truncates in the region of the first long α-helix (a.a. 621-668) of the helix-bundle was analyzed. None of these SecA derivatives can complement the SecA temperature-sensitive mutant *in vivo*. All of the N-fragments of SecA with various length of the α-helix show the response to lipids and slightly differ in the regulated intrinsic ATPase activities, suggesting that different elements are responsible for lipid stimulation and down-regulation. Moreover, N-fragments with half and longer α-helix form pore structures with liposomes as observed in AFM, indicating this region is critical for the structural role of SecA as part of the protein-conducting channels. Phe586 in the intramolecular regulator region was illustrated for important function. NBDII mutants of N68 and full-length SecA differ in the response to the ATPase inhibitor. C-terminal truncated SecA derivatives increase the resistance to inhibitors with the extension of the long α-helix. Thus, this part of C-regulatory domain may interfere with the approach of the inhibitor. These results demonstrate that the first long α-helix of HSD plays an important role in the structure and regulation of SecA ATPase.

3.2 Introduction

SecA plays the central role in the Sec-dependent protein translocation system; it is the most abundant component of the Sec system in the cell (Driessen 1994). It interacts with almost all the other components (Hartl, Lecker et al. 1990; Hendrick and Wickner

1991; Kimura, Akita et al. 1991; Snyders, Ramamurthy et al. 1997), indicating its importance for the protein translocation system in bacteria.

SecA consists of two separable domains, the N-terminal 68 kDa fragment (N68) and the C-terminal 34 kDa regulatory domain (C34). N68 holds high ATPase activity that is down-regulated by C34 (Karamanou, Vrontou et al. 1999). There are two nucleotide binding domains (NBDs) identified in SecA, NBDI and NBDII. NBDI, which is located in the N68 catalytic domain, contains the conserved Walker A and B motifs and is responsible for high affinity binding and hydrolysis of ATP (Mitchell and Oliver 1993; Sianidis, Karamanou et al. 2001). NBDII comprises a consensus sequence of Walker A and a putative Walker B motif (Mitchell and Oliver 1993). There is no experimental demonstration of nucleotide binding to NBDII. Instead, NBDII binds to NBDI and plays the role as intramolecular regulator of the hydrolysis of ATP (IRA2) (Sianidis, Karamanou et al. 2001). The predicted Walker B is outside of the N68 domain and located in a long α-helix (Figure 3.1). This α-helix is the first of the bundle of three α-helixes of the α-helical scaffold domain (HSD) in the C34 (Hunt, Weinkauf et al. 2002). Our preliminary genetic and biochemical data suggest that the interactions among the three α-helixes may be important for the function of SecA. The hydrophobic amino acid residue of the third α-helix of HSD (amino acid 810-829) is important for the minimal length of SecA (Na and Tai, unpublished data). In order to further identify the role of the first α-helix of HSD (amino acid 621-668), a series of C-terminal truncated SecA constructs of this region were made (Figure 3.1). This work provides more detailed structural analysis of SecA for understanding the mechanism of the Sec-dependent protein translocation across bacterial membranes.

3.3 Material and methods

Bacterial strains, medium, chemicals, and liposomes. *E. coli* DH5α was used for DNA cloning and plasmid isolation. *E. coli* BL21(λDE3) (Studier and Moffatt 1986) was used for overproduction of various truncated SecA proteins. SecA temperature-sensitive mutant *E. coli* BL21.19 (Mitchell and Oliver 1993) was used for the complementation assay. Luria-Bertani (LB) and TAG (1% (w/v) tryptone, 0.5% (w/v) NaCl, 40 mM potassium phosphate buffer (pH7.0), 7.6 mM ammonium sulfate, 1.6 mM sodium citrate, and 1% (w/v) glucose) liquid and solid (1.5% agar) media were used for bacterial growth. Chemicals were purchased from Sigma-Aldrich Corp (St. Louis, MO) and Fisher Scientific (Pittsburg, PA) unless indicated otherwise. *E. coli* total lipid extract was from Avanti Polar Lipids Inc. (Alabaster, Alabama). Liposomes were prepared by sonication (Sonic Dismembrator Model 500; Fisher Scientific, Pittsburgh, PA) from *E. coli* total lipid extract resuspended in TK buffer (10 mM Tris-HCl, pH7.6, and 50 mM KCl, for ATPase assay) or TKM buffer (TK with 2 mM $MgCl_2$, for AFM) as described previously (Wang, Chen et al. 2003). The size and quality of liposomes were determined by Submicron Particle Size Analyzer N5 (Beckman Coulter, Miami, FL).

Cloning, complementation test, and protein purification. To construct the C-terminal truncated SecA derivatives (Figure 3.2), DNA fragments were amplified by PCR (Mastercycler gradient; Eppendorf, Hauppauge, NY) with 5' primer (TATACATATGCTAATCAAATTGTTAACT) and 3' primers listed in Table 3.1 using pET5a-SecA as the template. The amplified DNA fragments encoding SecA with desired C-terminal ends were cloned to pET5a through *Nde*I and *Bam*HI. For N68R509K without N-terminal His-tag, pR509K (Mitchell and Oliver 1993) was used as the template to yield

N68R509K/pET5a. Plasmids carrying SecA derivatives were transformed into SecA temperature sensitive mutant BL21.19 for complementation test. Bacterial cells were streaked on LB/Amp plate and incubated at 42°C for overnight growth. A duplicate control plate was incubated at 30°C. SecA derivatives were over-expressed from plasmids constructed as listed in Table 3.1, pT7-SecA (Schmidt and Oliver 1989) (for full-length SecA), pIMBB28 (Karamanou, Vrontou et al. 1999) (for His-N68), pIMBB69 (Karamanou, Vrontou et al. 1999) (for His-N68R509K), and pR509K (Mitchell and Oliver 1993) (for SecAR509K), pN68R509K/pET5a (for N68R509K) in *E. coli* BL21(λDE3) and purified as previously described (Chen, Xu et al. 1996; Chen, Brown et al. 1998).

***In vitro* ATPase activity assay.** ATPase activity assays were performed as described (Lill, Dowhan et al. 1990) with minor modifications. For intrinsic, lipid, and membrane ATPase assay, 50 µL reaction mixture contained 3 µg of SecA derivatives (unless specified otherwise), 20 µg ovalbumin, 1.2 mM ATP, 50 mM Tris-HCl (pH7.6), 20 mM KCl, 20 mM NH_4Cl, 2 mM $Mg(OAc)_2$, 1 mM DTT, and 6 µg liposomes (for lipid ATPase) or 6 µg urea-washed *E. coli* BA13 membrane (for membrane ATPase). For translocation ATPase assay, reaction mixtures contained 1 µg proOmpA in addition to membranes. All reactions were done at 40°C or 30°C for an appropriate time. The ATPase activity was determined by the release of inorganic phosphate detected by the photometric method (Lanzetta, Alvarez et al. 1979) and the absorption at 660 nm was measured (SmartSpec Plus, Bio-Rad Laboratories, Inc.). The inhibitory effects were illustrated by the percentage (%) of remaining ATPase activity as compared to the controls in the

absence of potential inhibitors. All assays were performed at least in triplicate, and the results were presented as line graphs with a standard error of the mean.

Atomic force microscopy (AFM). AFM slides were prepared as previously described (Wang, Chen et al. 2003) with minor modifications. Briefly, the proper amount of SecA derivatives (2-5 μg) and liposomes (20 μg) in 10 μL TKM buffer were mixed by vortex and incubated on ice for 30 min. The mixtures were applied to freshly cleaved mica and then were held at room temperature for 15 min, rinsed three times with deionized water, and dried in a dessicator over night. AFM images were obtained with di Multi-Mode V (Veeco Instrument Inc., Woodburry, NY) by using the tapping mode and analyzed by image-processing software (Nanoscope v700) according to the manufacturer's manual. The size of the objectives was estimated by using gold particles as the standards.

3.4 Results and discussion

Lipids stimulated the ATPase activities of N-fragments of SecA. In the process of preparing the various HSD C-terminal truncated SecA fragments, we found that the over-expressed proteins with uncharged or hydrophobic amino acids at the C-terminus tend to form inclusion bodies. Most renatured proteins (except N75, which has the completed long α-helix) from 6M urea retained very low ATPase activities. Molecular modeling based on the crystal structure of *E. coli* SecA (Papanikolau, Papadovasilaki et al. 2007) suggests the hydrophobic interactions among the three α-helixes in the HSD are important for the function (Na and Tai, unpublished data). The hydrophobic amino acid at the C-terminus may destabilize the structure of the partial long α-helix of the fragments. These data indicate that the long α-helix is important for the conformation and

ATPase activity of the N-fragments of SecA. Charged amino acids were chosen from the neighboring region or introduced by PCR to obtain soluble and active SecA fragments (Figure 3.2). All N-fragments of SecA in this region (N68-N75) showed the stimulation effect by lipids (Figure 3.3). The intrinsic ATPase activity slightly decreased when the α-helix was extended (Figure 3.4a). Thus, the region between N68 and N75 confers domains in response to lipids and down-regulation elements. Since the lipid-stimulation effect appears in the shorter N-fragments (N68-N70) before the down-regulation occurs (N71.5D and longer N-fragments), the elements for these two events should locate differently. The ATPase activities of N-fragments (N68-N75) are significantly stimulated by lipids (2.5 to 4 fold) and membranes (milder effect, around 2 fold), but not by proOmA. In contrast, full-length SecA is obviously stimulated by lipids (3.6 fold), membranes (4.8 fold), and proOmA (up to 16 fold) (Figure 3.4b). These results suggest the long α-helix (a.a. 621-668) can "sense" and interact with lipids. Elements located in this region may be involved in the interaction with membrane proteins to cause the different responses to lipids and membranes. These N-fragments with a partial or whole α-helix possess high intrinsic ATPase activities since they do not contain the entire C-terminal regulatory domain; therefore, precursor proOmA does not further activate the ATPase activity.

His-tag changed the biochemical characteristics of N-terminal catalytic domain of SecA. Lipids can stimulate the ATPase of N68 significantly (up to 3 fold, Figure 3.3). This data is in controversy to a previous study that found N68 possess high basal ATPase activity equivalent to the fully activated translocation ATPase of SecA (Karamanou, Sianidis et al. 2005). Therefore, His-N68 from the same study was analyzed for comparison. As expected from the literature, lipids did not further stimulate the AT-

Pase activity of His-N68 (Figure 3.4). Besides, His-N68 and N68 showed different thermo-stabilities. His-N68 and N68 have similar activity at 30°C, but N68 has only about 50% activity of His-N68 at 40°C (Figure 3.3). The positive-charged His-tag may influence the neighboring structure, and the change of the β-sheet structure of the N-terminus of SecA affects the behavior in response to lipids (Floyd and Tai, unpublished data) and the biochemical function (Das, Stivison et al. 2008) (Floyd and Tai, unpublished data). The result indicates that His-tag may stabilize or change the conformation of N68, causing different responses to lipids and temperature change. The N-terminal fragments were constructed without His-tag in this study; therefore, the possible influence of His-tag could be excluded.

N-fragments of SecA formed ring-like structures induced by phospholipids. Ring-like structures of EcSecA and the tandem dimer EcSecAA upon interacting with phospholipids have been shown previously by AFM (Wang, Chen et al. 2003; Wang, Na et al. 2008). The lipid-specific domains, N39 and M48, also form a partial ring structure in the presence of phospholipids (Floyd and Tai, unpublished data). The N-fragments (N68-N75) contain the major part of M48. The ATPase activities of N68-N75 are greatly stimulated by lipids, indicating the drastic conformational changes induced by lipids. Therefore, the structures of these N-fragments in lipids were examined by the same approach. N71.5D ($SecA_{1\text{-}F639D}$) and larger fragments formed ring-like structures with shapes and depths that appear to be similar to full-length EcSecA (Figure 3.5). N-fragments without or with up to half of the long α-helix, N68-N71 ($SecA_{1\text{-}609}$ to $SecA_{1\text{-}632}$), did not form ring-like structures (Figure 3.5), even though the ATPase was also significantly activated by lipids. Thus, although the N-terminal part of the long α-helix can

interact with the lipids for stimulated ATPase, some elements located in the C-terminal half of the α-helix are required for composing the protein conducting channel.

N-fragments of SecA ($SecA_{1-609}$ to $SecA_{1-668}$) did not complement SecA mutant. The complementation ability of SecA fragments with truncated C-terminus was determined. None of the N-fragments in this region (N68-N75) could complement *E. coli* BL21.19 at the non-permissive temperature. The inability of complementation is consistent with our observation of the minimal length of functional SecA (Na and Tai, unpublished data) and a previous report of N-terminal truncate (SecA-N664) with similar length (Dapic and Oliver 2000). SecA-N664 does not have robust translocation ATPase activity and shows deficiency in protein translocation activity, which causes the failure of complementation in the same study. N68-N75 similarly possess low (uninducible) translocation ATPase; therefore, the defect of complementation may result in the insufficient protein secretion. Thus, although the long α-helix plays some critical roles, such as the interaction with lipids and membrane proteins, these N-fragments of SecA do not possess full physiological function.

Lipids did not stimulate the ATPase activity of N69F586L. In the process of PCR, a random mutagenesis happened and resulted in N69F586L, in which the 586^{th} amino acid residue phenylalanine was replaced by leucine. This mutation reduced the basal ATPase activity of N69 and abolished the stimulation effect of lipids (Figure 3.6). Phe586 is part of the conserved sequence of motif XI in the region of IRA2 (Sianidis, Karamanou et al. 2001). N69F586L and N69WT showed similar activities at 40°C, but the mutant only possesses less than 50% of activity as wild-type at 30°C (Figure 3.6).

Some IRA2 mutations that down-regulate the NBDI ATPase have been reported, and the inference is more severe at lower temperature (Sianidis, Karamanou et al. 2001). Interestingly, both N68R577K (Sianidis, Karamanou et al. 2001) and N69F586L are single point mutations in motif XI of IRA2 but have striking effects in response to lipids/membrane and/or preprotein. In these two mutants, the original amino acid residues are replaced by amino acids with similar characteristics; however, replacement still causes compromised function. Here we show another unassailable amino acid residue (Phe586) in IRA2 which is important for its function.

ATPase inhibitor showed different inhibitory effects on NBDII mutant of SecA. Previous studies suggest that the NBDII is a low-affinity ATP binding site and not essential for ATP hydrolysis since the NBDII mutant SecAR509K still keeps the high-affinity-ATP binding and basal ATPase activity. However, this mutant loses the response to the stimulatory effects of membranes and preproteins (Mitchell and Oliver 1993; Sianidis, Karamanou et al. 2001). The high catalytic ATPase activity of N68 is significantly reduced in the mutant N68R509K (Karamanou, Vrontou et al. 1999). These phenomena indicate the regulatory role of NBDII on hydrolysis of ATP. We recently found a fluorescence dye, Rose Bengal (RB) that may interfere with the two NBDs of SecA differently (Chapter 2, submitted for publication). Here, the SecA ATPase inhibitor, RB, is used as a probe for the mechanistic insight and structural understanding of the different NBDs. The inhibitory effects of RB on wild-type SecA and NBDII mutant (R509K) were determined. SecAR509K was slightly more sensitive to RB than the wild-type SecA, with IC_{50} about 20 μM and 30 μM, respectively (Figure 3.7a). The catalytic ATPase activity of

N68 was much more sensitive (IC_{50}= 0.75 μM) to RB than the full-length SecA (compare Figure 3.7a and 3.7b). Surprisingly, N68R509K showed high resistance to RB without significant inhibition up to 50 μM (Figure 3.7b). Wild-type and R509K mutant of N68 with His-tag were analyzed as well. Again, the ATPase activity of His-N68R509K was not significantly repressed by RB up to 50 μM, while wild-type His-N68 was very sensitive (IC_{50}= 0.5 μM, Figure 3.7c). His-tag does not influence their sensitivity to RB since N68 and His-N68 have similar values of IC_{50}. This result eliminates the possibility that the resistance is caused by the N-terminal His-tag. Molecular modeling suggests that Arg509 can interact with RB by forming a salt bridge, while the replacement Lys cannot. One possible explanation is that the C34 regulatory domain may interact with NBDII and suppress the primary effect of the inhibitor RB on NBDII.

N-fragments of SecA showed various sensitivities to ATPase inhibitor. Since NBDII mutant in Walker A motif (R509K) and wild-type SecA differ in response to inhibitor RB, we determined the inhibition of RB to the series of SecA fragments with various lengths of the predicted Walker B sequence of NBDII. Even though they have similar values of IC_{50}, the SecA fragments became more resistant to higher concentrations of RB while the α-helix extended, and the full-length SecA showed the highest resistance (Figure 3.8). This phenomenon suggests that the presence of the C-domain may mask the access of RB as a structural barrier. We have found that the sensitivity to RB of SecA is related to its conformation. Among the three forms of SecA ATPases, the translocation ATPase (in the presence of membrane and precursor proteins, the most open state of SecA) is the most sensitive to RB, while the intrinsic ATPase (closed state) is the least sen-

sitive (Chapter 2, Figure 2.4). Together with the increasing resistance with the extension of the C-regulatory domain, it shows the relationship of the structure and function of SecA.

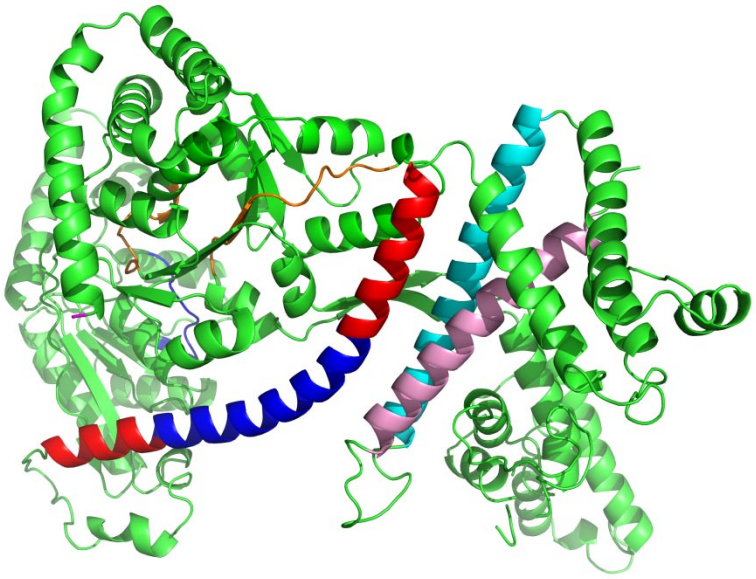

Figure 3.1. The structure of EcSecA. Some functional domains are labeled with colors: orange: NBDI: A_1(102-109), B_1(198-210); dark blue: NBDII: A_2(503-511), B_2(631-653); α-helical scaffold domain (HSD): red (621-668), light blue (756-788), pink (802-829).

```
                610        620        630        640        650        660        670        680
           ....|....|....|....|....|....|....|....|....|....|....|....|....|....|....|....|
EcSecA     DRVSGMMRKLGMKPGEAIEHPWVTKAIANAQRKVESRNFDIRKQLLEYDDVANDQRRAIYSQRNELLDVSDVSETINSIR
N68        DRVSGMMRK-------------------------------------------------------------------------
N69        DRVSGMMRKLGMKPGEAIE----------------------------------------------------------------
N70D       DRVSGMMRKLGMKPGEAIEHPWVTKAIAD------------------------------------------------------
N71        DRVSGMMRKLGMKPGEAIEHPWVTKAIANAQR---------------------------------------------------
N71.5D     DRVSGMMRKLGMKPGEAIEHPWVTKAIANAQRKVESRND--------------------------------------------
N71.6      DRVSGMMRKLGMKPGEAIEHPWVTKAIANAQRKVESRNFD-------------------------------------------
N72        DRVSGMMRKLGMKPGEAIEHPWVTKAIANAQRKVESRNFDIRK----------------------------------------
N73        DRVSGMMRKLGMKPGEAIEHPWVTKAIANAQRKVESRNFDIRKQLLEYD----------------------------------
N74R       DRVSGMMRKLGMKPGEAIEHPWVTKAIANAQRKVESRNFDIRKQLLEYDDVANDQRR-------------------------
N75        DRVSGMMRKLGMKPGEAIEHPWVTKAIANAQRKVESRNFDIRKQLLEYDDVANDQRRAIYSQRNELLD-------------
```

Figure 3.2. Sequence of the C-terminal truncated SecA fragments

Table 3.1. 3'primers used for construction of C-terminal truncated SecA fragments

N75	$SecA_{1-668}$	CGCTGGATCCTTATTAATCCAACAGTTCGT
N74	$SecA_{1-657}$	GCTGGGATCCTTATTAGCGACGCTGATCGT
N73	$SecA_{1-649}$	GATCGGATCCTTATTAATCATATTCCAGCA
N72	$SecA_{1-643}$	CCAGGGATCCTTATTACTTACGAATGTCGA
N71.6	$SecA_{1-640}$	GCAGGGATCCTTATTAGTCGAAGTTACGGC
N71.5D	$SecA_{1-639}$F639D*	GTTGGGATCCTTATTA***GTC***GTTACGGCTTTCAACTTTACG
N71	$SecA_{1-632}$	AGTTGGATCCTTATTATTTACGCTGGGCGT
N70D	$SecA_{1-629}$ N629D*	CAACGGATCCTTATTA***GTC***GGCAATCGCTTTAGTCACCCA
N69	$SecA_{1-619}$	TAGTGGATCCTTATTATTCAATGGCTTCGC
N68	$SecA_{1-609}$	CTGGGGATCCTTATTATTTACGCATCATGC
N68R509K	$SecA_{1-609}$R509K	CTGGGGATCCTTATTATTTACGCATCATGC

* Charged amino acid residues were introduced by the bold and italic sequence of primers

a

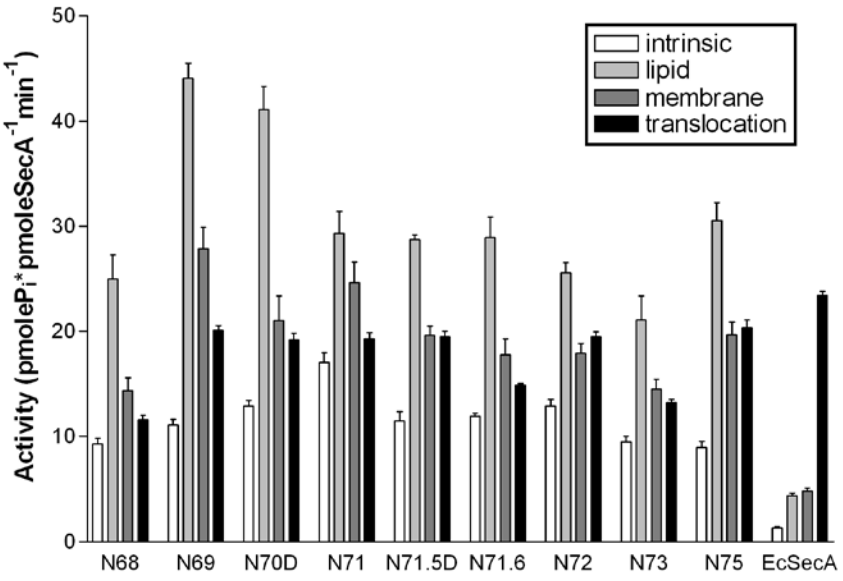

b

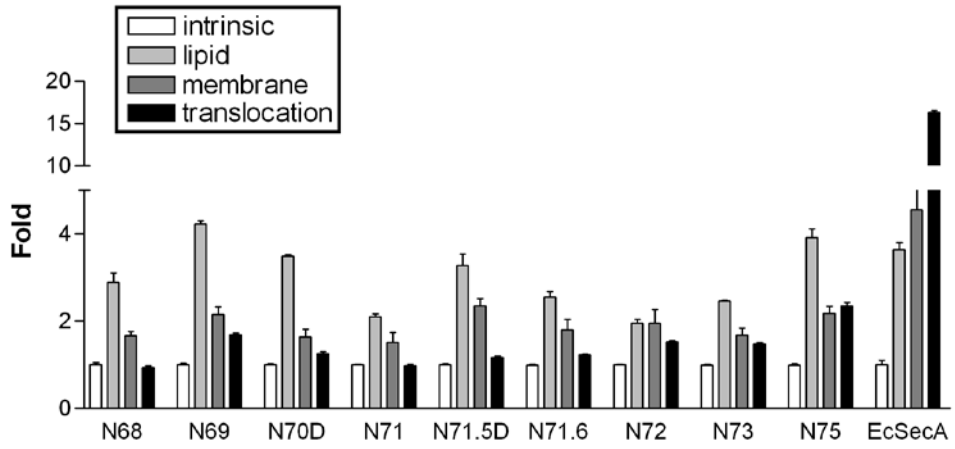

Figure 3.3. Different forms of ATPase of N-fragments of EcSecA. (a): specific activity; (b): stimulation effect illustrated in folds. The assays were carried out as described in Materials and Methods per 50 µL reaction with 3 µg of proteins at 30°C.

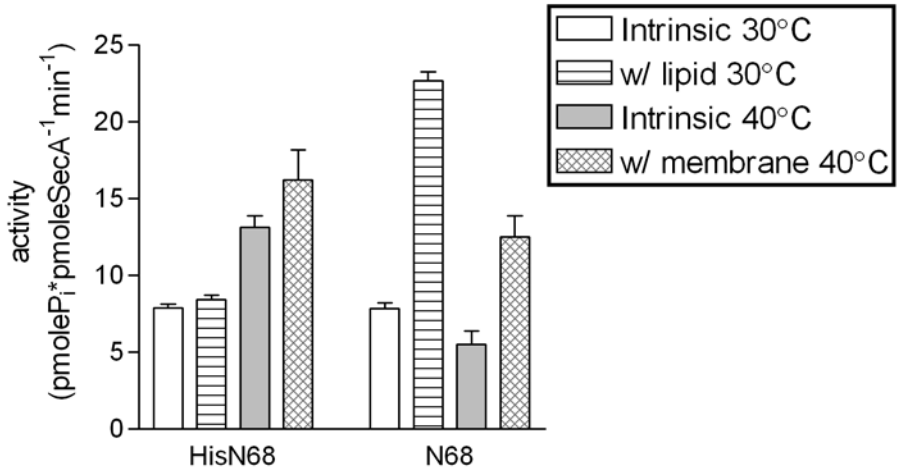

Figure 3.4. Lipid stimulation effect and thermo-stability of HisN68 and N68. The assays were carried out as described in Materials and Methods per 50 µL reaction with 3 µg of protein in the absence or presence of 6 µg of lipids or BA13 membrane.

Fragment	N68	N69	N70D	N71	N71.5D
AFM image	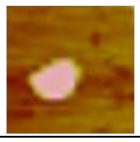	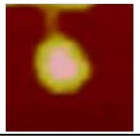	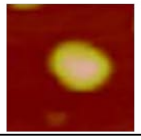	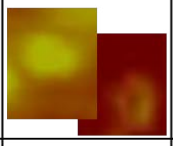	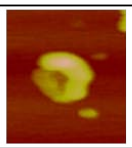
width (nm)				11.2±1.7 (n=23)	11.2±2.3 (n=100)
Fragment	N71.6	N72	N73	N75	EcSecA
AFM image	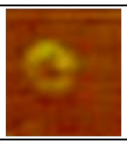	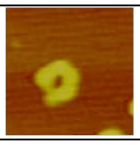		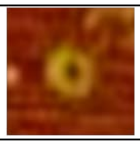	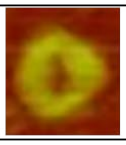
width (nm)	10.54±1.9 (n=100)	11.2±2.6 (n=100)	10.6±2.5 (n=100)	11.7±2.4 (n=100)	16.7±4.3 (n=100)

Figure 3.5. Ring-like pore structures of N-fragments of SecA observed by AFM.

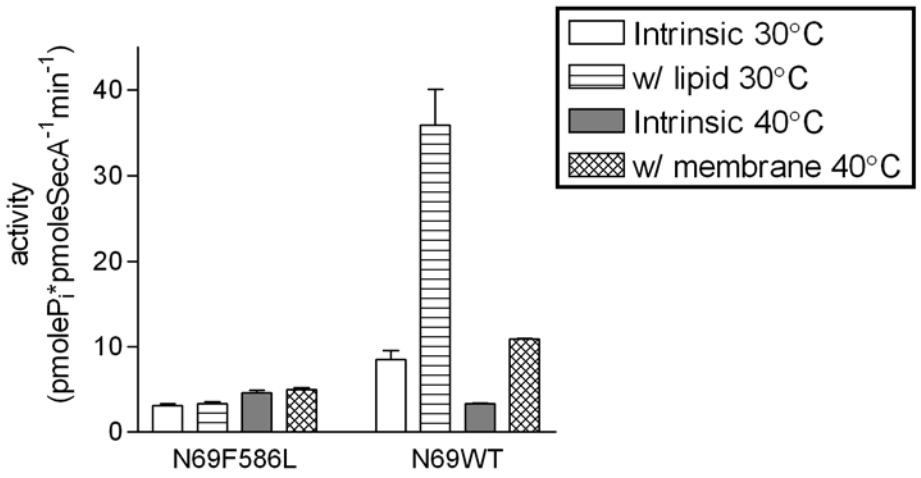

Figure 3.6. Lipid stimulation effect of IRA2 mutant N69F586L. The assays were carried out as described in Materials and Methods per 50 µL reaction with 3 µg of protein in the absence or presence of 6 µg of lipids or BA13 membrane.

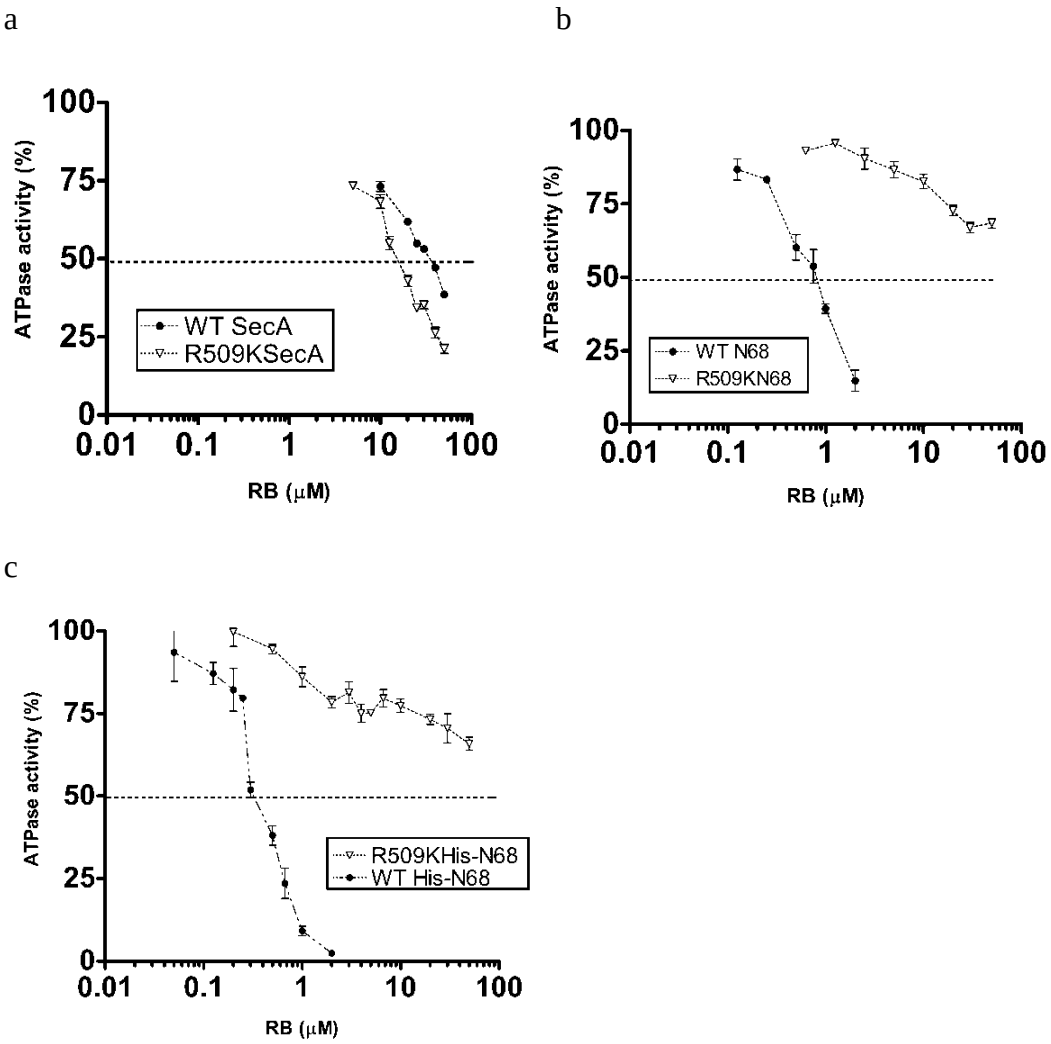

Figure 3.7. The inhibitory effect of RB against MBDII mutant R509K variants of SecA. The assays were carried out as described in Materials and Methods per 50 µL reaction with 1.5 µg of SecA derivatives (a) SecA, (b) N68, and (c) His-N68 at 40°C (a and c) or 30°C (b). The inhibitory effects were illustrated by the percentage (%) of remaining ATPase activity as compared to the controls in the absence of inhibitors.

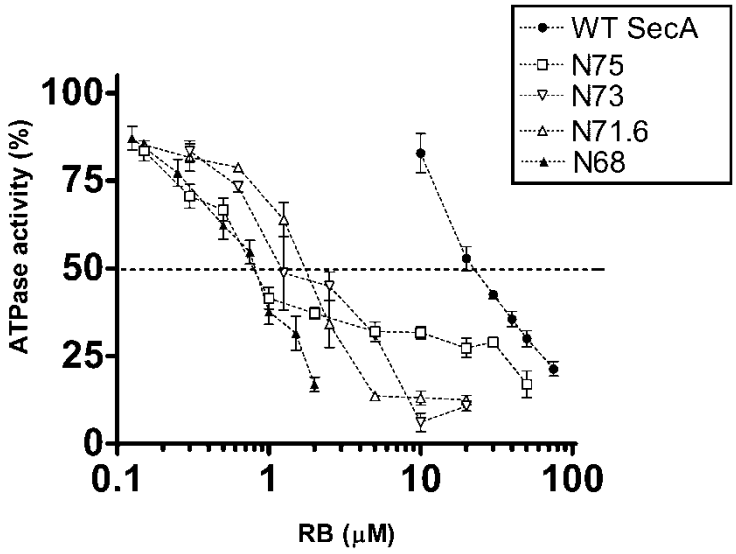

Figure 3.8. The inhibitory effect of RB against SecA variants with different lengths of C-domain. The assays were carried out as described in Materials and Methods per 50 µL reaction with 1.5 µg of SecA derivatives at 30°C. The inhibitory effects were illustrated by the percentage (%) of remaining ATPase activity as compared to the controls in the absence of inhibitors.

4 The structural and functional analysis of SecA from Gram-positive bacteria

Part of manuscript to be submitted for publication by

Ying-Ju Huang, Hsiuchin Yang, and Phang C. Tai

"The structural and functional analysis of SecA from Gram-positive bacteria"

4.1 Abstract

SecA plays an essential role in the Sec-dependent protein translocation in *Escherichia coli*. The genome sequence analysis indicates the similarities of the Sec-pathway between Gram-positive and Gram-negative bacteria. In this study, SecA from *Bacillus subtilis* (BsSecA) and *Streptococcus pyogenes* (SpSecA) were used for interspecies comparison. Although BsSecA and SpSecA are highly homologous to *Escherichia coli* SecA (EcSecA), neither of them can complement the growth of *E. coli* SecA temperature-sensitive mutants. Although the ATPase activities of BsSecA and SpSecA were not significantly stimulated by liposomes, conformational changes of BsSecA were induced by phospholipids, and proteolysis examinations revealed the lipid-specific domains corresponding to those of EcSecA. The ring-like structure of BsSecA was observed by atomic force microscope, suggesting that BsSecA interacts with phospholipids to form lipid-specific structures. These results indicate that, although EcSecA and BsSecA cannot complement each other, they share functional and structural similarities in the translocation machinery, constituting part of the protein-conduction channels.

4.2 Introduction

SecA plays an essential role in protein translocation. Besides the ATPase activity functioning as the molecular motor, recent studies have shown that SecA may be involved in the structure of the translocase. Analysis of protease-resistant fragments showed SecA integrates inner membranes in two forms (Chen, Xu et al. 1996; Chen, Brown et al. 1998). Phospholipids could induce conformational changes of SecA to form membrane-specific domains, resulting in resistance to proteolysis (You, Liao, and Tai,

unpublished data). SecA forms ring-like structures in lipids without SecYEG (Wang, Chen et al. 2003; Wang, Na et al. 2008). These data suggest that in addition to catalyzing ATP hydrolysis, certain domains of SecA play an important structural role in the translocation machinery, forming part of the protein-conduction channels.

Unlike in Gram-negative bacteria, secreted proteins in Gram-positive bacteria only need to cross a single membrane to reach the extra-cellular environment. Gram-positive bacteria (e.g., *Bacillus* species) have the ability to secrete a large amount of protein into the extra-cellular medium; therefore, they are often used in industry for commercial production of secreted proteins. The genome sequence analysis implies that the protein secretion systems of Gram-positive and Gram-negative bacteria may be similar because they share the major components (van Wely, Swaving et al. 2001). In Gram-positive bacteria, the Sec system generally controls the transport of newly translated proteins before folding has been completed. The Sec-dependent pathway consists of a series of Sec proteins. Membrane proteins SecY, SecE, and SecG constitute an oligomeric complex that is homologous to the Sec61 channel complex in the endoplasmic reticulum (Manting and Driessen 2000; van Wely, Swaving et al. 2001). SecA is an ATPase, driving the translocation of secretory proteins (Chen and Tai 1987; Lill, Cunningham et al. 1989; van Wely, Swaving et al. 2001). SecD and SecF stabilize the core structure and increase the efficiency of protein export (Mori and Ito 2001; van Wely, Swaving et al. 2001). The study of the crystallization and domain analysis of *B. subtilis* SecA enhances our understanding of its structure and function (Hunt, Weinkauf et al. 2002). The research in our lab centers on the structure and function of SecA, using *E. coli* as the model system. Currently, we are expanding our studies to other bacteria. In particular, SecA from

B. subtilis (BsSecA) and *S. pyogenes* (SpSecA) are used in this study as models of Gram-positive bacteria. BsSecA and SpSecA have high homologies (51% and 55.7% identities, respectively) to EcSecA. Previous study has shown that the characteristic membrane-associated conformation of EcSecA may be responsible for its function (You, Liao, and Tai, unpublished data). Based on the high homology among these proteins, we examined the structure and function of Gram-positive SecAs by similar approaches applied to Ec-SecA for the interspecies comparison. This study will help to elucidate the mechanisms of protein exporting in Gram-positive bacteria, which are of significant interest because of their potential biotechnological applications.

4.3 Material and methods

Bacterial strains, medium, and chemicals. *E. coli* DH5α was used for DNA cloning and plasmid isolation. *E. coli* BL21(λDE3) (Studier and Moffatt 1986) and BL21.19 (Mitchell and Oliver 1993) were used for overproduction of various SecA proteins. SecA mutants *E. coli* BL21.19, MM52 (Schmidt, Rollo et al. 1988), and BA13 (MC4100 *secA13(am) supF(ts)*) (Cabelli, Chen et al. 1988) were used for the complementation assay. *S. pyogenes* NZ131 was a gift from Z. Eichenbaum. Luria-Bertani (LB) liquid and solid (1.5% agar) media were used for *E. coli*, and Todd-Hewitt broth with 0.2% w/v yeast extract (THY) (Difco Laboratories, Sparks, MD) was used for the growth of *S. pyogenes*. *E. coli* total lipid extract was from Avanti Polar Lipids Inc. (Alabaster, Alabama). Other chemicals were purchased from Sigma-Aldrich Corp (St. Louis, MO) and Fisher Scientific (Pittsburg, PA), unless indicated otherwise.

Construction of plasmids carrying SecA derivatives. The gene encoding SecA was amplified by PCR (Mastercycler gradient; Eppendorf, Hauppauge, NY) with 5' primer (AAAGGGCATATGGCCAATATTCTACGCAAA) and 3' primer (GGGCCCCCATG GTTATGAGAAGGATTTACGAC) using the genomic DNA of *S. pyogenes* (a gift from Z. Eichenbaum) as the template and cloned to pET20b through *Nde*I and *Nco*I to yield SpSecA/pET20b. For tighter control of protein expression, the same DNA fragment was cloned to pBAD/Mys-HisC (Invitrogen, Carlsbad, CA) by the same method through *Nco*I and *Pst*I to yield SpSecA/pBAD. DNA encoding the N-fragment of BsSecA (Bs234) was amplified by PCR with genomic DNA of *B. subtilis*, and then cloned into expression vector pET20b via *Nde*I and *Nco*I to yield Bs234/pET20b. DNA encoding the chimeric BsEc was amplified by PCR using DNA encoding the N-terminal fragment of BsSecA (1-718 bp) and C-terminal fragment of Ec-secA (699-1189 bp) as the template, and then was cloned into pET5aEcSecA cassette via *Nde*I and *Sfu*I to yield BsEc/pET5a.

Preparation of SecA proteins and liposomes. SecA proteins of *E. coli* (EcSecA), *B. subtilis* (BsSecA) and *S. pyogenes* (SpSecA) were over-expressed from pT7-SecA (Cabelli, Chen et al. 1988), pT7div (McNicholas, Rajapandi et al. 1995), and SpSecA/pET20b, respectively, in *E. coli* BL21(λDE3) (Studier and Moffatt 1986) (for EcSecA) and BL21.19 (Mitchell and Oliver 1993) (after depletion of endogenous EcSecA, for BsSecA and SpSecA), and purified as described (Chen, Xu et al. 1996; Chen, Brown et al. 1998). Liposomes were prepared by sonication (Sonic Dismembrator Model 500; Fisher Scientific, Pittsburgh, PA) from purchased *E. coli* total lipid extract or phospholi-

pids of *S. pyogenes* prepared by methanol-chloroform (2:1, v/v) extraction, which were resuspended in TKM buffer (TK with 2 mM $MgCl_2$, for AFM) or in TK buffer (10 mM Tris-HCl, pH7.6, and 50 mM KCl, for ATPase assay and proteolysis assay) as described previously (Wang, Chen et al. 2003). The size and quality of liposomes were determined by Submicron Particle Size Analyzer N5 (Beckman Coulter, Miami, FL).

***In vitro* ATPase activity assay.** ATPase activity assays were performed as described (Lill, Dowhan et al. 1990) with minor modifications. For intrinsic, lipid, and membrane ATPase, 50 µL reaction mixture contained 3 µg EcSecA, BsSecA, or SpSecA, 1.2 mM of ATP, 50 mM Tris-HCl (pH 7.6), 20 mM KCl, 20 mM NH_4Cl, 2 mM $Mg(OAc)_2$, and 1 mM DTT, and 6 µg liposomes (for lipid ATPase) or urea-washed *E. coli* BA13 membrane (for membrane ATPase). For translocation ATPase, as well as the same amounts of BsSecA, ATP, BA13 membrane, 1 µg proOmpA and corresponding buffer were used. All reactions were done at 30°C (for intrinsic and lipid ATPases) or 40°C (for membrane and translocation ATPases) for an appropriate time and were stopped by the subsequent addition of 800 µL of malachite green and then 100 µL of 34% sodium citrate in one minute. After incubation at room temperature for 40 minutes, the absorption at 660 nm was measured (SmartSpec Plus; Bio-Rad Laboratories, Inc.). The ATPase activity was determined by the release of inorganic phosphate detected by the photometric method (Lanzetta, Alvarez et al. 1979). All assays were done at least in triplicate, and the results were presented as bar graphs with standard error of the mean.

Determination of lipid-specific domains of SecA by limited proteolysis. 10 μg of various SecA proteins were incubated in the presence or absence of 20 μg (unless specified otherwise) of liposomes in DTK buffer (1mM DTT, 10 mM Tris-HCl, pH 7.6, 50 mM KCl) on ice for 15 min. Then SecA proteins were digested with 3 μg/mL of trypsin on ice for 15 min. The proteolysis reaction was stopped by adding 4X SDS-sample buffer (0.25 M Tris-HCl, pH 6.8, 8% SDS, 40% glycerol, 0.04% Bromophenol Blue) and heated at 100°C for 15 min. Fragments of SecA were separated by SDS-PAGE and visualized by Coomassie blue staining. These fragments were transferred to PVDF membrane (ProBlott; Applied Biosystems, Foster City, CA), and individual bands were subjected to N-terminal sequencing carried out in the Core Facility of Georgia State University by using a protein sequencer (Procise 492cLC; Applied Biosystems, Foster City, CA).

Cellular fractionation of SpSecA. *S. pyogenes* cells were grown at 37°C until OD600 reached 2.0. The harvested cells were resuspended in phosphate buffer (25 mM KPO_4, pH6.4) and treated with lysozyme (0.5 mg/mL, 10 min). The spheroplast suspension was passed through the French Press (10,000 psi) three times and freeze-sorted three times to break cells. Unbroken cells and cellular debris were removed by centrifugation (6,000 g, 5 min, Centrifuge 5417R, Eppendorf, Hauppauge, NY). The supernatant was applied to ultra-centrifugation (265,100 xg, 60 min, Optima Ultracentrifuge, Beckman Coulter, Inc., Brea, CA) to separate the membrane and cytoplasmic fractions. The membrane fraction was resuspended with phosphate buffer. Both fractions were applied to SDS-PAGE, and SpSecA was detected by Western blot with polyclonal antibodies raised against BsSecA.

Atomic force microscopy (AFM). AFM slides were prepared as previously described (Wang, Chen et al. 2003) with minor modifications. In brief, the proper amount of SecA and liposomes (20 μg) in 10 μL TKM buffer were mixed by vortex and incubated on ice for 30 min. The mixtures were applied to freshly cleaved mica and then were held at room temperature for 10 min, rinsed three times with deionized water, and dried in a dessicator over night. AFM images were obtained with a CP-Autoprobe (Park Scientific, Sunnyvale, CA) by using the noncontact mode or di MultiMode V (Veeco Instrument Inc., Woodburry, NY) by using the tapping mode, and analyzed by image-processing software (SPMLab NT Ver. 5.01 or Nanoscope v700, respectively) according to the manufacturer's manual.

Complementation test. Plasmids carrying BsSecA, BsSecAN234, BsEcSecA, or SpSecA were transformed into SecA deficient mutants, BL21.19, MM52, or BA13. Bacterial cells were streaked on LB/Amp plate and incubated at 42°C for over-night growing. A duplicate control plate was incubated at 30°C.

4.4 Results and discussion

The lipid-specific domains of BsSecA were induced upon interaction with phospholipids. We have previously shown two membrane-integral forms of EcSecA from proteolysis-resistant fragments (Chen, Xu et al. 1996; Chen, Brown et al. 1998). We later proved that phospholipids could induce conformational change of EcSecA, generating a 39 kDa N-terminal domain (N39) and a 48 kDa domain located in the central region (M48) as membrane-embedded SecA (You, Liao, and Tai, unpublished data). To deter-

mine whether the lipid-specific domains exist in SecA of bacteria other than Gram-negative *E. coli*, the same approach was applied to SecA from Gram-positive bacteria. Limited proteolyses were performed with BsSecA and SpSecA, and the proteolytic profiles were analyzed. The tryptic digest patterns of BsSecA were similar to those of EcSecA, but each fragment was slightly smaller because BsSecA is 60 amino acid residues shorter than EcSecA. The profiles of proteolytic fragments of BsSecA were very distinct in the presence and absence of phospholipids (Figure 4.1a). Trypsin digestion of soluble BsSecA produced a major 64 kDa fragment. Differently, there were two major phospholipid-induced lipid-specific domains in BsSecA as verified by N-terminal sequencing: a 46 kDa fragment starting at ^{341}Glu, and a 36 kDa fragment starting at ^{1}Met, corresponding to M48 and N39 of EcSecA, respectively. The minor 64 kDa fragment starting at ^{15}Thr was probably integral $SecA_s$ form, as in EcSecA (Chen, Brown et al. 1998). Our data illustrate that phospholipids induce conformational changes of BsSecA to form lipid-specific domains similar to EcSecA, indicating these two proteins share functional and structural similarities. On the other hand, no lipid-specific domains of SpSecA were detected in the presence of various amounts of Ec or Sp phospholipids (Figure 4.1b). It is presumably because there are more trypsin-cutting sites in SpSecA. Therefore, the conformational change might be hard to be detected by this approach. It has been reported previously that SecA is distributed unevenly into a unique microdomain of the cellular membrane in *S. pyogenes* (Rosch and Caparon 2004). This microdomain is named ExPortal and has been proposed as an organelle involved in the biogenesis of secreted proteins in *S. pyogenes* (Rosch and Caparon 2005). However, a subsequent study showed that SpSecA is located throughout the periphery and cytoplasm of cells (Carlsson,

Stalhammar-Carlemalm et al. 2006). Here traditional biochemical immunoblot was applied to resolve these contradictory results. Soluble and membrane-associated SpSecAs were separated by untra-centrifugation, analyzed by SDS-PAGE, Western Blot, and quantified by Quantity One (BioRad, Hercules, CA). Our data showed that the majority (about 80%) of SpSecA is membrane-associated, but not exclusively (Figure 4.2, comparing lane 3 and 4). The specific localization of SecA is also detected in *B. subtilis* within clusters located along spiral-like structures, and the distribution could be influenced by the change of phospholipid contents (Campo, Tjalsma et al. 2004). The lipid-specific domains of BsSecA reveal the interactions between SecA and phospholipids, which may contribute the subcellular distribution of SecA in Gram-positive bacteria.

BsSecA formed ring-like structures induced by phospholipids. Ring-like structures of EcSecA and the tandem dimer EcSecAA have been shown previously by AFM (Wang, Chen et al. 2003; Wang, Na et al. 2008). Based on the high homologies between EcSecA and BsSecA, we examined the structure of BsSecA in lipids by the same approach. BsSecA forms ring-like pore structures in the presence of phospholipids (Figure 4.3). The shape of this structure is remarkably similar to what was observed in EcSecA, and with estimated 15-20 nm diameter and a hole 4-6 nm wide which are similar as compared to EcSecA detected by the new AFM machine (Figure 3.5). This unique structure could only be observed upon the interaction with phospholipids, indicating that it may be related to the lipid-specific domains described earlier. Our observation suggests that the ring-like pore structures may represent the structural role of BsSecA as part of the core of bacterial protein-conducting channel. Moreover, we prove that the potential

structural role of SecA in the protein translocation machinery is not restricted to Gram-negative bacteria, suggesting a universal case also in Gram-positive bacteria.

BsSecA and SpSecA do not complement EcSecA mutant. Previous studies showed that even though the full-length BsSecA failed to restore the growth and protein translocation, the N-terminal fragment containing 234 amino acid residues of BsSecA can complement the EcSecA temperature-sensitive mutant MM52 (Takamatsu, Nakane et al. 1994). A subsequent study demonstrated the full ability of complementation of a chimeric protein that contains the first 242 amino acid residues of BsSecA and the rest of EcSecA (McNicholas, Rajapandi et al. 1995). These studies suggest the barrier between species locates at the C-terminal of SecA. Surprisingly, the corresponding fragment from *Pseudomonas aeruginosa* did not show the ability to complement the SecA-deficient mutant of *E. coli* (Yu and Tai, unpublished data). However, in the N-terminal region, *P. aeruginosa* (Pa) SecA has higher homology (71% identity) to EcSecA than BsSecA (64% identity). To confirm this result and for interspecies comparison, N-terminal fragment of BsSecA (BsSecAN234) and chimeric BsEcSecA which contains N-234 BsSecA and the rest part of EcSecA were cloned, and the streak test was performed in this study. Since an unknown leakage of over-expression occurs, we were able to observe a plasmid effect on *E. coli* MM52, a strain lacking an essential factor to over-produce a gene carried by the T7 promoter. Unexpectedly, BsSecAN234 could not complement *E. coli* MM52 at the non-permissive temperature. Immunoblotting did not detect the intact N-fragment but did detect some degraded pieces (Figure 4.4). It indicates that BsSecAN234 may not be stable in cells under this condition. In the previous study, the N-234 fragment is fused with

LacZ (Takamatsu, Nakane et al. 1994). It might have stabilized the protein and caused the inconsistent result. The chimeric BsEcSecA could complement both *E. coli* MM52 and BL21.19. This result is consistent with the earlier study (McNicholas, Rajapandi et al. 1995), while our construct has slightly shorter N-domain of BsSecA. Another Gram-positive SecA from *S. pyogenes* (SpSecA) with high homology (55.7% identity) with EcSecA was cloned, and the ability of complementation was verified. Although SpSecA could be steadily expressed, it could not complement *E. coli* BL21.19 (Figure 4.5). In a system with tighter control, SpSecA/pBAD could be expressed but still fail to complement *E. coli* BA13 with various amounts of arabinose (0.002%-0.2%, Figure 4.6). These data once more show evidence for the difference between Gram-positive and Gram-negative SecA proteins. Immunoblotting observed successfully expressed and stable BsSecA and SpSecA in *E. coli* SecA defect mutants; therefore, failure to complement was not caused by incomplete or unstable Gram-positive SecA proteins in *E. coli*.

The ATPase activities of BsSecA and SpSecA were not significantly stimulated by lipids, membrane, and precursor proteins. EcSecA has low intrinsic ATPase activity, while the lipid ATPase could be stimulated by anionic phospholipids. In the presence of SecYEG complex and precursor proteins, the activity would be fully activated and referred to as translocation ATPase (Lill, Dowhan et al. 1990). BsSecA has relatively high intrinsic ATPase activity, about 4.5 times of EcSecA, in terms of specific activity (Figure 4.7). Interestingly, in the presence of lipids, the ATPase activity was only slightly stimulated up to 1.4 fold (Figure 4.7), which is comparable to an earlier report (van der Wolk, Klose et al. 1993). A substantial activating effect on BsSecA could be de-

tected when a high concentration of *B. subtilis* lipid is used (van der Wolk, Klose et al. 1993). Similar to BsSecA, SpSecA possesses a high endogenous ATPase activity that was not notably stimulated by lipids (Figure 4.7). Under this experimental condition, when the same ratios of SecA/membrane and precursor protein (proOmA) were used, the membrane ATPase and translocation ATPase of BsSecA were only slightly stimulated (up to 1.5 fold), while the corresponding of EcSecA was dramatically activated (up to 5 fold for membrane ATPase and higher than 15 fold for translocation ATPase, Figure 3.4). A moderate stimulation (about 3 fold) is observed even when high concentrations of components (BsSecA, Ec membrane, proOmA, and EcSecB) are applied (van der Wolk, Klose et al. 1993). One possible explanation is that since the heterogeneous components (Ec membrane/SecYEG and proOmA) are used in the assay, the ideal conformational changes of the membrane and translocation ATPase may not be completed. It has been reported that BsSecA cannot function in the translocation system of *E. coli in vivo* and *in vitro*, suggesting that the inefficient interaction between BsSecA and EcSecYEG causes the incompatibility (Takamatsu, Fuma et al. 1992; McNicholas, Rajapandi et al. 1995). A subsequent study reveals a rigid requirement of homologous BsSecYEG in the BsSecA dependent *in vitro* translocation, although still minor stimulation of translocation ATPase is observed (Swaving, van Wely et al. 1999). The C-terminal linker (amino acid residues 781-819) of Gram-positive SecA is not highly conserved to Gram-negative SecA (Kakeshita, Kageyama et al. 2010), and this region is in the vicinity of the intramolecular regulator of ATP hydrolysis (IRA) (Karamanou, Vrontou et al. 1999). It raises the possibility of differences between BsSecA and EcSecA with regard to the C-terminal-domain-mediated regulatory mechanisms.

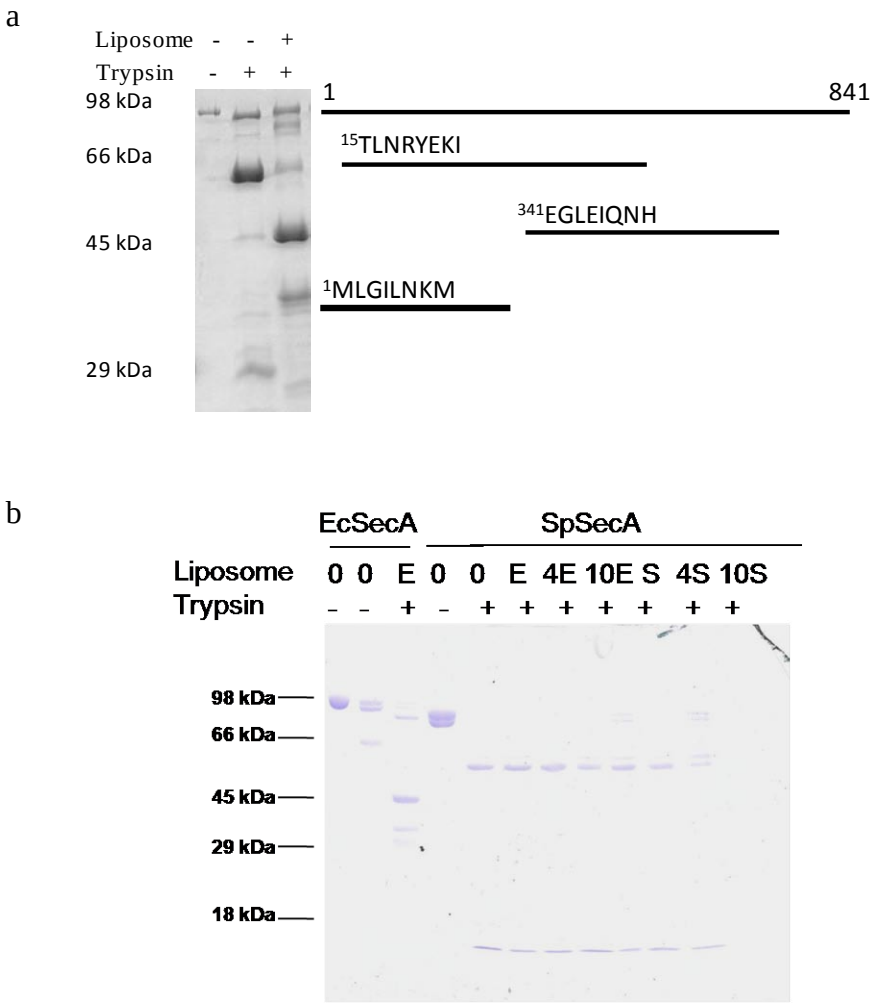

Figure 4.1. Comparison of the proteolysis pattern of soluble SecA and phospholipid-associated SecA. (a) Phospholipids induce conformational changes of BsSecA detected by limited-proteolysis. Left panel: the proteolysis patterns of BsSecA in the presence and absence of lipids. After proteolysis as described in Materials and Methods, protein fragments were separated by SDS-PAGE and visualized by Coomassie blue staining. Right panel: schematic presentation of identification of lipid-specific fragments of BsSecA. Numbers and letters represent the starting point and amino acid residues of fragments verified by N-terminal sequencing. (b) No lipid-specific fragment of SpSecA is detected by limited-proteolysis. Comparison of Ec and SpSecA with different liposomes (Ec lipid mixture (E) and Sp phospholipids (S); numbers indicate the ratio of SecA/lipids, w/w). Positions of molecular weight markers are shown by bars.

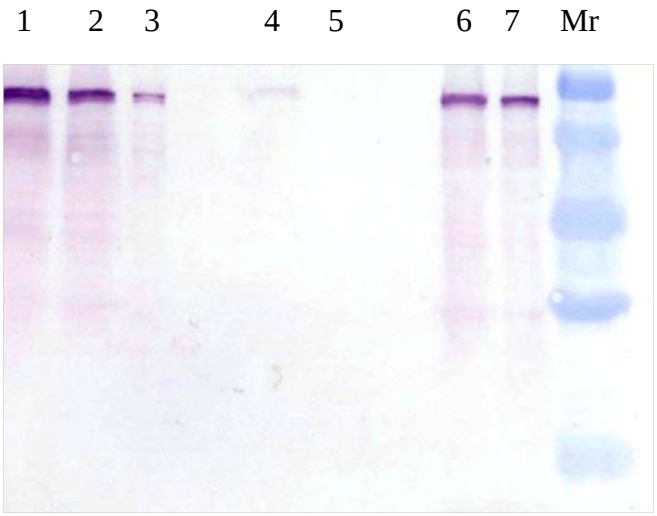

Figure 4.2. Cellular distribution of SpSecA. Cellular fractionation was performed as described in Materials and Methods. SpSecA was detected by antibody against BsSecA. Lane 1-3: membrane fraction (equivalent to fractions from 600, 300, and 30 µL of cell lysate); lane 4-5: cytoplasm (30 and 10 µL); lane 6-7: unbroken cells and cellular debris; Mr: molecular weight marker.

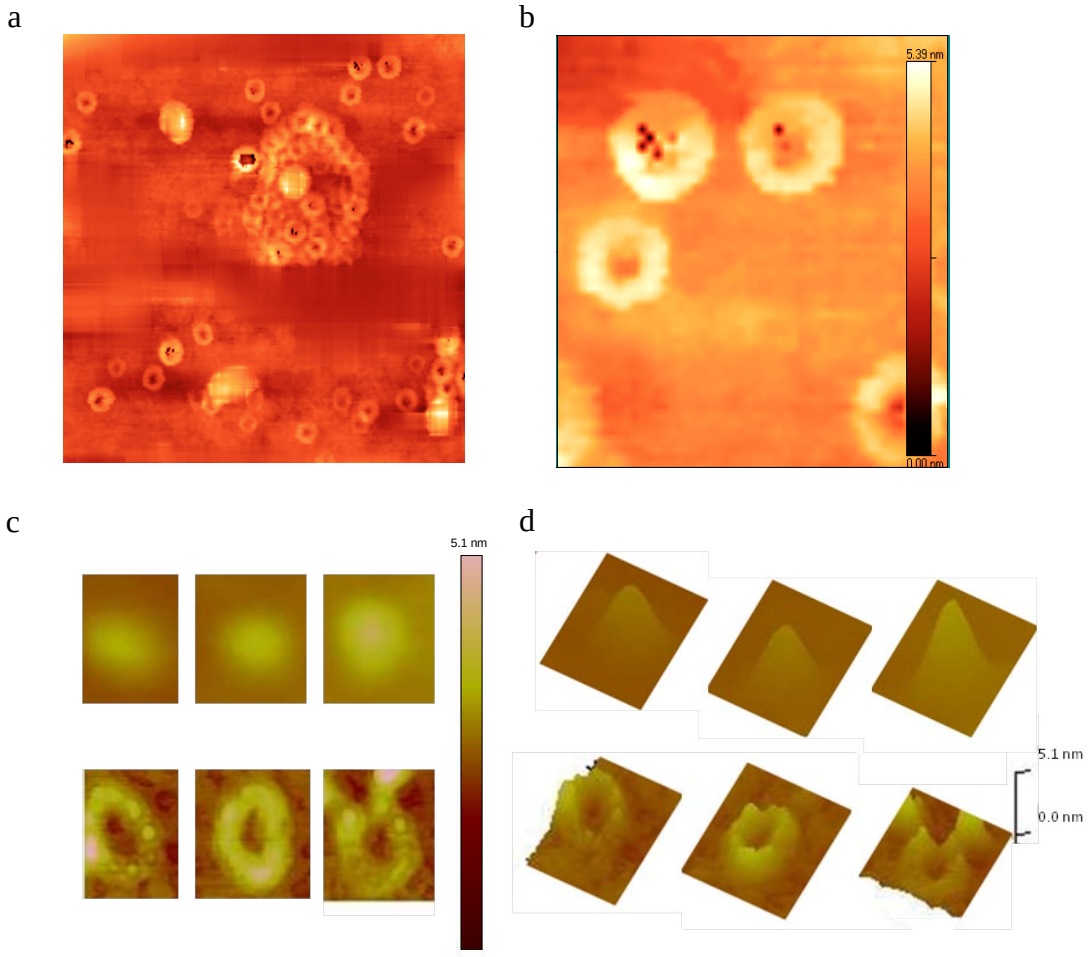

Figure 4.3. BsSecA forms ring-like pore structures in lipids as observed by AFM. Purified BsSecA was incubated with (a, b, lower panel of c and d) or without (upper panel of c and d) lipid bilayers prepared from *E. coli* total lipid extract and applied to freshly cleaved mica as described in Material and Methods. (a-b): image obtained by CP-Autoprobe (Park Scientific) using the noncontact mode; (b): a zoom-in image of (a); (c-d): image obtained by di MultiMode V di MultiMode V (Veeco Instrument Inc.) using the tapping mode; upper panel: BsSecA with lipids; lower panel: BsSecA along. (d): 3-D image of (c). The bars in (b-d) show the depth of the image.

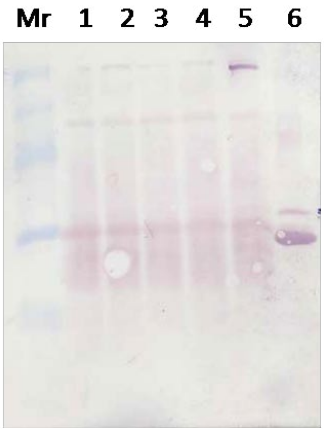

Figure 4.4. Stability of BsSecAN234 in *E. coli* MM52. Expressing BsSecAN234 (lane 1-4) and EcSecA (lane 5) in MM52 by leakage of over-expression; lane 6: over-expressing BsSecAN234 in BL21.19; Mr: molecular weight marker. SecAs were detected by polyclonal antibodies against BsSecA.

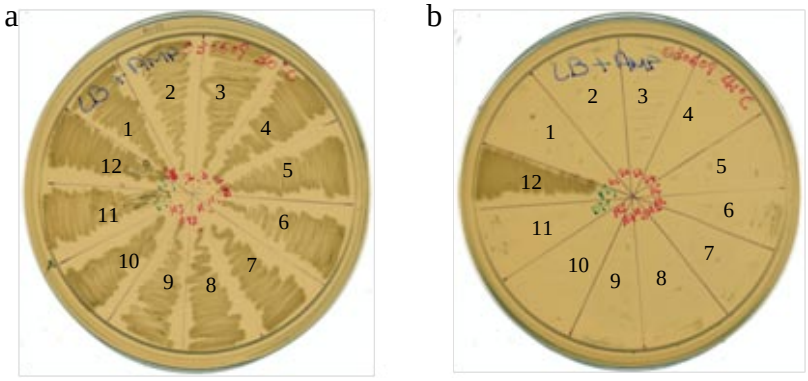

Figure 4.5. Complementation test of SpSecA to *E. coli secA* mutant BL21.19. (a): 30°C; (b): 42°C. SecAs were induced by 5μM IPTG. 1-10: SpSecA/pET20b/BL21.19; 11: pT7Div/BL21.19; 12: pT7-SecA/BL21.19.

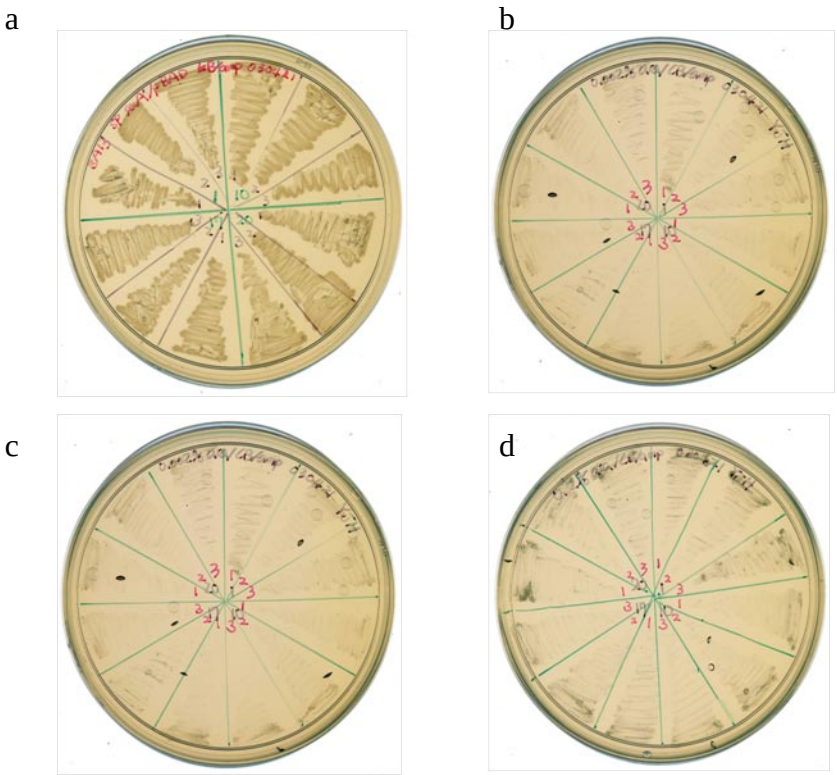

Figure 4.6. Complementation test of SpSecA to *E. coli secA* mutant BA13. SpSecA/pBAD/BA13 was grown at (a): 30°C; (b-d): 42°C. (b, c, and d): SpSecA were induced by arabinose (0.002%, 0.02% and 0.2%, respectively).

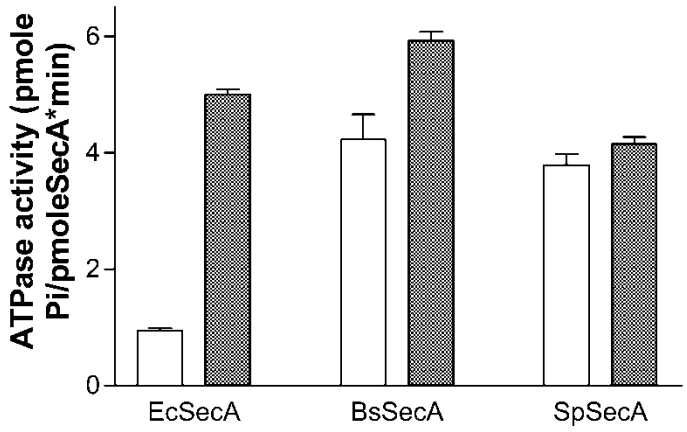

Figure 4.7. *In vitro* ATPase activities of BsSecA and SpSecA are not significantly stimulated by lipids. The intrinsic ATPase (open bars) and lipid ATPase (close bars) of Ec, Bs, and SpSecA were performed as described in Materials and Methods. All assays were done in multiples, and the result was presented as bar graphs with standard error of the mean.

5 CONCLUSIONS

5.1 General conclusion and discussion

The over-all aim of our research is to understand the mechanism of protein secretion in bacteria, with a focus on the SecA-dependent protein translocation. In this study, multiple approaches were used to analyze the structure and function of SecA.

SecA ATPase inhibitors and possible applications. We found that fluorescein analogs Rose Bengal (RB) and Erythrosin B (EB) can inhibit all three forms of SecA ATPase as well as *in vitro* protein translocation effectively. Most likely, the fluorescein analogs are general ATPase inhibitors because various ATPases are repressed by these compounds (Morris, Silbergeld et al. 1982; Silbergeld, Anderson et al. 1982; Fricke 1985). However, SecA may still be the more susceptible target of RB and EB in bacteria, because the catalytic ATPase is more sensitive than F_1F_0-proton ATPase. These compounds also exhibit bacteriostatic and bactericidal effects on both Gram-negative and Gram-positive bacteria in the presence of glucose to minimize the effects on F_1F_0-proton ATPase. In the experimental condition, photo-oxidation is not the primary mechanism for the antimicrobial activities and inhibitory effect against ATPase of RB, as previously reported (Watson and Haynes 1982; Banks, Board et al. 1985; Glaser, Cadenas et al. 1988; Rasooly and Weisz 2002; Kim, Park et al. 2008; Waite and Yousef 2009). Our results show that SecA is one of the targets of fluorescein analogs, and the antibacterial effects can be caused by the inhibition of ATPase and protein translocation.

Only a few SecA inhibitors have been found to date. The well-known SecA inhibitor, sodium azide, merely prevents the translocation ATPase and *in vitro* protein translocation at mM range, which is a thousand times weaker than RB, and has no effect on

the intrinsic and membrane ATPase (Oliver, Cabelli et al. 1990; Nakane, Takamatsu et al. 1995). Inhibitory effects against ATPase or bacterial growth are observed from other inhibitors from natural sources, such as CJ21058 (Sugie, Inagaki et al. 2002) and pannomycin (Parish, de la Cruz et al. 2009), or synthesis (Li, Huang et al. 2008; Chen, Huang et al. 2010; Akula, Zheng et al. 2011; Jang, De Jonghe et al. 2011), although none of them have been reported to hold compatible potency and the comprehensive effects both *in vitro* and *in vivo* as RB. The fluorescein analogs are commercially available, with high solubility for easy manipulation, and with relatively low or no toxicity for food and drug application. Therefore, they can serve as good starting materials for further structural optimization. Taken together, our data suggest that fluorescein analogs are good candidates for development of new antibacterial agents using SecA as the target. Being the central component of the protein secretion pathway and without a counterpart in humans, SecA provides an ideal target for potential medicines through an alternative action with existing antibiotics. This new strategy may help solve the serious problem of antibiotic resistance.

SecA possesses three levels of ATPase activities: intrinsic, membrane, and translocation ATPases, depending on the conformation, which is in response to the presence of legends or other components of the Sec system (Lill, Dowhan et al. 1990). RB shows dramatically different inhibitory effects and mechanisms against three forms of SecA ATPase, suggesting the inhibition is related to the conformation of SecA. RB and EB inhibit the intrinsic ATPase of SecA competitively at low ATP concentration and non-competitively at high ATPase concentration, indicating they influence the two non-identical nucleotide binding sites of SecA. Kinetics study suggests that RB and EB prefer to bind to the high-affinity site, acting as a competitive inhibitor at low ATP concentra-

tion. NBDII acts as a sensor for the signal from high ATP concentration to increase the activity. RB and EB then inhibit the raised activity non-competitively. This interpretation is consistent with the most widely accepted view of SecA: NBDI is responsible for the high-affinity binding and acts as the real catalytic site. NBDII is a regulatory site for the activity of NBDI and has been suggested as the intramolecular regulator of ATP hydrolysis (IRA2) (Karamanou, Vrontou et al. 1999; Nakatogawa, Mori et al. 2000; Sianidis, Karamanou et al. 2001). These interesting features of RB and EB lead to a potential application. Specifically, these inhibitors or their derivatives can provide useful tools for biochemical analysis, such as to probe the conformational changes of SecA during protein translocation and to clarify the functional significance of the two nucleotide binding sites of SecA.

The structural role of the C-terminal domain of SecA: Can (and which domain of) SecA form the protein-conducting channel? The current model for Sec-dependent protein transportation (Wickner and Leonard 1996) illustrates that the core channel for protein translocation is formed by heterotrimeric SecYEG complex (Akimaru, Matsuyama et al. 1991; Nishiyama, Mizushima et al. 1992; Hanada, Nishiyama et al. 1994). The peripheral protein SecA hydrolyzes ATP to provide the energy required for the movement of preproteins across the plasma membrane (Eichler and Wickner 1997). However, membranes with deletion of SecY and SecE are still active in translocation of some precursor proteins, suggesting these two proteins are not essential for the transportation of all proteins (Watanabe, Nicchitta et al. 1990; Watanabe and Blobel 1993; Yang, Lian et al. 1997; Yang, Yu et al. 1997). The membrane-integral form of SecA and two lipid-specific domains have been identified (Chen, Xu et al. 1996). 2-D

and 3-D structures of EcSecA in lipids detected by electronic microscopy (EM) and atomic force microscopy (AFM) reveal the ability of SecA itself to form the channel-like structure that is independent of ATP or on-going protein translocation (Wang, Chen et al. 2003). Electro-physiological data show EcSecA, but not SecYEG, is the major contributor for channel activity, providing more evidence that SecA can form the protein-conducting channel (Lin, dissertation, 2006) (Hsieh, Zhang et al. 2011). In this study, we investigated the structural role and function of the first long α-helix of C-terminal domain of SecA. This α-helix is not necessary for ATPase activity because N68 without the helix possesses high intrinsic ATPase and responds to the interaction with lipids with stimulated activity. We have found that the lack of stimulation in the literature is the effect from the N-terminal His-tag. On the other hand, the α-helix is important for the membrane interaction and the ring-like structure of SecA with lipids. This helix is located at the middle of the lipid-specific domain M48, which can form a partial pore-like structure in lipids (You and Tai, unpublished data). Here $SecA_{1\text{-}F639D}$ to $SecA_{1\text{-}668}$ (N71.5D-N75), which contains major part of M48 and whole N39 (the other lipid-specific domain), can form a comparable ring structure similar to the full length of SecA. Thus, the minimal essential elements for the ring structure should be located in this region, and the precise position still needs to be defined.

The structural role of SecA has been analyzed in our lab using EcSecA as the model. In order to confirm that our finding is not an extraordinary case that can only be detected in this specific protein, BsSecA was analyzed in the comparative study. With the same approaches, a lipid-specific domain corresponding to M48 of EcSecA is determined. The ring-like structure of BsSecA in lipids is also similar to what has been found

in EcSecA by AFM. With this supporting evidence, we can conclude that the structural role of SecA is not an exceptional event in *E. coli,* but is universal in bacteria. SecA from Gram-positive and G-negative bacteria share common features of their structural role in the protein transportation machinery, even though the species barrier exists in other bio-chemical functions. Thus, EcSecA and BsSecA are not exchangeable and cannot com-plement each other (Takamatsu, Fuma et al. 1992; van der Wolk, Klose et al. 1993; McNicholas, Rajapandi et al. 1995; Swaving, van Wely et al. 1999).

In this study, the structure and function of SecA from various bacteria are further examined. We show more evidence to support our working hypothesis that SecA can form a protein-conducting channel. These comparative studies provide a more compre-hensive view to understand the protein translocation in bacterial physiology.

5.2 Future directions

Based on what we have accomplished in this study, we will further determine the structures and function of SecA in two aspects: (1) to examine SecA inhibitors and the applications; and (2) to further characterize the structure and function of lipid-specific domains of SecA and the structural role of SecA as part of the protein-conducting chan-nel.

RB and EB will be applied for further structural optimization for several aims, such as to increase the potency, to decrease the molecular weight for better permeability, and to verify the functional group of the compound. The binding site of the inhibitor may be determined by cross-linking. RB, EB, or their derivatives may be applied in co-crystallization for the structural study.

We found that the SecA variant containing the C-terminal portion of the α-helix starts to gain the ability to form the ring-like structure in the presence of lipids. The SecA derivatives beyond the first α-helix will be constructed, to determine the role of the other two α-helixes of HSD. The minimum required elements for pore-structure forming and functional channels need to be defined. SecA domain mapping will be achieved with multiple approaches, including structural studies with AFM, the electro-physiological studies for the channel activity, and *in vitro* translocation for biochemical functions. With these comprehensive data, we will try to correlate the structural and functional role of various SecA domains.

6 REFERENCES

Abdou, I. M. and L. Strekowski (2000). "A Facile Synthesis of 6-Aryl-5-cyano-1-(b-d-pyranosyl or b-d-furanosyl)-2-thiocytosines." Tetrahedron **56**: 8631-8636.

Akimaru, J., S. Matsuyama, et al. (1991). "Reconstitution of a protein translocation system containing purified SecY, SecE, and SecA from Escherichia coli." Proc Natl Acad Sci U S A **88**(15): 6545-6549.

Akita, M., A. Shinkai, et al. (1991). "SecA, an essential component of the secretory machinery of *Escherichia coli*, exists as homodimer." Biochem. Biophys. Res. Commun. **174**(1): 211-216.

Akula, N., H. Zheng, et al. (2011). "Discovery of novel SecA inhibitors of Candidatus Liberibacter asiaticus by structure based design." Bioorg Med Chem Lett **21**(14): 4183-4188.

Alami, M., K. Dalal, et al. (2007). "Nanodiscs unravel the interaction between the SecYEG channel and its cytosolic partner SecA." EMBO J **26**(8): 1995-2004.

Bajorath, J. (2002). "Integration of Virtual and High-Throughput Screening." Nat. Rev. Drug Discov. **1**(11): 882-894.

Banks, J. G., R. G. Board, et al. (1985). "The cytotoxic and photodynamic inactivation of micro-organisms by Rose Bengal." J Appl Bacteriol **58**(4): 391-400.

Benach, J., Y. T. Chou, et al. (2003). "Phospholipid-induced monomerization and signal-peptide-induced oligomerization of SecA." J. Biol. Chem. **278**(6): 3628-3638.

Berndt, J. D., N. L. Callaway, et al. (2001). "Effects of chronic sodium azide on brain and muscle cytochrome oxidase activity: a potential model to investigate environmental contributions to neurodegenerative diseases." J Toxicol Environ Health A **63**(1): 67-77.

Bologa, C. G., C. M. Revankar, et al. (2006). "Virtual and Biomolecular Screening Converge on a Selective Agonist for GPR30." Nat. Chem. Biol. **2**(4): 207-212.

Bowler, M. W., M. G. Montgomery, et al. (2006). "How Azide Inhibits ATP Hydrolysis by the F-ATPases." Proc. Natl. Acad. Sci. U S A **103**(23): 8646-8649.

Breukink, E., N. Nouwen, et al. (1995). "The C terminus of SecA is involved in both lipid binding and SecB binding." J Biol Chem **270**(14): 7902-7907.

Cabelli, R. J., L. Chen, et al. (1988). "SecA protein is required for secretory protein translocation into E. coli membrane vesicles." Cell **55**(4): 683-692.

Cabelli, R. J., K. M. Dolan, et al. (1991). "Characterization of membrane-associated and soluble states of SecA protein from wild-type and SecA51(TS) mutant strains of Escherichia coli." J Biol Chem **266**(36): 24420-24427.

Campo, N., H. Tjalsma, et al. (2004). "Subcellular sites for bacterial protein export." Mol Microbiol **53**(6): 1583-1599.

Carlsson, F., M. Stalhammar-Carlemalm, et al. (2006). "Signal sequence directs localized secretion of bacterial surface proteins." Nature **442**(7105): 943-946.

Casadaban, M. J. (1976). "Transposition and fusion of the lac genes to selected promoters in Escherichia coli using bacteriophage lambda and Mu." J Mol Biol **104**(3): 541-555.

Case, D. A., T. E. Cheatham, 3rd, et al. (2005). "The Amber biomolecular simulation programs." J Comput Chem **26**(16): 1668-1688.

Chen, L. F., T. Chopra, et al. (2009). "Pathogens resistant to antibacterial agents." Infect Dis Clin North Am **23**(4): 817-845, vii.

Chen, L. L. and P. C. Tai (1987). "Evidence for the involvement of ATP in co-translational protein translocation." Nature **328**(6126): 164-166.

Chen, M., K. Xie, et al. (2002). "YidC, a newly defined evolutionarily conserved protein, mediates membrane protein assembly in bacteria." Biol Chem **383**(10): 1565-1572.

Chen, W., Y. J. Huang, et al. (2010). "The first low microM SecA inhibitors." Bioorg Med Chem **18**(4): 1617-1625.

Chen, X., T. Brown, et al. (1998). "Identification and characterization of protease-resistant SecA fragments: secA has two membrane-integral forms." J Bacteriol **180**(3): 527-537.

Chen, X., H. Xu, et al. (1996). "A significant fraction of functional SecA is permanently embedded in the membrane. SecA cycling on and off the membrane is not essential during protein translocation." J. Biol. Chem **271**(47): 29698-29706.

Chitlaru, T., O. Gat, et al. (2006). "Differential proteomic analysis of the Bacillus anthracis secretome: distinct plasmid and chromosome CO2-dependent cross talk mechanisms modulate extracellular proteolytic activities." J Bacteriol **188**(10): 3551-3571.

Dapic, V. and D. Oliver (2000). "Distinct membrane binding properties of N- and C-terminal domains of Escherichia coli SecA ATPase." J Biol Chem **275**(32): 25000-25007.

Das, S., E. Stivison, et al. (2008). "Reexamination of the role of the amino terminus of SecA in promoting its dimerization and functional state." J Bacteriol **190**(21): 7302-7307.

de Keyzer, J., E. O. van der Sluis, et al. (2005). "Covalently dimerized SecA is functional in protein translocation." J. Biol. Chem. **280**(42): 35255-35260.

de Leeuw, E., T. Granjon, et al. (2002). "Oligomeric properties and signal peptide binding by Escherichia coli Tat protein transport complexes." J Mol Biol **322**(5): 1135-1146.

DeLano, W. L. (2006). The PyMOL Molecular Graphics System, DeLano Scientific, San Carlos, CA, USA**:** http://www.pymol.org**.**

Dempsey, B. R., A. Economou, et al. (2002). "The ATPase domain of SecA can form a tetramer in solution." J. Mol. Biol. **315**(4): 831-843.

Ding, H., J. F. Hunt, et al. (2003). "*Bacillus subtilis* SecA ATPase exists as an antiparallel dimer in solution." Biochemistry **42**(29): 8729-8738.

Driessen, A. J. (1993). "SecA, the peripheral subunit of the *Escherichia coli* precursor protein translocase, is functional as a dimer." Biochemistry **32**(48): 13190-13197.

Driessen, A. J. (1994). "How proteins cross the bacterial cytoplasmic membrane." J Membr Biol **142**(2): 145-159.

Driessen, A. J. and N. Nouwen (2008). "Protein translocation across the bacterial cytoplasmic membrane." Annu Rev Biochem **77**: 643-667.

Economou, A. (2001). "Sec, drugs and rock'n'roll: antibiotic targeting of bacterial protein translocation." Expert Opin Ther Targets **5**(2): 141-153.

Economou, A., P. J. Christie, et al. (2006). "Secretion by numbers: Protein traffic in prokaryotes." Mol Microbiol **62**(2): 308-319.

Economou, A., J. A. Pogliano, et al. (1995). "SecA membrane cycling at SecYEG is driven by distinct ATP binding and hydrolysis events and is regulated by SecD and SecF." Cell **83**(7): 1171-1181.

Eichler, J. and W. Wickner (1997). "Both an N-terminal 65-kDa domain and a C-terminal 30-kDa domain of SecA cycle into the membrane at SecYEG during translocation." Proc Natl Acad Sci U S A **94**(11): 5574-5581.

Eldridge, M. D., C. W. Murray, et al. (1997). "Empirical scoring functions: I. The development of a fast empirical scoring function to estimate the binding affinity of ligands in receptor complexes." J Comput Aided Mol Des **11**(5): 425-445.

Erlandson, K. J., S. B. Miller, et al. (2008). "A role for the two-helix finger of the SecA ATPase in protein translocation." Nature **455**(7215): 984-987.

Ewing, T. J., S. Makino, et al. (2001). "DOCK 4.0: Search Strategies for Automated Molecular Docking of Flexible Molecule Databases." J. Comput. Aided. Mol. Des. **15**(5): 411-428.

Feher, M. (2006). "Consensus scoring for protein-ligand interactions." Drug Discov Today **11**(9-10): 421-428.

Fekkes, P., J. G. de Wit, et al. (1999). "Zinc stabilizes the SecB binding site of SecA." Biochemistry **38**(16): 5111-5116.

Fekkes, P. and A. J. Driessen (1999). "Protein targeting to the bacterial cytoplasmic membrane." Microbiol Mol Biol Rev **63**(1): 161-173.

Foote, M. C., B. H. Burmeister, et al. (2010). "A novel treatment for metastatic melanoma with intralesional rose bengal and radiotherapy: a case series." Melanoma Res **20**(1): 48-51.

Foster, D. L. and R. H. Fillingame (1979). "Energy-transducing H+-ATPase of Escherichia coli. Purification, reconstitution, and subunit composition." J Biol Chem **254**(17): 8230-8236.

Fricke, U. (1985). "Erythrosin B inhibits high affinity ouabain binding in guinea-pig heart Na+-K+-ATPase without influence on cardiac glycoside induced contractility." Br J Pharmacol **85**(2): 327-334.

Glaser, E., E. Cadenas, et al. (1988). "Inhibition of the mitochondrial F1-ATPase by rose bengal mediated photooxidation. Interaction of the Fe2+ chelate of bathophenanthroline with the sensitizer." Acta Chem Scand B **42**(3): 175-182.

Hanada, M., K. I. Nishiyama, et al. (1994). "Reconstitution of an efficient protein translocation machinery comprising SecA and the three membrane proteins, SecY, SecE, and SecG (p12)." J Biol Chem **269**(38): 23625-23631.

Hartl, F. U., S. Lecker, et al. (1990). "The binding cascade of SecB to SecA to SecY/E mediates preprotein targeting to the E. coli plasma membrane." Cell **63**(2): 269-279.

Hendrick, J. P. and W. Wickner (1991). "SecA protein needs both acidic phospholipids and SecY/E protein for functional high-affinity binding to the Escherichia coli plasma membrane." J Biol Chem **266**(36): 24596-24600.

Hsieh, Y. H., H. Zhang, et al. (2011). "SecA alone can promote protein translocation and Ion-channel activity:SecYEG increases efficiency and signal peptide specificity." J Biol Chem.

Hunt, J. F., S. Weinkauf, et al. (2002). "Nucleotide control of interdomain interactions in the conformational reaction cycle of SecA." Science **297**(5589): 2018-2026.

Jacobsberg, L. B., E. R. Kantrowitz, et al. (1975). "Interaction of tetraiodofluorescein with aspartate transcarbamylase and its isolated catalytic and regulatory subunits." J Biol Chem **250**(24): 9238-9249.

Jakalian, A., B. L. Bush, et al. (2000). "Fast, Efficient Generation of High-Quality Atomic Charges. AM1-BCC Model: I. Method." J. Comput. Chem. **21**(2): 132-146.

Jakalian, A., D. B. Jack, et al. (2002). "Fast, Efficient Generation of High-Quality Atomic Charges. AM1-BCC Model: II. Parameterization and Validation." J. Comput. Chem. **23**(16): 1623-1641.

Jang, M. Y., S. De Jonghe, et al. (2011). "Synthesis of novel 5-amino-thiazolo[4,5-d]pyrimidines as E. coli and S. aureus SecA inhibitors." Bioorg Med Chem **19**(1): 702-714.

Jilaveanu, L. B. and D. Oliver (2006). "SecA dimer cross-linked at its subunit interface is functional for protein translocation." J. Bacteriol. **188**(1): 335-338.

Jilaveanu, L. B., C. R. Zito, et al. (2005). "Dimeric SecA is essential for protein translocation." Proc. Natl. Acad. Sci. U S A **102**(21): 7511-7516.

Jorgensen, W. L., J. Chandrasekhar, et al. (1983). "Comparison of simple potential functions for simulating liquid water." J Chem Phys **79**(2): 926-935.

Kakeshita, H., Y. Kageyama, et al. (2010). "Enhanced extracellular production of heterologous proteins in Bacillus subtilis by deleting the C-terminal region of the SecA secretory machinery." Mol Biotechnol **46**(3): 250-257.

Kanazawa, H., T. Miki, et al. (1979). "Specialized transducing phage lambda carrying the genes for coupling factor of oxidative phosphorylation of Escherichia coli: increased synthesis of coupling factor on induction of prophage lambda asn." Proc Natl Acad Sci U S A **76**(3): 1126-1130.

Karamanou, S., G. Sianidis, et al. (2005). "*Escherichia coli* SecA truncated at its termini is functional and dimeric." FEBS Lett. **579**(5): 1267-1271.

Karamanou, S., E. Vrontou, et al. (1999). "A molecular switch in SecA protein couples ATP hydrolysis to protein translocation." Mol Microbiol **34**(5): 1133-1145.

Kim, Y. S., S. J. Park, et al. (2008). "Antibacterial compounds from Rose Bengal-sensitized photooxidation of beta-caryophyllene." J Food Sci **73**(7): C540-545.

Kimura, E., M. Akita, et al. (1991). "Determination of a region in SecA that interacts with presecretory proteins in Escherichia coli." J Biol Chem **266**(10): 6600-6606.

Knott, T. G. and C. Robinson (1994). "The secA inhibitor, azide, reversibly blocks the translocation of a subset of proteins across the chloroplast thylakoid membrane." J Biol Chem **269**(11): 7843-7846.

Lanzetta, P. A., L. J. Alvarez, et al. (1979). "An improved assay for nanomole amounts of inorganic phosphate." Anal Biochem **100**(1): 95-97.

Li, M., Y. J. Huang, et al. (2008). "Discovery of the first SecA inhibitors using structure-based virtual screening." Biochem Biophys Res Commun **368**(4): 839-845.

Li, M., N. Ni, et al. (2008). "Structure-based discovery and experimental verification of novel AI-2 quorum sensing inhibitors against Vibrio harveyi." ChemMedChem **3**(8): 1242-1249.

Li, M. and B. Wang (2006). "Computational studies of H5N1 hemagglutinin binding with SA-alpha-2, 3-Gal and SA-alpha-2, 6-Gal." Biochem. Biophys. Res. Commun. **347**(3): 662-668.

Li, M. and B. Wang (2007). "Homology modeling and examination of the effect of the D92E mutation on the H5N1 nonstructural protein NS1 effector domain." J. Mol. Model. **13**(12): 1237-1244.

Lill, R., K. Cunningham, et al. (1989). "SecA protein hydrolyzes ATP and is an essential component of the protein translocation ATPase of Escherichia coli." Embo J **8**(3): 961-966.

Lill, R., W. Dowhan, et al. (1990). "The ATPase activity of SecA is regulated by acidic phospholipids, SecY, and the leader and mature domains of precursor proteins." Cell **60**(2): 271-280.

Linnertz, H., H. Kost, et al. (1998). "Erythrosin 5'-isothiocyanate labels Cys549 as part of the low-affinity ATP binding site of Na+/K+-ATPase." FEBS Lett **441**(1): 103-105.

Linnertz, H., P. Urbanova, et al. (1998). "Molecular distance measurements reveal an (alpha beta)2 dimeric structure of Na+/K+-ATPase. High affinity ATP binding site and K+-activated phosphatase reside on different alpha-subunits." J Biol Chem **273**(44): 28813-28821.

Lyne, P. D. (2002). "Structure-based virtual screening: an overview." Drug Discov Today **7**(20): 1047-1055.

Maloney, P. R., D. J. Parks, et al. (2000). "Identification of a Chemical Tool for the Orphan Nuclear Receptor FXR." J. Med. Chem. **43**: 2971-2974.

Manting, E. H. and A. J. Driessen (2000). "Escherichia coli translocase: the unravelling of a molecular machine." Mol Microbiol **37**(2): 226-238.

Marklund, S. L. (1984). "Properties of extracellular superoxide dismutase from human lung." Biochem J **220**(1): 269-272.

McDonald, I. K. and J. M. Thornton (1994). "Satisfying hydrogen bonding potential in proteins." J. Mol. Biol. **238**(5): 777-793.

McGann, M. R., H. R. Almond, et al. (2003). "Gaussian docking functions." Biopolymers **68**(1): 76-90.

McNicholas, P., T. Rajapandi, et al. (1995). "SecA proteins of Bacillus subtilis and Escherichia coli possess homologous amino-terminal ATP-binding domains regulating integration into the plasma membrane." J Bacteriol **177**(24): 7231-7237.

Mignaco, J. A., O. H. Lupi, et al. (1996). "Two simultaneous binding sites for nucleotide analogs are kinetically distinguishable on the sarcoplasmic reticulum Ca(2+)-ATPase." Biochemistry **35**(13): 3886-3891.

Mitchell, C. and D. Oliver (1993). "Two distinct ATP-binding domains are needed to promote protein export by *Escherichia coli* SecA ATPase." Mol. Microbiol. **10**(3): 483-497.

Mori, H. and K. Ito (2001). "The Sec Protein-translocation Pathway." Trends Microbiol. **9**(10): 494-500.

Mori, H., H. Sugiyama, et al. (1998). "Amino-terminal region of SecA is involved in the function of SecG for protein translocation into Escherichia coli membrane vesicles." J Biochem **124**(1): 122-129.

Morris, S. J., E. K. Silbergeld, et al. (1982). "Erythrosin B (USFD&C RED 3) inhibits calcium transport and atpase activity of muscle sarcoplasmic reticulum." Biochem Biophys Res Commun **104**(4): 1306-1311.

Moustakas, D. T., P. T. Lang, et al. (2006). "Development and Validation of a Modular, Extensible Docking Program: DOCK 5." J. Comput. Aided Mol. Des. **20**(10-11): 601-619.

Muegge, I. (2003). "Selection criteria for drug-like compounds." Med Res Rev **23**(3): 302-321.

Muller, J. P., J. Ozegowski, et al. (2000). "Interaction of Bacillus subtilis CsaA with SecA and precursor proteins." Biochem J **348 Pt 2**: 367-373.

Murray, C. W., T. R. Auton, et al. (1998). "Empirical scoring functions. II. The testing of an empirical scoring function for the prediction of ligand-receptor binding affinities and the use of Bayesian regression to improve the quality of the model." J Comput Aided Mol Des **12**(5): 503-519.

Nakane, A., H. Takamatsu, et al. (1995). "Acquisition of azide-resistance by elevated SecA ATPase activity confers azide-resistance upon cell growth and protein translocation in Bacillus subtilis." Microbiology **141 (Pt 1)**: 113-121.

Nakatogawa, H., H. Mori, et al. (2000). "Two independent mechanisms down-regulate the intrinsic SecA ATPase activity." J. Biol. Chem. **275**(43): 33209-33212.

Nishiyama, K., S. Mizushima, et al. (1992). "The carboxyl-terminal region of SecE interacts with SecY and is functional in the reconstitution of protein translocation activity in Escherichia coli." J Biol Chem **267**(10): 7170-7176.

Oliver, D. B., R. J. Cabelli, et al. (1990). "Azide-resistant Mutants of *Escherichia coli* Alter the SecA Protein, An Azide-sensitive Component of the Protein Export Machinery." Proc. Natl. Acad. Sci. USA **87**: 8227–8231.

Or, E., A. Navon, et al. (2002). "Dissociation of the dimeric SecA ATPase during protein translocation across the bacterial membrane." EMBO. J. **21**(17): 4470-4479.
Osborne, A. R. and T. A. Rapoport (2007). "Protein translocation is mediated by oligomers of the SecY complex with one SecY copy forming the channel." Cell **129**(1): 97-110.
Osborne, A. R., T. A. Rapoport, et al. (2005). "Protein translocation by the Sec61/SecY channel." Annu Rev Cell Dev Biol **21**: 529-550.
Pallen, M. J. (2002). "The ESAT-6/WXG100 superfamily -- and a new Gram-positive secretion system?" Trends Microbiol **10**(5): 209-212.
Papanikolau, Y., M. Papadovasilaki, et al. (2007). "Structure of dimeric SecA, the Escherichia coli preprotein translocase motor." J Mol Biol **366**(5): 1545-1557.
Papanikou, E., S. Karamanou, et al. (2005). "Identification of the preprotein binding domain of SecA." J Biol Chem **280**(52): 43209-43217.
Papanikou, E., S. Karamanou, et al. (2007). "Bacterial protein secretion through the translocase nanomachine." Nat Rev Microbiol **5**(11): 839-851.
Parish, C. A., M. de la Cruz, et al. (2009). "Antisense-guided isolation and structure elucidation of pannomycin, a substituted cis-decalin from Geomyces pannorum." J Nat Prod **72**(1): 59-62.
Payne, D. J. (2008). "Microbiology. Desperately seeking new antibiotics." Science **321**(5896): 1644-1645.
Pearlman, R. S. (1987). "CONCORD: Rapid Generation of High Quality Approximate 3D Molecular Structures." Chem. Des. Autom. News **2**(1): 1-7.
Pohlschroder, M., E. Hartmann, et al. (2005). "Diversity and evolution of protein translocation." Annu Rev Microbiol **59**: 91-111.
Rambow-Larsen, A. A. and A. A. Weiss (2004). "Temporal expression of pertussis toxin and Ptl secretion proteins by Bordetella pertussis." J Bacteriol **186**(1): 43-50.
Randall, L. L. and M. T. Henzl (2010). "Direct identification of the site of binding on the chaperone SecB for the amino terminus of the translocon motor SecA." Protein Sci **19**(6): 1173-1179.
Rasooly, A. and A. Weisz (2002). "In vitro antibacterial activities of phloxine B and other halogenated fluoresceins against methicillin-resistant Staphylococcus aureus." Antimicrob Agents Chemother **46**(11): 3650-3653.
Rosch, J. and M. Caparon (2004). "A microdomain for protein secretion in Gram-positive bacteria." Science **304**(5676): 1513-1515.
Rosch, J. W. and M. G. Caparon (2005). "The ExPortal: an organelle dedicated to the biogenesis of secreted proteins in Streptococcus pyogenes." Mol Microbiol **58**(4): 959-968.
Ruiz, N., B. Falcone, et al. (2005). "Chemical conditionality: a genetic strategy to probe organelle assembly." Cell **121**(2): 307-317.
Saier, M. H. (2006). "Protein Secretion and Membrane Insertion Systems in Gram-negative Bacteria." J. Membr. Biol. **214**(2): 75-90.
Samuelson, J. C., M. Chen, et al. (2000). "YidC mediates membrane protein insertion in bacteria." Nature **406**(6796): 637-641.
Sardis, M. F. and A. Economou (2010). "SecA: a tale of two protomers." Mol Microbiol **76**(5): 1070-1081.
Schmidt, M. G. and D. B. Oliver (1989). "SecA protein autogenously represses its own translation during normal protein secretion in Escherichia coli." J Bacteriol **171**(2): 643-649.

Schmidt, M. G., E. E. Rollo, et al. (1988). "Nucleotide sequence of the secA gene and secA(Ts) mutations preventing protein export in Escherichia coli." J Bacteriol **170**(8): 3404-3414.

Schneider, G. and H. J. Bohm (2002). "Virtual screening and fast automated docking methods." Drug Discov Today **7**(1): 64-70.

Segers, K. and J. Anne (2011). "Traffic jam at the bacterial sec translocase: targeting the SecA nanomotor by small-molecule inhibitors." Chem Biol **18**(6): 685-698.

Serres, M. H., S. Goswami, et al. (2004). "GenProtEC: an updated and improved analysis of functions of Escherichia coli K-12 proteins." Nucleic Acids Res **32**(Database issue): D300-302.

Sharma, V., A. Arockiasamy, et al. (2003). "Crystal structure of Mycobacterium tuberculosis SecA, a preprotein translocating ATPase." Proc Natl Acad Sci U S A **100**(5): 2243-2248.

Shin, J. Y., M. Kim, et al. (2006). "Effects of signal peptide and adenylate on the oligomerization and membrane binding of soluble SecA." J Biochem Mol Biol **39**(3): 319-328.

Sianidis, G., S. Karamanou, et al. (2001). "Cross-talk between catalytic and regulatory elements in a DEAD motor domain is essential for SecA function." Embo J **20**(5): 961-970.

Silbergeld, E. K., S. M. Anderson, et al. (1982). "Interactions of erythrosin B (U.S. F, D & C Red 3) with rat cortical membranes." Life Sci **31**(10): 957-969.

Snyders, S., V. Ramamurthy, et al. (1997). "Identification of a region of interaction between Escherichia coli SecA and SecY proteins." J Biol Chem **272**(17): 11302-11306.

Stahl, M. and M. Rarey (2001). "Detailed analysis of scoring functions for virtual screening." J Med Chem **44**(7): 1035-1042.

Stephens, C. and L. Shapiro (1997). "Bacterial protein secretion--a target for new antibiotics?" Chem Biol **4**(9): 637-641.

Stewart, J. J. (1990). "MOPAC: a semiempirical molecular orbital program." J Comput Aided Mol Des **4**(1): 1-105.

Stoddard, B. L., D. Ringe, et al. (1990). "The Structure of Iron Superoxide Dismutase from Pseudomonas ovalis Complexed with the Inhibitor Azide." Protein Eng. **4**(2): 113-119.

Studier, F. W. and B. A. Moffatt (1986). "Use of bacteriophage T7 RNA polymerase to direct selective high-level expression of cloned genes." J Mol Biol **189**(1): 113-130.

Sugie, Y., S. Inagaki, et al. (2002). "CJ-21,058, a new SecA inhibitor isolated from a fungus." J Antibiot (Tokyo) **55**(1): 25-29.

Swaving, J., K. H. van Wely, et al. (1999). "Preprotein translocation by a hybrid translocase composed of Escherichia coli and Bacillus subtilis subunits." J Bacteriol **181**(22): 7021-7027.

Tai, P. C., G. Tian, et al. (1991). "In vitro protein translocation into Escherichia coli inverted membrane vesicles." Methods Cell Biol **34**: 167-187.

Takamatsu, H., S. Fuma, et al. (1992). "In vivo and in vitro characterization of the secA gene product of Bacillus subtilis." J Bacteriol **174**(13): 4308-4316.

Takamatsu, H., A. Nakane, et al. (1994). "A truncated Bacillus subtilis SecA protein consisting of the N-terminal 234 amino acid residues forms a complex with Escherichia coli SecA51(ts) protein and complements the protein translocation defect of the secA51 mutant." J Biochem (Tokyo) **116**(6): 1287-1294.

Tanfani, F., H. Linnertz, et al. (2000). "Effects of fluorescent pseudo-ATP and ATP-metal analogs on secondary structure of Na(+)/K(+)-ATPase." Biochim Biophys Acta **1457**(1-2): 94-102.

Thompson, J. F., P. Hersey, et al. (2008). "Chemoablation of metastatic melanoma using intralesional Rose Bengal." Melanoma Res **18**(6): 405-411.

Tjalsma, H., H. Antelmann, et al. (2004). "Proteomics of protein secretion by Bacillus subtilis: separating the "secrets" of the secretome." Microbiol Mol Biol Rev **68**(2): 207-233.

Tsai, K.-C., S.-H. Wang, et al. (2008). "The Effect of Different Electrostatic Potentials on Docking Accuracy: A Case Study Using DOCK5.4." Bioorg. Med. Chem. Lett. **18**(12): 3509-3512.

Tsukazaki, T., H. Mori, et al. (2008). "Conformational transition of Sec machinery inferred from bacterial SecYE structures." Nature **455**(7215): 988-991.

US, G. (2011). "Code of Federal Regulations. Title 21, part 74.303." U.s. Government Printing Office, Washington, D.C. **1**.

Van den Berg, B., W. M. Clemons, Jr., et al. (2004). "X-ray structure of a protein-conducting channel." Nature **427**(6969): 36-44.

van der Sluis, E. O. and A. J. Driessen (2006). "Stepwise evolution of the Sec machinery in Proteobacteria." Trends Microbiol **14**(3): 105-108.

van der Wolk, J., M. Klose, et al. (1993). "Characterization of a Bacillus subtilis SecA mutant protein deficient in translocation ATPase and release from the membrane." Mol Microbiol **8**(1): 31-42.

van der Wolk, J. P., A. Boorsma, et al. (1997). "The low-affinity ATP binding site of the Escherichia coli SecA dimer is localized at the subunit interface." Biochemistry **36**(48): 14924-14929.

van Klompenburg, W., A. N. Ridder, et al. (1997). "In vitro membrane integration of leader peptidase depends on the Sec machinery and anionic phospholipids and can occur post-translationally." FEBS Lett **413**(1): 109-114.

van Wely, K. H., J. Swaving, et al. (2001). "Translocation of proteins across the cell envelope of Gram-positive bacteria." FEMS Microbiol Rev **25**(4): 437-454.

Verkhivker, G. M., D. Bouzida, et al. (2000). "Deciphering common failures in molecular docking of ligand-protein complexes." J Comput Aided Mol Des **14**(8): 731-751.

Voulhoux, R., G. Ball, et al. (2001). "Involvement of the twin-arginine translocation system in protein secretion via the type II pathway." EMBO J **20**(23): 6735-6741.

Vrontou, E. and A. Economou (2004). "Structure and function of SecA, the preprotein translocase nanomotor." Biochim Biophys Acta **1694**(1-3): 67-80.

Vrontou, E., S. Karamanou, et al. (2004). "Global co-ordination of protein translocation by the SecA IRA1 switch." J Biol Chem **279**(21): 22490-22497.

Waite, J. G. and A. E. Yousef (2009). "Chapter 3: Antimicrobial properties of hydroxyxanthenes." Adv Appl Microbiol **69**: 79-98.

Wallace, A. C., R. A. Laskowski, et al. (1995). "LIGPLOT: a program to generate schematic diagrams of protein-ligand interactions." Protein Eng. **8**(2): 127-134.

Wang, H., B. Na, et al. (2008). "Additional in vitro and in vivo evidence for SecA functioning as dimers in the membrane: dissociation into monomers is not essential for protein translocation in Escherichia coli." J Bacteriol **190**(4): 1413-1418.

Wang, H. W., Y. Chen, et al. (2003). "Ring-like pore structures of SecA: implication for bacterial protein-conducting channels." Proc Natl Acad Sci U S A **100**(7): 4221-4226.

Wang, L., A. Miller, et al. (2000). "Signal peptide determinants of SecA binding and stimulation of ATPase activity." J Biol Chem **275**(14): 10154-10159.

Watanabe, M. and G. Blobel (1993). "SecA protein is required for translocation of a model precursor protein into inverted vesicles of Escherichia coli plasma membrane." Proc Natl Acad Sci U S A **90**(19): 9011-9015.

Watanabe, M., C. V. Nicchitta, et al. (1990). "Reconstitution of protein translocation from detergent-solubilized Escherichia coli inverted vesicles: PrlA protein-deficient vesicles efficiently translocate precursor proteins." Proc Natl Acad Sci U S A **87**(5): 1960-1964.

Watson, B. D. and D. H. Haynes (1982). "Structural and functional degradation of Ca2+:Mg2+-ATPase rich sarcoplasmic reticulum vesicles photosensitized by erythrosin B." Chem Biol Interact **41**(3): 313-325.

Wickner, W. and M. R. Leonard (1996). "Escherichia coli preprotein translocase." J Biol Chem **271**(47): 29514-29516.

Woodbury, R. L., S. J. Hardy, et al. (2002). "Complex behavior in solution of homodimeric SecA." Protein. Sci. **11**(4): 875-882.

Yang, Y. B., J. Lian, et al. (1997). "Differential translocation of protein precursors across SecY-deficient membranes of Escherichia coli: SecY is not obligatorily required for translocation of certain secretory proteins in vitro." J Bacteriol **179**(23): 7386-7393.

Yang, Y. B., N. Yu, et al. (1997). "SecE-depleted membranes of Escherichia coli are active. SecE is not obligatorily required for the in vitro translocation of certain protein precursors." J Biol Chem **272**(21): 13660-13665.

Yip, B. P. and F. B. Rudolph (1976). "Interaction of tetraiodofluorescein with yeast hexokinase." J Biol Chem **251**(22): 7157-7161.

Yoshikawa, S., K. Shinzawa-Itoh, et al. (1998). "Redox-coupled Crystal Structural Changes in Bovine Heart Cytochrome c Oxidase." Science **280**(5370): 1723-1729.

Yound, J. M. and J. H. Wang (1971). "The Nature of Binding of Competitive Inhibitors to Alcohol Dehydrogenases." J. Biol. Chem. **246**(9): 2815-2821.

Zaitsev, V. N., I. Zaitseva, et al. (1999). "An X-ray Crystallographic Study of the Binding Sites of the Azide Inhibitor and Organic Substrates to Ceruloplasmin, A Multi-copper Oxidase in the Plasma." J. Biol. Inorg. Chem. **4**(5): 579-587.

Zheng, S., G. Kaur, et al. (2008). "Design, synthesis, and structure-activity relationship, molecular modeling, and NMR studies of a series of phenyl alkyl ketones as highly potent and selective phosphodiesterase-4 inhibitors." J. Med. Chem. **51**(24): 7673-7688.

Zhou, M., D. Theunissen, et al. (2010). "LAB-Secretome: a genome-scale comparative analysis of the predicted extracellular and surface-associated proteins of Lactic Acid Bacteria." BMC Genomics **11**: 651.

Zimmer, J., Y. Nam, et al. (2008). "Structure of a complex of the ATPase SecA and the protein-translocation channel." Nature **455**(7215): 936-943.

7 APPENDICES

Appendix A: Discovery of the First SecA Inhibitors Using Structure-Based Virtual Screening

This work has been published by

Minyong Li, Ying-Ju Huang, Phang C. Tai, and Binghe Wang,

"Discovery of SecA inhibitors using structure-based virtual screening". (2008) *Biochem Biophys Res Commun.* 368**(4)**:839-845

The biochemical assay was done by Ying-Ju Huang. The computer simulation was done by Minyong Li.

7.1 Abstract

Bacterial protein secretion is a critical and complex process. The Sec machinery provides a major pathway for protein translocation across and integration into the cellular membrane in bacteria. Small molecule probes that perturb the functions of individual member proteins within the Sec machinery will be very important research tools as well as leads for future antimicrobial agent development. Herein we describe the discovery of inhibitors, through virtual screening, that specifically act on SecA ATPase, which is a critical member of the Sec system. These are the very first inhibitors reported for intrinsic SecA ATPase.

7.2 Introduction

It is well known that protein synthesis primarily occurs in the cytosolic ribosomes. However, their sites of eventual localization vary. It has been said that no less than 10% of protein products cross a membrane before arriving at the final location of function (Mori and Ito 2001). There are others that need to be integrated into a membrane. Therefore, protein transport across and integration into membranes are very important to their proper functions. However, the study of protein transport is not a trivial task. In bacteria, there are several protein transport mechanisms (Saier 2006). Among them, the Sec machinery (or translocase) provides a major pathway of protein translocation from the cytosol across or into the cytoplasmic membrane. The Sec machinery has seven proteins including SecA, SecD, SecE, SecF, SecG, SecY, and YajC. They also form complexes such as SecYEG and SecYEGDFYajC in the membrane as functional units for protein transport. Among the Sec proteins, SecA is found both in the cytoplasm

and bound to the inner membrane. When SecA is bound to the SecYEG complex, acidic phospholipids and a precursor protein such as proOmpA (the precursor of outer membrane protein A), it becomes fully active as an ATPase, which drives protein translocation (Lill, Dowhan et al. 1990; van Klompenburg, Ridder et al. 1997). Small molecule probes that perturb the function of individual components of the Sec family will be very important for studying the details of the transport mechanisms for various proteins. They are also useful tools to examine the detailed mechanisms of how the Sec system functions. SecA has no human counterpart. Therefore, SecA inhibitors also have the potential to be of a novel class of antimicrobial agents with minimal toxicity. In our own research, we are in need of inhibitors of SecA ATPase as tools to probe the detailed mechanism of function of the SecYEG-SecA transport system. Currently, inorganic azide is the only inhibitor available (IC50: 1 mM) as a research tool to probe the SecA system (Knott and Robinson 1994). However, such inhibitory activities are only known for the SecYEG-SecA translocase activities, not for the intrinsic SecA ATPase activities though azide-resistant mutation has been mapped on SecA (Oliver, Cabelli et al. 1990). In addition, azide is also an inhibitor of many other enzymes such as cytochrome c oxidase (Yoshikawa, Shinzawa-Itoh et al. 1998; Bowler, Montgomery et al. 2006), superoxide dismutase (Stoddard, Ringe et al. 1990) alcohol dehydrogenase (Yound and Wang 1971), and ceruloplasmin (Zaitsev, Zaitseva et al. 1999). Its multitude of activities make azide a poor probe for SecA functions in vivo or in cellular preparations. In 2002, Sugie reported an organic compound (CJ-21058) that inhibits SecYEG-SecA translocase activities using partially purified membrane preparations (Sugie, Inagaki et al. 2002). It was inferred that the observed effect was due to SecA ATPase inhibition. However, no enzyme inhibition

studies were conducted to allow for true characterization of the compound as a SecA ATPase inhibitor or whether the inhibition mechanism was due to its effect on other factors. Furthermore, CJ-21058 is a natural product isolated from marine source and is not readily available to those interested in using it a research probe. Therefore, up to date and to the best our knowledge, there has not been a confirmed organic SecA ATPase inhibitor reported in the published literature. Herein we report the discovery of inhibitors of SecA ATPase by taking advantage of the newly available E. coli SecA crystal structure through virtual screening (Papanikolau, Papadovasilaki et al. 2007). The inhibitors identified will be extremely important tools to labs interested in studying bacterial protein transport. Furthermore these inhibitors are commercially available from Maybridge, which will make it very convenient for interested labs to obtain. In the long term, the inhibitors identified can also serve as important structural leads for the development of SecA inhibitors as novel antimicrobial agents with minimal host toxicity.

For our effort to discover SecA ATPase inhibitors, we decided to use structure-based virtual screening. This decision was largely due to the recent availability of the published crystal structure of *E. coli* SecA ATPase (Papanikolau, Papadovasilaki et al. 2007). In a structure-based virtual screening approach, large compound databases can be docked into the active site/binding pocket and estimated binding free energies are used to select compounds for experimental testing (Lyne 2002; Schneider and Bohm 2002). There have been many examples in which such an approach was used successfully (Bajorath 2002; Bologa, Revankar et al. 2006). With the available SecA ATPase crystal structure, we screened compounds in the MayBridge Screening Collection against the *holo*-form (PDB entry: 2FSG) (Papanikolau, Papadovasilaki et al. 2007). Figure 7.1

represents the docking conformations of these 31 hits and ATP around the ATP-site of SecA ATPase. All hit compounds seem to have similar proposed orientations as ATP when binding with *E. coli* SecA. The chemical structures and docking scores for all these 31 compounds (1-31) are presented as supplementary information (Figure 7.2 and Table 7.1).

7.3 Material and methods

Protocol of virtual screening. The 2D structures of these compounds were first converted into 3D structures using the CONCORD program (Pearlman 1987). Before docking, hydrogen atoms were added into the protein structure and all atoms were assigned with Kollman-all charges by the SYBYL 7.1 program (2005). Hydrogen atoms were added to the 3D ligand structures and all atoms were assigned with AM1-BCC partial charges (Jakalian, Bush et al. 2000; Jakalian, Jack et al. 2002) by the QuACPAC 1.1 software (2007). Residues within a radius of 6 Å around the center of ATP were defined as the active site to construct a grid for the virtual screening. The active site included residues Gly80, Mse81, Arg82, His83, Phe84, Gln87, Arg103, Thr104, Gly105, Glu106, Gly107, Lys108, Thr109, Leu110, Arg138, Asp209, Glu210, Arg509 and Gln578. The Maybridge database, containing about 60,000 compounds, was screened and scored on a 40-node Linux Biocluster. The position and conformation of each compound were optimized first by the anchor fragment orientation and then by the torsion minimization method implemented in the DOCK 6 program (Ewing, Makino et al. 2001; Moustakas, Lang et al. 2006). Fifty conformations and a maximum of 100 anchor orientations for each compound were generated, and all of the docked conformations were energy minimized

by 100 iterations following procedures as described in literature (Moustakas, Lang et al. 2006). The docked molecules were ranked based on the sum of the *van der Waals* and electrostatic energies implemented in the DOCK 6 program to obtain the top 1000 compounds. After collecting the top hits, re-analysis of virtual screening results was conducted using drug-like property criteria (Muegge 2003) by the FILTER 2.0.1 software.(2007) We then performed consensus scoring evaluation (Feher 2006) by ChemScore (Eldridge, Murray et al. 1997; Murray, Auton et al. 1998), PLP (Verkhivker, Bouzida et al. 2000), ScreenScore (Stahl and Rarey 2001), ChemGauss and ShapeGauss (McGann, Almond et al. 2003) implemented in the FRED 2.2.3 software (2007) as well as hydrogen bond and hydrophobic profiles checked by the IDEA 8.8 software (2007). As the final step, a manual binding orientation and conformational analysis was performed to come up with the final 31 hits for biological evaluation.

Molecular simulation of docking complexes. Molecular simulations were performed on a 40-node Linux Biocluster following similar procedures as described in earlier publications from our lab (Li and Wang 2006; Li and Wang 2007). In brief, the docked complexes were solvated by using the TIP3P water model (Jorgensen, Chandrasekhar et al. 1983), subjected to 500-steps of molecular mechanics minimization and molecular dynamics simulations at 300 K for 1.5 ns using the SANDER module in AMBER 8 program (Case, Cheatham et al. 2005). The resulting structures were then analyzed using PyMOL 0.99 (DeLano 2006), HBPLUS 3.06 (McDonald and Thornton 1994) and Ligplot 4.22 (Wallace, Laskowski et al. 1995) programs to identify specific contacts between ligands and SecA.

Assays of compounds against EcN68 SecA ATPase. EcN68 was over-expressed from pT7-SecA (Schmidt and Oliver 1989) and pIMBB-8 (Karamanou, Vrontou et al. 1999) and purified as described in the literatures (Chen, Xu et al. 1996; Chen, Brown et al. 1998). ATPase activities were determined by the release of phosphate (Pi) detected spectrophotometrically using malachite green (Sugie, Inagaki et al. 2002). All potential inhibitors were dissolved in 100% DMSO (Sigma) to make a 10 mM stock solution and kept at 4 °C before use. Potential inhibitors were diluted to proper concentrations with DMSO. SecA ATPase assay was performed as described in the literature (Lill, Dowhan et al. 1990) in the presence of 10% (vol/vol) DMSO. The malachite green solution was incubated on ice for at least 2 hours (Sugie, Inagaki et al. 2002). Briefly, reaction mixture in 50 μL contained 9 μg EcSecA or 2.25 μg N68, 2 mM ATP, 50 mM Tris-HCl (pH7.6), 20 mM KCl, 20 mM NH_4Cl, 1 mM DTT, and 2 mM $Mg(OAc)_2$. Tubes were incubated at 40 °C for 40 or 20 minutes for EcSecA or N68, respectively. The reactions were stopped by adding 800 μL of malachite green and then 100 μL of 34% citric acid in 1 min. The mixtures were incubated at room temperature for 40 minutes and then the absorptions at 660 nm were measured. Inhibition is illustrated by showing the percentage (%) of the remaining ATPase activities.

7.4 Results and discussion

These compounds were purchased from Maybridge Chemical Company (Trevillet, Tintagel, Cornwall PL34 OHW, UK). ATPase assays with E coli N68SecA (SecA residue #1-610) were conducted to test their inhibitory activities. N68SecA ATPase does

not have the 34kDa regulatory domain and represents the unregulated ATPase activity (Dempsey, Economou et al. 2002). Several compounds showed significant inhibitory effects as shown in Figure 7.3. For example, at 100 μM, about one third of the tested compounds, including 9, 11, 13, 15, 16, 19, 20, 21, 23 and 25, showed >50% inhibition of the E coli SecA activities with 15 and 16 showing the highest activities with about 80% inhibition.

The six most potent compounds, 9, 13, 15, 16, 20 and 21 (Figure 7.4), were further studied for their fifty-percent inhibitory concentrations (IC_{50}) as described in literature (Lill, Dowhan et al. 1990). The IC_{50} values of the two most potent compounds 15 (HTS-12302) and 16 (SEW-05929) were about 30 μM. The IC_{50} values were about 80 μM for 20 (BTB-06881) and 21 (CD-09529) and 150 μM for 9 (KM-03277) and 13 (SP-00934). The inhibitory curves for these six compounds are represented in Figure 7.4.

Full kinetic studies were performed for 16 and 21. Both compounds were competitive inhibitors of SecA ATPase with K_i of 18 μM for 16 and 40 μM for 21. Using the same method, we also examined azide, which is known to inhibit the SecYEG-SecA translocase activities with IC_{50} of about 1 mM (Oliver, Cabelli et al. 1990). No inhibition was observed of the N68SecA ATPase activities at concentrations as high as 10 mM. Such results indicate that azide has no inhibitory activities on the unregulated SecA ATPase.

The structures of 16 and 21 were re-docked into the active site and the interactions were optimization by molecular mechanics and molecular dynamics. After refinements, compound 16 seems to bind with SecA by forming hydrogen bonds with Lys108,

Glu210 and Arg509 and through hydrophobic interactions with residues Thr104, Gly105, Gly107, Gly392, Gly510 and Thr511 as shown in Figure 7.5.

Compared with 16, compound 21 has a slightly different binding profile with SecA. It mainly depends on strong hydrophobic interactions with Phe 84, Gln106 and Gln578, as well as hydrogen bond interactions with Gly105, Gly107 and Lys108. The proposed binding profile of compound 21 is depicted in Figure 7.6.

7.5 Conclusion

In summary, this study describes the successful discovery of the first SecA ATPase inhibitors using structure-based virtual screening against *E. coli* SecA. In the initial screening, ten compounds (hit rate of 10/31 = 32%), including 9, 11, 13, 15, 16, 19, 20, 21, 23 and 25, showed >50% inhibitory activities against *E coli* SecA at 100 μM concentrations. Among them, two compounds, 16 and 21, showed K_i values of 18 and 40 μM, respectively. These inhibitors will be extremely useful to researchers interested in examining the roles that SecA ATPase plays in the transport of various bacterial proteins. Furthermore, since SecA has no human counterpart, the inhibitor structures identified can serve as important lead scaffolds for structural optimization for the eventual development of a new class of antimicrobial agents with minimal toxicity.

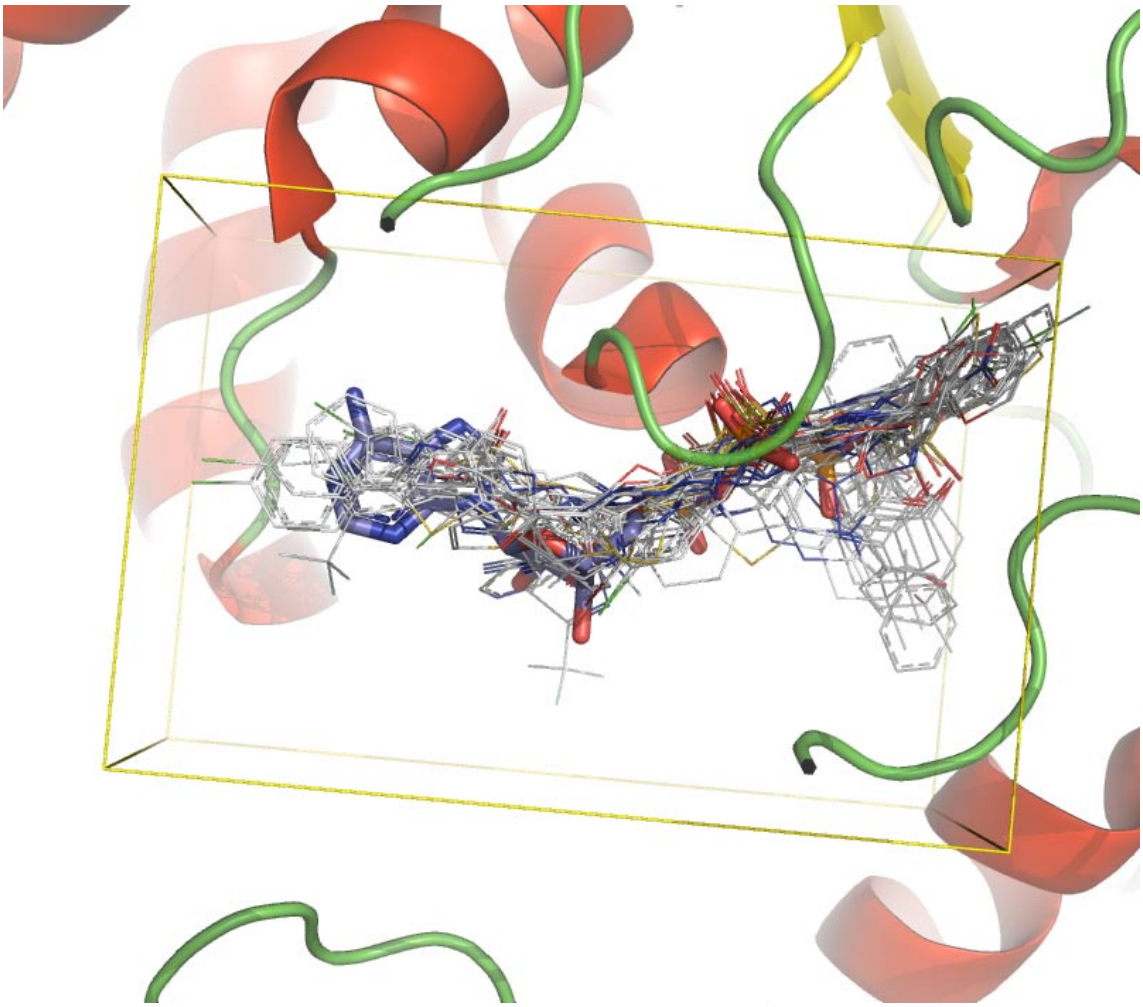

Figure 7.1. Docking conformations of 31 hits (white lines) and ADP (purple sticks) around the ATP-site (yellow box) of *E. coli* SecA (ribbons).

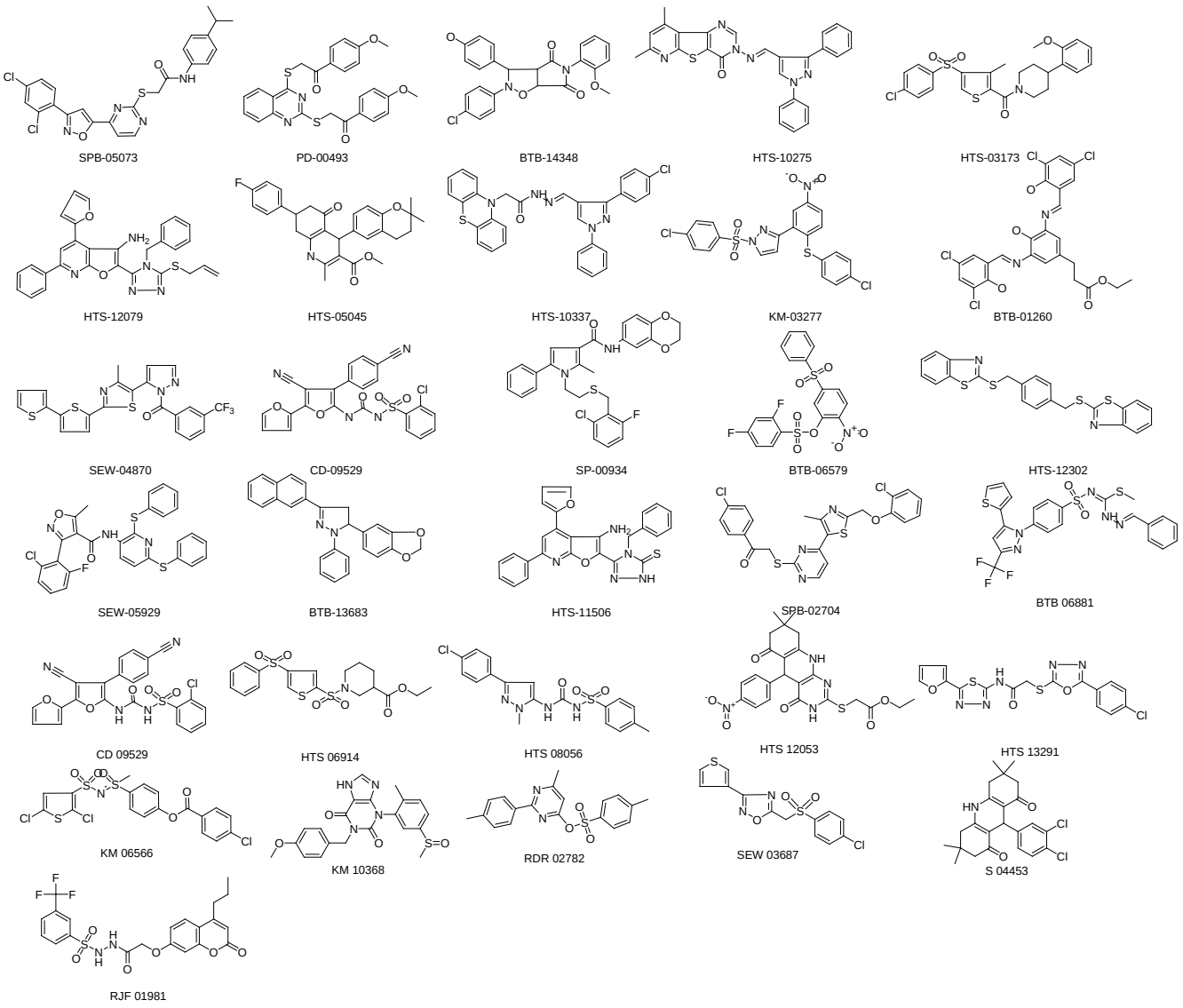

Figure 7.2. The chemical structures of all 31 hit compounds.

Table 7.1 Consensus scores of all 31 hit compounds

Cmpd	Name	ChemScore		ChemGauss		PLP		ScreenScore		ShapeGauss		Consensus
		Score	Rank	Score	Rank	Score	Rank	Score	Rank	Score	Rank	Score
1	SPB-05073	-12.65	25	-57.58	64	-51.14	3	-123.73	0	-507.9	20	112
2	PD-00493	-12.28	34	-56.66	77	-40.9	49	-100.01	8	-503.28	26	194
3	BTB-14348	-7.79	189	-61.43	23	-42.82	24	-89.08	27	-519.26	15	278
4	HTS-10275	-8.35	155	-60.42	33	-41.89	33	-85.44	46	-499.07	31	298
5	HTS-03173	-14.83	8	-55.11	99	-44.88	14	-79.5	83	-448.22	121	325
6	HTS-12079	-11.26	51	-59.05	45	-35.53	113	-80.88	74	-471.26	70	353
7	HTS-05045	-9	121	-57.21	68	-36.44	95	-87.42	36	-496.8	35	355
8	HTS-10337	-7.28	222	-56.57	78	-46.54	8	-96.52	13	-492.26	43	364
9	KM-03277	-7.09	230	-66.28	5	-40.07	55	-84.5	52	-491.73	46	388
10	BTB-01260	-7.43	211	-54.82	107	-42.39	28	-88.05	31	-518.6	16	393
11	SEW-04870	-6.54	275	-65.39	9	-39.5	58	-82.98	65	-590.92	3	410
12	CD-09529	-8.3	161	-56.69	74	-38.02	72	-78.31	90	-498.7	32	429
13	SP-00934	-10.72	61	-59.38	43	-41.73	35	-89.47	26	-417.97	264	429
14	BTB-06579	-11.24	52	-53.55	139	-37.21	84	-79.83	82	-466.09	80	437
15	HTS-12302	-10.89	56	-53.1	151	-33.11	151	-90.34	23	-482.68	59	440
16	SEW-05929	-20.22	0	-50.55	218	-56.58	0	-103.95	2	-424.78	222	442
17	BTB-13683	-12.18	37	-53.06	152	-46.28	10	-97.21	11	-420.15	249	459
18	HTS-11506	-14.3	13	-55.62	90	-44.21	16	-92.64	18	-403.23	356	493
19	SPB-02704	-11.46	47	-48.36	300	-46.51	9	-111.22	1	-434.49	170	527
20	BTB 06881	-5.27	356	-74.32	0	-36.73	90	-79.26	84	-580.23	5	535
21	CD 09529	-6.61	267	-55.85	87	-43.52	19	-94.09	14	-438.01	155	542
22	HTS 06914	-6.7	256	-58.63	51	-32.14	166	-84.86	49	-505.23	24	546
23	HTS 08056	-10.58	67	-53.92	129	-53.85	1	-102.41	5	-404	351	553
24	HTS 12053	-11.38	48	-55.16	98	-34.58	129	-87.31	38	-419.5	252	565
25	HTS 13291	-7.9	183	-53.22	148	-38.78	67	-83.21	63	-450.15	110	571
26	KM 06566	-12.45	28	-55.01	102	-30.39	189	-67.26	167	-458.23	90	576
27	KM 10368	-8.91	126	-53.34	144	-43.07	22	-102.64	4	-414.52	281	577
28	RDR 02782	-7.57	201	-71.01	2	-27.93	244	-73.01	124	-547.53	8	579
29	SEW 03687	-10.63	64	-54.62	112	-36.17	98	-72.21	130	-432.65	185	589
30	S 04453	-5.68	323	-53.44	142	-44.2	17	-103.59	3	-450.87	106	591
31	RJF 01981	-5.38	349	-60.88	26	-36.56	93	-73.51	122	-528.12	11	601

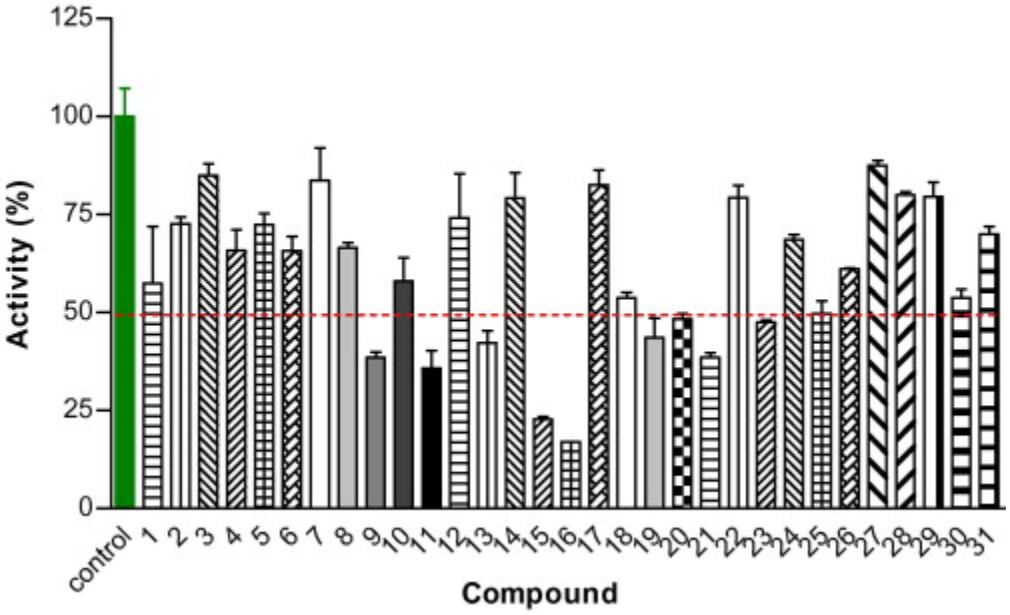

Figure 7.3. Inhibition of unregulated SecA ATPase activities by tested compounds at 100 μM

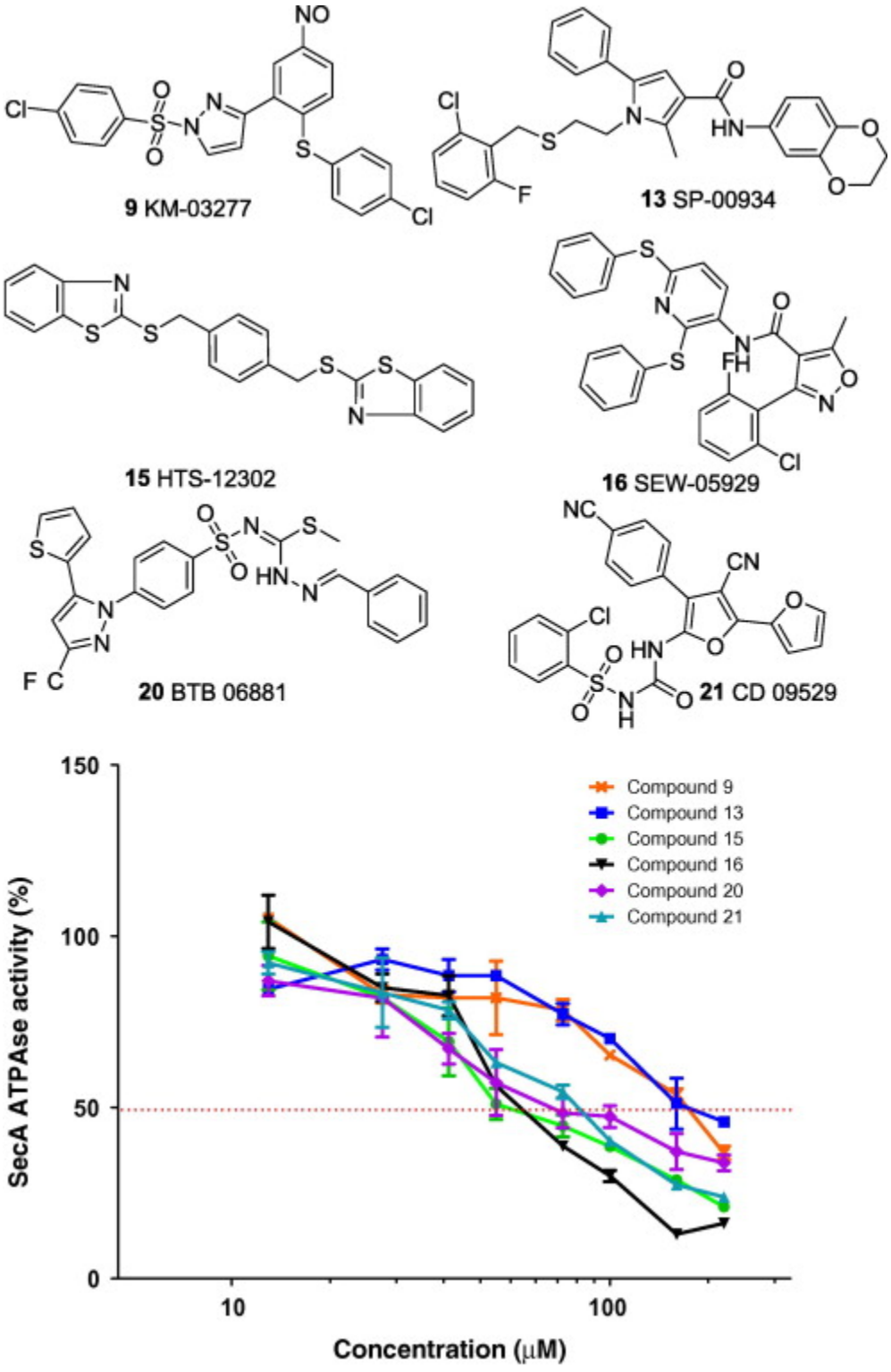

Figure 7.4. The chemical structures of SecA inhibitors and their inhibitory curves against *E. coli* SecA.

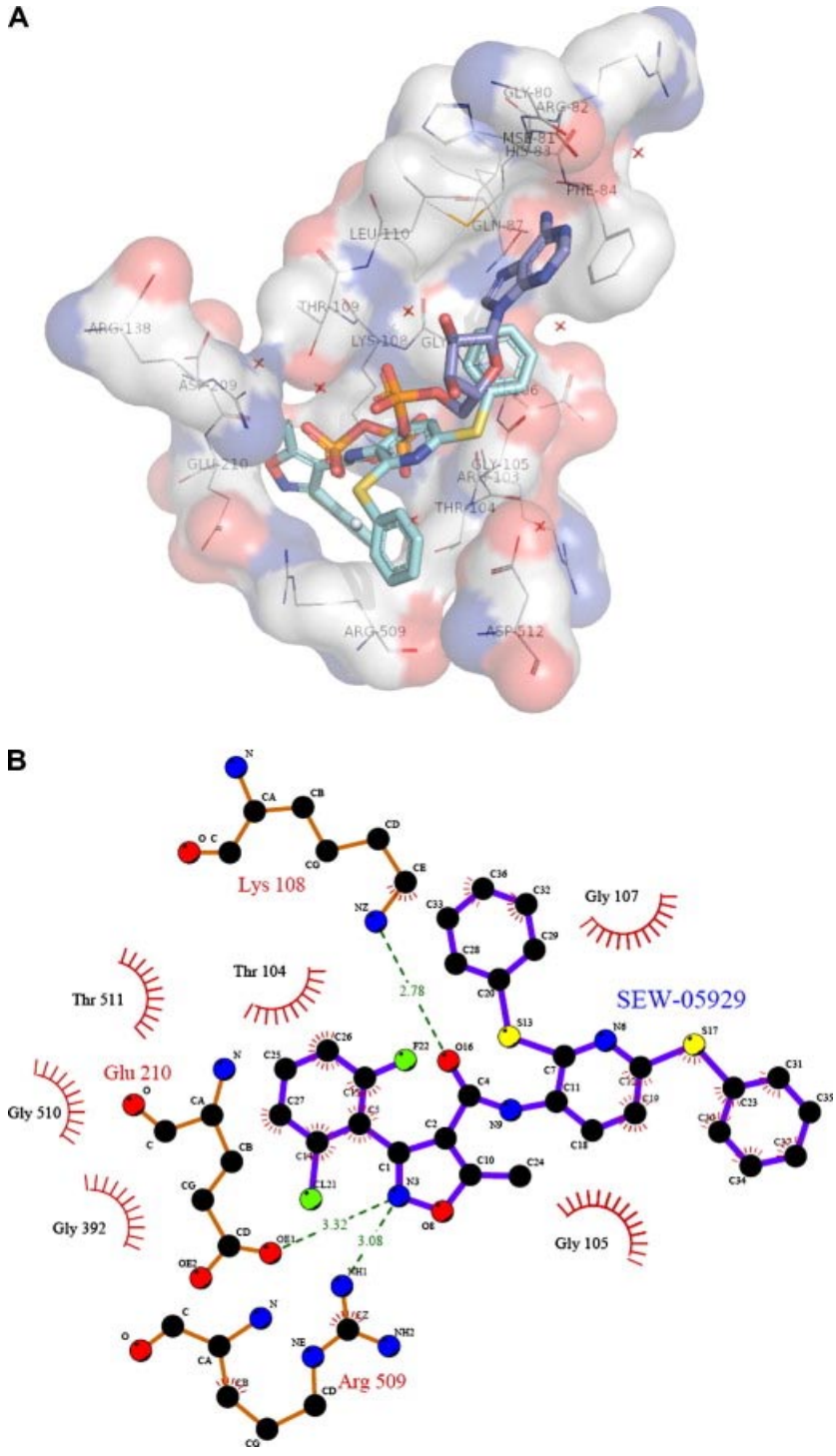

Figure 7.5. (A) The proposed docking conformation of compound 16 **(blue sticks) and ATP (purple sticks) around SecA ATP-site; (B) the proposed schematic interactions of compound** 16 **with SecA.** (For interpretation of color mentioned in this figure the reader is referred to the web version of the article.)

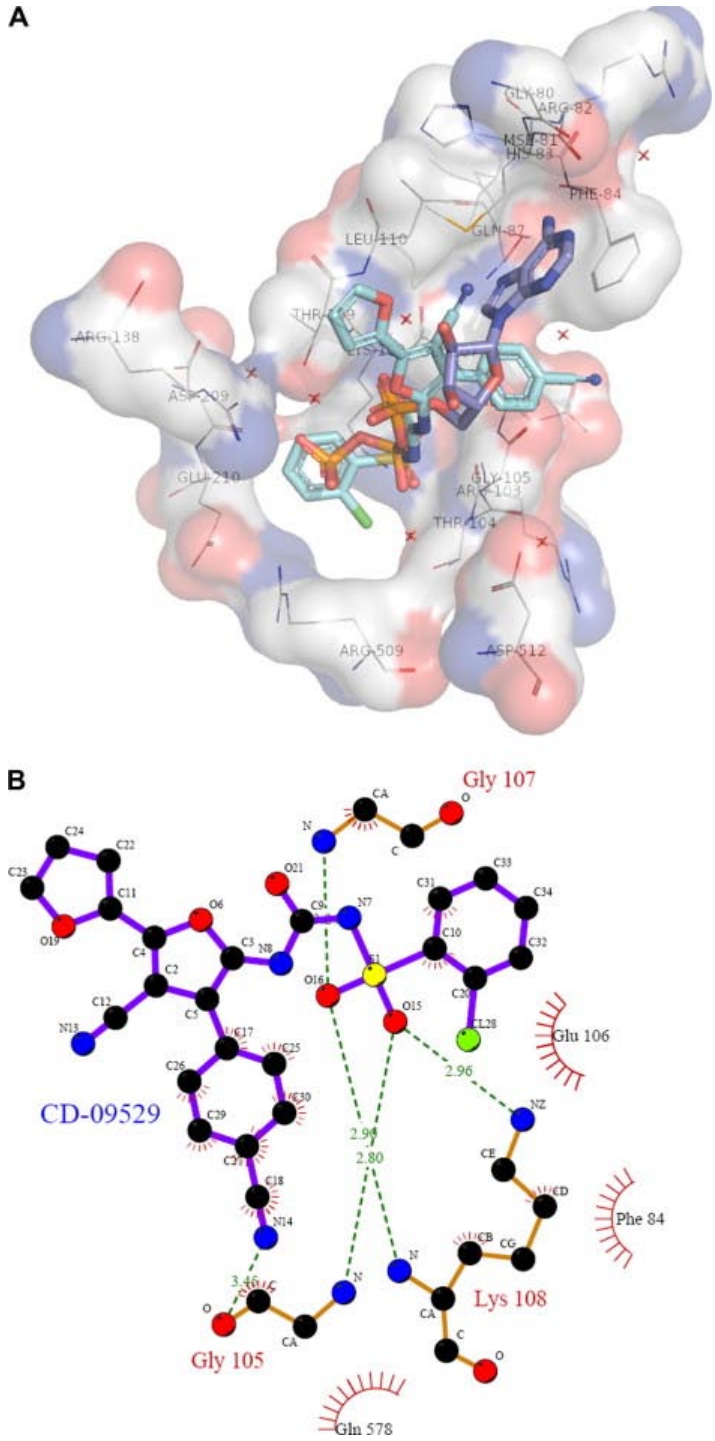

Figure 7.6. (A) The proposed docking conformation of compound 21 **(blue sticks) and ATP (purple sticks) around SecA ATP-site; (B) the proposed schematic interactions of compound** 21 **with SecA.** (For interpretation of color mentioned in this figure the reader is referred to the web version of the article.

Appendix B: First Low μM SecA Inhibitors

This work has been published by

Weixuan Chen, Ying-Ju Huang, Sushma Reddy Gundala, Hsiuchin Yang, Minyong Li, Phang C. Tai, and Binghe Wang, as part of

"The first low μM SecA inhibitors". (2010) *Bioorg Med Chem.*18(4):1617-25.

The biological assays were done by Y. Huang. The synthesis of chemicals was done by W. Chen, and the computer simulation was done by M. Li.

7.6 Abstract

SecA ATPase is a critical member of the Sec family, which is important in the translocation of membrane and secreted polypeptides/proteins in bacteria. Small molecule inhibitors can be very useful research tools as well as leads for future antimicrobial agent development. Based on previous virtual screening work, we optimized the structures of two hit compounds and obtained SecA ATPase inhibitors with IC_{50} in the single digit micromolar range. These represent the first low micromolar synthetic inhibitors of bacterial SecA and will be very useful for mechanistic studies.

7.7 Introduction

With the rapid emergence of drug resistant bacteria, there is an urgent need for the development of new antimicrobial agents, especially those with a unique mechanism of action. With this ultimate goal in mind, we are interested in the development of inhibitors of bacterial protein translocation. Several protein transport mechanisms exist in bacteria (Saier 2006). Among them, the Sec machinery (or translocase) provides a major pathway of protein translocation from the cytosol across or into the cytoplasmic membrane. The Sec machinery has seven proteins including SecA, SecD, SecE, SecF, SecG, SecY, and YajC. Assembly and complex formation are required to yield the functional translocase. Among the Sec proteins, SecA is found both in the cytoplasm and bound to the inner membrane. When SecA is bound to the SecYEG complex, acidic phospholipids and a precursor protein such as proOmpA (the precursor of outer membrane protein A), it becomes fully active as an ATPase and a protein translocase (Lill, Dowhan et al. 1990; van Klompenburg, Ridder et al. 1997). Recently, several seminal papers described in intricate

details as to how the SecA machinery functions in transporting proteins (Erlandson, Miller et al. 2008; Tsukazaki, Mori et al. 2008; Zimmer, Nam et al. 2008).

It has been said that in any given organism, membrane and secreted polypeptides/proteins comprise more than 30% of the proteome; and no less than 10% of proteins cross a membrane before arriving at their final locations of function (Mori and Ito 2001; Vrontou and Economou 2004). Such actions are often mediated by protein translocases. Therefore SecA is essential for bacterial survival. We envision that inhibitors of SecA can be very useful tools for studying bacterial protein transport and potential antimicrobial agents, especially because SecA has no human counterpart. We have previously reported effort in using virtual screening against the *Escherichia coli* SecA crystal structure (Papanikolau, Papadovasilaki et al. 2007) to search for possible structural features suitable for SecA inhibitor development (Li, Huang et al. 2008). In this paper, we describe our effort in optimizing the structural features of the initial hits for the development of bacterial SecA inhibitors. Several low μM inhibitors have been found. Considering the fact that currently inorganic azide, which is a SecA inhibitor with an IC_{50} value of about 3 mM, has cross reactivities against a number of enzymes (Stoddard, Ringe et al. 1990; Bowler, Montgomery et al. 2006) and is the primary research tool for probing bacterial protein translocation, the newly discovered SecA inhibitors will be very important.

7.8 Results and Discussions

7.8.1. Chemistry

In our earlier virtual screening efforts, two hits, **1** (SEW-05929) and **2** (HTS-12302), were shown to have modest SecA inhibitory activities (IC_{50} values of about 100 μM) (Li, Huang et al. 2008). In our earlier screening, these two compounds were found to have IC50 values of about 30 μM. However, upon more rigorous studies, 2 was found to have IC50 of 100 μM. 1 showed similar inhibition activities as 2, but started having solubility problems when approaching 100 μM. Since there were no other known SecA inhibitors except one natural product, for which the true inhibition mechanism was not known (Sugie, Inagaki et al. 2002), our effort to search for potent SecA inhibitors started with the optimization of these two modest inhibitors (Figure 7.7).

Our optimization effort first started with the isoxazole carboxamide series (**1**) with the focus being on optimizing the aryl group attached to the amide. In this series, 14 analogs were synthesized. The synthesis started with conversion of halogenated benzaldehyde **3** to the corresponding oxime **4** (Scheme 1). Isoxazole acid **6** was prepared by reacting **5** with ethyl acetoacetate followed by hydrolysis.(Maloney, Parks et al. 2000) Subsequent coupling/amidation reactions using EDCI and DMAP gave the final isoxazole carboxamide derivatives **7a-7n**. In this series, there were amides of aniline compounds **7a-g**, primary alkylamines **7h, i**, secondary alkyamines **7j-l**, and benzylamines **7m,n**.

In optimizing the second series (**2,** Figure 7.7), we first started by testing different aryl structures flanking the central ring. In our initial effort, 6-chloro-2-mercaptobenzothiazole and 2-mercaptobenzoxazole derivatives were prepared by react-

ing potassium ethylxanthate **8** with 2,4-dichloroaniline **9** or substituted 2-aminophenol **10** (Scheme 2). Further, 5-cyano-6-aryl-2-thiouracils were prepared “by condensation of an aldehyde with ethyl cyanoacetate and thiourea in the presence of piperidine”.(Abdou and Strekowski 2000) The symmetrical compounds **15a-g** or **16a-i** were obtained by reacting two equivalents of compounds **11a-g** or **14a-i** with *p*-xylylene dibromide in acetonitrile in the presence of K_2CO_3 (Scheme 3). One successful series of analogs was the 2,2'-(α,α’-xylene)bis(sulfanediyl)bis-(6-aryl-5-cyano-4-oxopyrimidine) **16a-i** (see below for biological results). For this series, we were interested in further simplifying the structure to understand the core structural need. Therefore, "monomer" series **17d,e,g-i** was prepared by benzylation of compounds **14d,e,g-i** with benzyl chloride, and the difference in activities between the "dimer" and "monomer" series was also studied.

7.8.2. Biological evaluation

7.8.2.1. In vitro study

The synthesized compounds were first evaluated using EcN68 SecA, which is a truncated version without the C-terminal regulatory/inhibitory domain, by following procedures published earlier (Li, Huang et al. 2008). Briefly, ATPase activities were determined by the release of phosphate (Pi), which can be detected spectrophotometrically using malachite green (Sugie, Inagaki et al. 2002). For compounds **7a-n,** none of them showed improved activities over the original hit (**1**) or significant inhibition at 100 μM (Figure 7.8). Such results coupled with the weak activities of the original hit compound led to the decision of not pursuing this class of compounds any further.

For analogs of **2,** compounds **15a-g** did not show significant improvement over the initial hit (data not shown). However, the substituted thiouracils (**16**) showed very significant activities when screened at 100 (data not shown) and 30 μM (Figure 7.9). Those compounds that showed potent inhibition at 30 μM were further screened at 5 μM (Figure 7.10). Within the symmetrical compound series **16a-i**, there were two substitution patterns: one with a phenyl ring substituted at the 4-position and the other with a phenyl ring substituted at the 3-position. The results showed that the 4-substituted analogs were more potent than the 3-substituted class, which was in turn slightly more potent than the ones without phenyl substituent. For example the activities of the 4-methyl substituted (**16c,** Figure 7.9) was higher than the 3-methyl analog (**16b,** Figure 7.9**)**, which was in turn higher than the unsubstituted one **(16a,** Figure 7.9). With the initial indication that derivatives with a phenyl ring bearing a 4-substituent were more active, the subsequent effort was focused on optimizing this series of compounds. One approach adopted was to use relatively bulky alkyl groups at the 4-position. It turned out that these compounds were more potent than the corresponding 4-methyl substituted compounds. Among these compounds, those with an electron donating (e.g., methoxy) substituent seemed to be less active than the unsubstituted ones (*e.g.*, **16f < 16a,** Figure 7.9). At 5 μM, analogs with a halogen or aryl group substitution at the 4-position were more potent than the analogues with an alkyl substitution (*e.g.*, **16g,h,i > 16c,d,e** Figure 7.10). For the examination of the difference between the “dimers” and “monomers”, *S*-benzyl-2-thiouracils analogues **17d, e, g-i** were also tested (Figure 7.11). First of all, both thiouracil-based “dimer” and “monomer” compounds showed more potent inhibition than the benzothiazole or benzoxazole compounds **15a-g**. However, the "dimer" series **16d,e,g-i** were more potent than

the "monomer" series **17d,e,g-i**, respectively. This higher potency for the “dimer” series seems to come from better fitting of the binding pocket of these compounds (see below). In the “monomer” series, it was observed that a large sized R’ group seemed to confer high potency (*e.g.*, **17h > 17g ≈ 17e > 17d**). However, when the substituented phenyl ring was replaced by a larger 1-naphthyl group, the activity seemed to decrease slightly.

We determined the IC_{50} values of compound **16 g** and **16 h** since they showed the most potent activities of all the compounds screened at 5 μM. The result showed they had low micro molar inhibition (IC_{50}: 2 μM, Figure 7.12), which is 50-fold more potent than the hit compound **2 (**IC_{50}: 100 μM) (Li, Huang et al. 2008).

Inhibition tests using whole EcSecA gave similar results (**16g** IC_{50}: 20 μM, **16h** IC_{50}: 50 μM and **17h** IC_{50}: 60 μM, Figure 7.13), which suggested that the EcN68 inhibition assay was more sensitive than the whole SecA inhibition assay. This is understandable since EcSecA contains a regulatory domain, which is essentially an inhibitor.

7.8.2.2. In vivo study

The biological activities of “dimer” and “monomer” compounds **16h** and **17h** were assessed against leaky mutant NR698 and wild-type *E. coli* strain MC4100 by determining the minimum inhibition concentration (MIC) (Figure 7.14). “Monomer” compound **17h** exhibited the most potent inhibition effects against NR698, whereas “dimer” compounds **16h** did not exhibit significantly antimicrobial activities. However, neither **17h** nor **16h** exhibited inhibition effects against wild-type *E. coli* strain MC4100. Such results suggested that the permeability of **16h** against NR698 and **17h** against MC4100

might be a key factor and for *in vivo* applications future studies should focus on low molecular weight compounds such as **17h** for structural optimization.

7.8.3. Computational modeling

In order to achieve a detailed understanding the binding mode between SecA and our compounds, *in silico* modeling was conducted by using molecular simulation (Li and Wang 2006; Li and Wang 2007; Li, Ni et al. 2008; Zheng, Kaur et al. 2008). Herein, the parent compound, HTS-12302 and the most active compound, **16g**, were docked into the ATP site of SecA using DOCK 5.4. The docked complexes were then optimized by molecular mechanics and molecular dynamics simulation implemented in AMBER 8. Finally, the possible ligand-protein interactions were examined by following similar procedures we used in previous studies (Li, Huang et al. 2008). After molecular simulation, compound HTS-12302 seems to bind SecA through interactions with Thr 104 by forming hydrogen bond and with Met 81, Phe 84, Gln 87, Gly 105, Glu 106, Gly 107, Lys 108, Thr 109, Leu 110, Gly 392 and Arg 509 through hydrophobic interactions (Figure 7.15). Compound **16g** has a similar binding conformation and orientation, in which it seems to engage in more hydrogen bond interactions with Phe 84, Gln 87, Lys 108 and Glu 210. Moreover, compound **16g** still bears hydrophobic interactions with Met 81, Thr 104, Gly 105, Glu 106, Gly 107, Leu 110 and Arg 509. Upon analysis of the structural features of these two compounds, it seems that the inclusion of the thiouracil moiety may contribute to the inhibitory activity because of more hydrophobic interaction and hydrogen bonds when compared with lead compound HTS-12302. Such structural insights will play a very critical role in future design of potent SecA inhibitors and in further structural optimizations.

7.8.4. Conclusion

Through optimization of two hit compounds **1** (SEW-05929) and **2** (HTS-12302) identified from virtual screening, we have found a series of thiouracil derivatives that are much more potent than the primary hits. The two most potent compounds, **16g** and **16h**, are 50-fold more active than the hit compounds. Results of antimicrobial tests suggest that future work should focus on low molecular weight analogs of **17h** for *in vivo* applications. These compounds are the first in its class and should be very useful as research tools in studying bacterial protein transport. The new inhibitory structural features identified should also be very useful for further structural optimization in search of even more potent inhibitors as potential antimicrobial agents.

7.9 Experimental

7.9.1. Chemistry

General Chemical Methods. All reagents and solvents were reagent grade or were purified by standard methods before use. Column chromatography was carried out on flash silica gel (Sorbent 230-400 mesh). TLC analysis was conducted on silica gel plates (Sorbent Silica G UV254). NMR spectra were recorded at ^{1}H (400 MHz) and ^{13}C (100 MHz) with a Bruker instrument. Chemical shifts (δ values) and coupling constants (J values) are given in ppm and Hz, respectively, using TMS (^{1}H NMR) and solvents (^{13}C NMR) as internal standards.

General procedure for the preparation of isoxazole carboxamide derivatives (7a-7n). Under N_2 atmosphere, a solution of an isoxazole carboxylic acid (**6**, 0.1 mmol), amine (0.12 mmol), EDCI (23 mg, 0.12 mmol), DMAP (14.7 mg, 0.12 mmol) and HOBt

(27 mg, 0.2 mmol) in DMF (2.5 mL) was stirred at room temperature overnight. Then most of the solvent was removed under reduced pressure. To the residue was added 10 mL H_2O and 10 mL EtOAc. Then the aqueous solution was extract by EtOAc (20 mL × 2). The organic layer was subsequently washed with brine (20 mL). The crude compound was purified by flash chromatography on silica gel using hexane and EtOAc (9:1) as the mobile phase to give **7a-7n**.

3-(2,6-Dichlorophenyl)-5-methyl-*N*-m-tolylisoxazole-4-carboxamide (7a). Yield 76%; ^{1}H NMR ($CDCl_3$) δ 1.70 (s, 3H), 2.86 (s, 3H), 6.74 (bs, 1H), 7.00-7.07 (m, 2H), 7.18 (td, 1H, *J* = 1.6 Hz, 7.2 Hz), 7.44 (dd, 1H, *J* = 6.4 Hz, 9.6 Hz), 7.50 (m, 2H), 7.90 (d, 1H, *J* = 8.0 Hz); ^{13}C NMR ($CDCl_3$) δ 13.7, 16.9, 112.0, 123.0, 125.4, 127.0, 127.3, 128.3, 129.1, 130.6, 132.7, 135.3, 136.6, 155.7, 159.0, 176.4. HRMS-ESI (+): Calc. for $C_{18}H_{15}N_2O_2Cl_2$: 361.0511. Found: 361.0527 $[M+H]^+$.

***N*-(3-Bromobenzyl)-3-(2,6-dichlorophenyl)isoxazole-4-carboxamide (7b).** Yield 71%; ^{1}H NMR ($CDCl_3$) δ 2.27 (s, 3H), 2.84 (s, 3H), 6.85 (m, 3H), 7.11 (m, 2H), 7.48 (dd, 1H, *J* = 6.4 Hz, 9.6 Hz), 7.54 (m, 2H); ^{13}C NMR ($CDCl_3$) δ 13.5, 21.7, 112.1, 117.1, 120.8, 125.8, 127.3, 129.0, 129.0, 132.7, 136.4, 137.2, 139.3, 155.9, 158.9, 175.7. HRMS-ESI (+): Calc. for $C_{18}H_{15}N_2O_2Cl_2$: 361.0511. Found: 361.0516 $[M+H]^+$.

(3-(2,6-Dichlorophenyl)-5-methylisoxazol-4-yl)(morpholino)methanone (7c). Yield 81%; ^{1}H NMR ($CDCl_3$) δ 1.63 (s, 3H), 2.18 (s, 3H), 2.80 (s, 3H), 6.62 (bs, 1H), 6.82 (s, 1H), 6.92 (d, 1H, *J* = 8.4 Hz), 7.37 (dd, 1H, *J* = 6.4 Hz, 9.6 Hz), 7.44 (m, 2H), 7.66 (d, 1H, *J* = 8.4 Hz); ^{13}C NMR ($CDCl_3$) δ 13.7, 16.9, 21.0, 112.0, 123.2, 127.4, 127.5, 128.6, 129.0, 131.2, 132.7, 135.3, 136.6, 155.7, 159.0, 176.2. HRMS-ESI (+): Calc. for $C_{19}H_{17}N_2O_2Cl_2$: 375.0667. Found: 375.0679 $[M+H]^+$.

(3-(2,6-Dichlorophenyl)-5-methylisoxazol-4-yl)(piperidin-1-yl)methanone (7d). Yield 67%; ^{1}H NMR ($CDCl_3$) δ 2.24 (s, 3H), 2.78 (s, 3H), 6.70 (dd, 1H, *J* = 2.4 Hz, 8.4 Hz), 6.75 (bs, 1H), 7.12 (d, 1H, *J* = 2.4 Hz), 7.29 (d, 1H, 8.8 Hz), 7.43 (dd, 1H, *J* = 6.4 Hz, 9.6 Hz), 7.49 (m, 2H), 7.62 (m, 5H); ^{13}C NMR ($CDCl_3$) δ 13.6, 23.3, 111.9, 118.8, 120.1, 122.2, 127.2, 129.0, 132.8, 132.8, 136.3, 136.5, 139.0, 155.8, 158.8, 175.9. HRMS-ESI (+): Calc. for $C_{18}H_{14}N_2O_2Cl_2Br$: 438.9616. Found: 438.9633 $[M+H]^+$.

3-(2,6-Dichlorophenyl)-*N*-(2,4-dimethylphenyl)-5-methylisoxazole-4-carboxamide (7e). Yield 55%; ^{1}H NMR ($CDCl_3$) δ 2.87 (s, 3H), 6.92-6.99 (m, 2H), 7.08 (t, 1H, *J* = 7.6 Hz), 7.20 (bs, 1H), 7.47 (dd, 1H, *J* = 6.4 Hz, 9.6Hz), 7.52 (m, 2H), 8.33 (td, 1H, *J* = 1.6 Hz, 8.0 Hz); ^{13}C NMR ($CDCl_3$) δ 13.7, 111.8, 114.7, 114.9, 121.6, 124.7, 124.8, 124.8, 124.8, 126.3, 129.1, 132.8, 136.3, 153.4, 155.9, 158.8, 176.4. HRMS-ESI (+): Calc. for $C_{17}H_{12}N_2O_2Cl_2F$: 365.0260. Found: 365.0269 $[M+H]^+$.

***N*-(3-Chlorophenyl)-3-(2,6-dichlorophenyl)-5-methylisoxazole-4-carboxamide (7f).** Yield 42%; ^{1}H NMR ($CDCl_3$) δ 2.79 (s, 3H), 6.81 (bs, 1H), 6.84 (m, 1H), 6.98 (m, 1H), 7.09 (t, 1H, *J* = 8.0 Hz), 7.30 (t, 1H, *J* = 1.6 Hz), 7.45(dd, 1H, *J* = 6.4 Hz, 9.6 Hz), 7.50 (m, 2H); ^{13}C NMR ($CDCl_3$) δ 90.2, 113.8, 128.2, 128.6, 132.0, 158.2, 160.2, 176.0. HRMS-ESI (+): Calc. for $C_{17}H_{12}N_2O_2Cl_3$: 380.9964. Found: 380.9962 $[M+H]^+$.

***N*-Cyclohexyl-3-(2,6-dichlorophenyl)-5-methylisoxazole-4-carboxamide (7g).** Yield 59%; ^{1}H NMR ($CDCl_3$) δ 2.83 (s, 3H), 6.83 (bs, 1H), 6.87 (m, 1H), 6.98 (t, 1H, *J* = 8.8 Hz), 7.42 (dd, 1H, *J* = 2.8 Hz, 6.8 Hz), 7.50 (dd, 1H, *J* = 6.4 Hz, 9.6 Hz), 7.55 (m, 2H); ^{13}C NMR ($CDCl_3$) δ 13.6, 111.7, 116.8, 117.0, 119.6, 119.7, 121.4, 121.6, 122.4, 127.1, 129.1, 132.9, 133.8, 136.3, 154.0, 155.7, 156.4, 158.9, 176.1. HRMS-ESI (+): Calc. for $C_{17}H_{11}N_2O_2FCl_3$: 398.9870. Found: 398.9885 $[M+H]^+$.

3-(2,6-Dichlorophenyl)-5-methyl-*N*-o-tolylisoxazole-4-carboxamide (7h). Yield 79%; ^{1}H NMR ($CDCl_3$) δ 0.83 (m, 2H), 1.04 (m, 1H), 1.19-1.32 (m, 4H), 1.39 (m, 1H), 2.02 (m, 2H), 2.73 (s, 3H), 3.74 (m, 1H), 5.02 (m, 1H), 7.39 (dd, 1H, *J* = 6.4 Hz, 9.6 Hz), 7.45 (m, 2H); ^{13}C NMR ($CDCl_3$) δ 13.3, 24.1, 25.5, 32.5, 47.4, 112.0, 127.8, 128.7, 132.4, 136.3, 156.1, 159.9, 174.7. HRMS-ESI (+): Calc. for $C_{17}H_{19}N_2O_2Cl_2$: 353.0824. Found: 353.0838 $[M+H]^+$.

***N*-(4-Bromo-3-methylphenyl)-3-(2,6-dichlorophenyl)-5-methylisoxazole-4-carboxamide (7i).** Yield 82%; ^{1}H NMR ($CDCl_3$) δ 0.28 (m, 2H), 0.65-0.70 (m, 4H), 0.81 (d, 2H, *J* = 6.8 Hz), 0.94 (m, 2H), 1.16-1.25 (m, 2H), 1.31-1.44 (m, 4H), 1.49-1.58 (m, 4H), 1.75 (m, 2H), 3.63 (m, 1H), 4.10 (m, 1H), 7.39-7.51 (m, 5H); ^{13}C NMR ($CDCl_3$) δ13.2, 13.4, 22.2, 22.3, 29.6, 29.8, 31.5, 31.9, 32.9, 33.6, 44.3, 48.3, 111.8, 112.0, 127.7, 127.9, 128.7, 128.9, 132.3, 132.6, 136.2, 136.4, 156.0, 156.2, 159.8, 160.0, 174.5, 175.3. HRMS-ESI (+): Calc. for $C_{18}H_{21}N_2O_2Cl_2$: 367.0980. Found: 367.0991 $[M+H]^+$.

(3-(2,6-Dichlorophenyl)-5-methylisoxazol-4-yl)(thiomorpholino)methanone (7j). Yield 85%; ^{1}H NMR ($CDCl_3$) δ 1.34 (bs, 4H), 1.52 (m, 2H), 2.56 (s, 3H), 3.38 (bs, 4H), 7.32 (m, 1H), 7.40 (m, 2H); ^{13}C NMR ($CDCl_3$) δ 12.4, 24.4, 25.9, 113.6, 127.7, 128.4, 131.5, 135.9, 157.5, 161.6, 169.6. HRMS-ESI (+): Calc. for $C_{16}H_{17}N_2O_2Cl_2$: 339.0667. Found: 339.0668$[M+H]^+$.

3-(2,6-Dichlorophenyl)-*N*-(2-fluorophenyl)-5-methylisoxazole-4-carboxamide (7k). Yield 84%; ^{1}H NMR ($CDCl_3$) δ 2.52 (s, 3H), 3.36 (bs, 8H), 7.30 (dd, 1H, *J* = 6.4 Hz, 9.6Hz), 7.37 (m, 2H); ^{13}C NMR ($CDCl_3$) δ 12.6, 66.7, 112.8, 127.4, 128.6, 131.8, 135.9, 157.3, 161.9, 170.4. HRMS-ESI (+): Calc. for $C_{15}H_{15}N_2O_3Cl_2$: 341.0460. Found: 341.0466 $[M+H]^+$.

***N*-(3-Chloro-4-fluorophenyl)-3-(2,6-dichlorophenyl)-5-methylisoxazole-4-carboxamide (7l).** Yield 72%; ^{1}H NMR ($CDCl_3$) δ 2.30 (bs, 4H), 2.52 (s, 3H), 3.62 (bs, 4H), 7.30 (dd, 1H, *J* = 6.4 Hz, 9.6Hz), 7.37 (m, 2H); ^{13}C NMR ($CDCl_3$) δ 12.6, 27.8, 113.0, 127.4, 128.6, 131.9, 135.9, 157.2, 162.2, 170.4. HRMS-ESI (+): Calc. for $C_{15}H_{15}N_2O_2SCl_2$: 357.0231. Found: 357.0237 $[M+H]^+$.

***N*-(2-Bromobenzyl)-3-(2,6-dichlorophenyl)-5-methylisoxazole-4-carboxamide (7m).** Yield 73%; ^{1}H NMR ($CDCl_3$) δ 2.73 (s, 3H), 4.37 (d, 2H, *J* = 6.0 Hz), 5.62 (bs, 1H), 7.04 (m, 1H), 7.16 (m, 2H), 7.26-7.33 (m, 3H), 7.38 (d, 1H, *J* = 8.0 Hz); ^{13}C NMR ($CDCl_3$) δ 13.4, 43.9, 111.6, 123.9, 127.3, 127.9, 128.8, 129.5, 130.6, 132.3, 132.8, 136.2, 136.9, 156.1, 160.6, 175.2. HRMS-ESI (+): Calc. for $C_{18}H_{14}N_2O_2Cl_2Br$: 438.9616. Found: 438.9627 $[M+H]^+$.

3-(2,6-Dichlorophenyl)-5-methyl-*N*-(4-methylcyclohexyl)isoxazole-4-carboxamide (mixture of cis & trans) (7n). Yield 93%; ^{1}H NMR ($CDCl_3$) δ 2.74 (s, 3H), 4.28 (d, 2H, *J* = 5.6 Hz), 5.27 (bs, 1H), 6.91 (d, 1H, *J* = 7.2 Hz), 7.04 (m, 2H), 7.29 (d, 2H, *J* = 7.6 Hz), 7.34 (d, 2H, *J* = 7.6 Hz); ^{13}C NMR ($CDCl_3$) δ 13.4, 42.9, 111.5, 122.9, 126.2, 127.3, 128.8, 130.2, 130.4, 132.5, 136.0, 139.8, 156.1, 160.7, 175.2. HRMS-ESI (+): Calc. for $C_{18}H_{14}N_2O_2Cl_2Br$: 438.9616. Found: 438.9635 $[M+H]^+$.

General procedures for the preparation of and 2-mercaptobenzoxazole (11b – 11g). To a solution of a substituted 2-aminophenol (3 mmol) was added potassium ethylxanthate (484 mg, 3 mmol) in absolute ethanol (10 mL). The resulting mixture was heated under reflux overnight and then cooled to room temperature. The precipitate was dissolved in H_2O (10 mL) and washed with ethyl acetate (10 mL × 3) and the aqueous

solution was then neutralized to pH = 5 by slow addition of glacial acetic acid. Then the product precipitated (crystallized) out to give **11b – 11g**.

2-Mercaptobenzoxazole (11b). Yield 52%; ^{1}H NMR (DMSO-d_6) δ 7.29 (m, 3H), 7.53 (d, 1H, J = 7.6 Hz), 13.90 (bs, 1H); ^{13}C NMR (DMSO-d_6) δ 110.0, 110.5, 123.7, 125.1, 131.2, 148.1, 180.1. HRMS-ESI (+): Calc. for C_7H_6NOS: 152.0170. Found: 152.0170 $[M+H]^+$.

2-Mercapto-5-methylbenzoxazole (11c). Yield 45%; ^{1}H NMR (DMSO-d_6) δ 2.37 (s, 3H), 7.05 (m, 2H), 7.34 (m, 1H), 13.73 (bs, 1H); ^{13}C NMR (DMSO-d_6) δ 20.8, 109.4, 110.4, 124.2, 131.2, 134.7, 146.3, 180.2. HRMS-ESI (+): Calc. for C_8H_8NOS: 166.0327. Found: 166.0333 $[M+H]^+$.

2-Mercapto-6-methylbenzoxazole (11d). Yield 64%; ^{1}H NMR (DMSO-d_6) δ 2.39 (s, 3H), 7.10 (d, 1H, J = 7.6 Hz), 7.16 (t, 1H, J = 7.6 Hz), 7.31 (d, 1H, J = 7.6 Hz), 13.95 (bs, 1H); ^{13}C NMR (DMSO-d_6) δ 16.1, 107.2, 121.1, 123.6, 126.0, 130.4, 147.9, 180.1. HRMS-ESI (+): Calc. for C_8H_8NOS: 166.0327. Found: 166.0333 $[M+H]^+$.

2-Mercapto-3-nitrobenzoxazole (11e). Yield 14%; ^{1}H NMR (DMSO-d_6) δ 7.44 (t, 1H, J = 8.0Hz), 7.91 (d, 1H, J = 8.0 Hz), 8.06 (d, 1H, J = 8.0 Hz); ^{13}C NMR (DMSO-d_6) δ 115.8, 119.8, 123.4, 128.0, 131.4, 149.8, 181.7. HRMS-ESI (+): Calc. for $C_7H_5N_2O_3S$: 197.0021. Found: 197.0013 $[M+H]^+$.

2-Mercapto-5-nitrobenzoxazole (11f). Yield 25%; ^{1}H NMR (DMSO-d_6) δ 7.17 (d, 1H, J = 8.8 Hz), 7.95 (d, 1H, J = 2.4 Hz), 7.99 (dd, 1H, J = 2.4 Hz, 8.8 Hz); ^{13}C NMR (DMSO-d_6) δ 101.8, 112.3, 119.8, 139.7, 150.3, 153.2, 188.4. HRMS-ESI (+): Calc. for $C_7H_5N_2O_3S$: 197.0021. Found: 197.0018 $[M+H]^+$.

2-Mercapto-5-chlorobenzoxazole (11g). Yield 36%; ^{1}H NMR (DMSO-d_6) δ 7.30 (d, 2H, J = 7.6 Hz), 7.53 (d, 1H, J = 8.0 Hz), 14.04 (bs, 1H); ^{13}C NMR (DMSO-d_6) δ 110.3, 111.2, 123.5, 129.3, 132.6, 147.0, 180.8. HRMS-ESI (+): Calc. for C_7H_5NOSCl: 185.9780. Found: 185.9789 [M+H]+.

General procedures for the preparation of 2-thiouracils 14a – 14i. To a solution of an aldehyde (RCHO, 10 mmol), ethyl cyanoacetate (1.0 mL, 10 mmol), and thiourea (0.76 g, 10 mmol) in absolute ethanol (50 mL) was added piperidine (2.0 mL, 20 mmol); the mixture was heated under reflux overnight and then cooled to room temperature. The precipitate was dissolved in 0.5M NaOH (20 mL) and washed with ethyl acetate (10 mL × 3). The aqueous solution was then neutralized to pH = 2 by slow addition of 1M HCl. Then the product precipitated (crystallized) out to give **14a – 14i**.

5-Cyano-6-phenyl-2-thiouracil (14a). Yield 67%; ^{1}H NMR (DMSO-d_6) δ 7.62 (m, 5H), 13.19 (s, 1H), 13.32 (bs, 1H); ^{13}C NMR (DMSO-d_6) δ 90.2, 113.8, 128.2, 128.6, 132.0, 158.2, 160.2, 176.0. MS-ESI (+): 252.0 $[M+Na]^+$.

5-Cyano-6-(3-tolyl)-2-thiouracil (14b). Yield 31%; ^{1}H NMR (DMSO-d_6) δ 2.39 (s, 3H), 7.46 (m, 4H), 13.17 (s, 1H), 13.26 (bs, 1H); ^{13}C NMR (DMSO-d_6) δ 20.9, 90.6, 114.7, 125.9, 128.4, 129.1, 129.2, 132.8, 137.9, 158.5, 160.9, 176.2. HRMS-ESI (+): Calc. for $C_{12}H_{10}N_3OS$: 244.0545. Found: 244.0555 $[M+H]^+$.

5-Cyano-6-(4-tolyl)-2-thiouracil (14c). Yield 43%; ^{1}H NMR (DMSO-d_6) δ 2.45 (s, 3H), 7.41 (d, 2H, J = 7.6 Hz), 7.61 (d, 2H, J = 8.4 Hz); ^{13}C NMR (DMSO-d_6) δ 12.2, 81.7, 105.9, 118.4, 120.1, 121.2, 135.3, 150.9, 153.2, 168.2. HRMS-ESI (+): Calc. for $C_{13}H_{12}N_3OS$: 258.0701. Found: 258.0702 $[M+H]^+$.

5-Cyano-6-(4-ethylphenyl)-2-thiouracil (14d). Yield 25%; ^{1}H NMR (DMSO-d_6) δ 1.22 (t, 3H, J = 7.6 Hz), 2.71 (q, 2H, J = 7.6 Hz), 7.42 (d, 2H, J = 8.0 Hz), 7.61 (d, 2H, J = 8.0 Hz), 13.15 (bs, 1H); ^{13}C NMR (DMSO-d_6) δ 15.2, 28.1, 90.4, 114.8, 126.6, 127.9, 128.9, 148.6, 158.5, 160.9, 176.2. HRMS-ESI (+): Calc. for $C_{14}H_{14}N_3OS$: 272.0858. Found: 272.0867 $[M+H]^+$.

5-Cyano-6-(4-isopropylphenyl)-2-thiouracil (14e). Yield 37%; ^{1}H NMR (DMSO-d_6) δ 1.24 (d, 6H, J = 6.8 Hz), 3.00 (septet, 1H, J = 6.8 Hz), 7.46 (d, 2H, J = 8.0 Hz), 7.62 (d, 2H, J = 8.0 Hz), 13.15 (bs, 2H); ^{13}C NMR (DMSO-d_6) δ 23.6, 33.5, 90.3, 114.9, 126.5, 126.7, 129.0, 153.1, 158.6, 160.8, 176.2. HRMS-ESI (+): Calc. for $C_{14}H_{14}N_3OS$: 272.0858. Found: 272.0867 $[M+H]^+$.

5-Cyano-6-(4-methoxyphenyl)-2-thiouracil (14f). Yield 21%; ^{1}H NMR (DMSO-d_6) δ 3.86 (s, 3H), 7.12 (d, 2H, J = 8.8 Hz), 7.68 (d, 2H, J = 8.8 Hz), 13.13 (bs, 2H); ^{13}C NMR (DMSO-d_6) δ 55.7, 89.9, 114.0, 115.2, 121.1, 131.0, 158.8, 160.6, 162.5, 176.3. HRMS-ESI (+): Calc. for $C_{12}H_{10}N_3O_2S$: 260.0494. Found: 260.0496 $[M+H]^+$.

5-Cyano-6-(4-bromophenyl)-2-thiouracil (14g). Yield 39%; ^{1}H NMR (DMSO-d_6) δ 7.63 (d, 2H, J = 8.4 Hz), 7.80 (d, 2H, J = 8.4 Hz), 13.21 (s, 1H), 13.37 (bs, 1H); ^{13}C NMR (DMSO-d_6) δ 91.1, 114.6, 125.9, 128.5, 130.9, 131.6, 158.4, 160.0, 176.2. HRMS-ESI (+): Calc. for $C_{11}H_7N_3OSBr$: 307.9493. Found: 307.9504 $[M+H]^+$.

5-Cyano-6-(biphenyl-4-yl)-2-thiouracil (14h). Yield 75%; ^{1}H NMR (DMSO-d_6) δ 7.45 (t, 1H, J = 7.2 Hz), 7.53 (t, 2H, J = 7.2 Hz), 7.78 (d, 4H, J = 8.4 Hz), 7.89 (d, 2H, J = 8.4Hz) 13.19 (s, 1H), 13.35 (bs, 1H); ^{13}C NMR (DMSO-d_6) δ 90.6, 114.8, 126.6, 127.0, 128.1, 128.4, 129.2, 129.6, 138.7, 143.7, 158.5, 160.5, 176.2. HRMS-ESI (+): Calc. for $C_{17}H_{12}N_3OS$: 306.0701. Found: 306.0714 $[M+H]^+$.

5-Cyano-6-(1-naphthyl)-2-thiouracil (14i). Yield 22%; ^{1}H NMR (DMSO-d_6) δ 7.64 (m, 3H), 7.74 (d, 1H, *J* = 6.8 Hz), 7.99 (dd, 1H, *J* = 6.0 Hz, 6.4 Hz), 8.06 (dd, 1H, *J* = 6.0 Hz, 6.4 Hz,), 8.15 (d, 1H, *J* = 8.4 Hz), 13.11 (s, 1H), 13.46 (bs, 1H); ^{13}C NMR (DMSO-d_6) δ 93.1, 114.5, 124.7, 125.2, 126.8, 127.2, 127.5, 128.3, 128.5, 129.5, 131.2, 132.8, 158.7, 161.1, 176.8. HRMS-ESI (+): Calc. for $C_{15}H_{10}N_3OS$: 280.0545. Found: 280.0554 $[M+H]^+$.

General procedure for the preparation of 2,2'-(α,α'-Xylene)bis(sulfanediyl)bisbenzothiazole (15a), 2,2'-(α,α'-Xylene)bis(sulfanediyl)bisbenzoxazole (15b-g), and 2,2'-(α,α'-Xylene)bis(sulfanediyl)bis-4-oxopyrimidine (16a-i). To a solution of the 2-mercaptobenzothiazole, 2-mercaptobenzoxazole, or 2-thiouracil derivatives (**11a-g or 10a-h**, 0.1 mmol) and α, α'-xylenedibromide (12 mg, 0.045 mmol) in acetonitrile (2.5 mL) was added K_2CO_3 (42 mg, 0.3 mmol). The mixture was heated under reflux over-night and then cooled to room temperature. The liquid was removed on a rotavapor and the residue was washed with 0.5M NaOH (20 mL). Then the white solid residue was dried in vacuum oven at 40 ºC overnight to give **15a-15g** or **16a-16h**.

2,2'-(α,α'-Xylene)bis(sulfanediyl)bis-(6-chlorobenzothiazole) (15a). Yield 84%; ^{1}H NMR (DMSO-d_6) δ 4.62 (s, 4H), 7.45 (s, 4H), 7.47 (dd, 2H, *J* = 2.0 Hz, 8.4 Hz), 7.84 (d, 2H, *J* = 8.4 Hz), 8.11 (d, 2H, *J* = 2.0 Hz); ^{13}C NMR (DMSO-d_6) δ 36.3, 120.8, 121.7, 126.2, 128.7, 135.4, 135.9, 151.0, 166.6. HRMS-ESI (+): Calc. for $C_{22}H_{15}N_2S_4Cl_2$: 504.9495. Found: 504.9499 $[M+H]^+$.

2,2'-(α,α'-Xylene)bis(sulfanediyl)bis(benzoxazole) (15b). Yield 35%; ^{1}H NMR (DMSO-d_6) δ 4.60 (s, 4H), 7.34 (m, 4H), 7.49 (m, 4H), 7.65 (m, 4H); ^{13}C NMR (DMSO-

d$_6$) δ 35.1, 110.2, 118.3, 124.3, 124.6, 129.2, 136.1, 141.2, 151.3, 163.8. HRMS-ESI (+): Calc. for $C_{22}H_{17}N_2O_2S_2$: 405.0731. Found: 405.0732$[M+H]^+$.

2,2'-(α,α'-Xylene)bis(sulfanediyl)bis-(5-methylbenzoxazole) (15c). Yield 57%; ^{1}H NMR (DMSO-*d*$_6$) δ 2.40 (s, 6H), 4.57 (s, 4H), 7.12 (d, 2H, *J* = 8.0 Hz), 7.46 (m, 8H); ^{13}C NMR (DMSO-*d*$_6$) δ 20.9, 35.1, 109.6, 118.3, 125.1, 129.2, 134.0, 136.2, 141.4, 149.5, 163.6. HRMS-ESI (+): Calc. for $C_{24}H_{21}N_2O_2S_2$: 433.1044. Found: 433.1041 $[M+H]^+$.

2,2'-(α,α'-Xylene)bis(sulfanediyl)bis-(6-methylbenzoxazole) (15d). Yield 86%; ^{1}H NMR (DMSO-*d*$_6$) δ 2.49 (s, 6H), 4.59 (s, 4H), 7.18 (m, 4H), 7.43 (d, 2H, *J* = 7.6 Hz), 7.49 (s, 4H); ^{13}C NMR (DMSO-*d*$_6$) δ 16.0, 35.2, 107.5, 124.0, 125.1, 128.3, 129.3, 136.2, 140.4, 151.0, 162.6. HRMS-ESI (+): Calc. for $C_{24}H_{21}N_2O_2S_2$: 433.1044. Found: 433.1050 $[M+H]^+$.

2,2'-(α,α'-Xylene)bis(sulfanediyl)bis-(4-nitrobenzoxazole) (15e). Yield 61%; ^{1}H NMR (DMSO-*d*$_6$) δ 4.66 (s, 4H), 7.50 (t, 4H, *J* = 8.0 Hz), 7.52 (s, 4H), 8.01 (d, 2H, *J* = 8.0 Hz), 8.08 (d, 2H, *J* = 8.0 Hz); ^{13}C NMR (DMSO-*d*$_6$) δ 35.3, 115.6, 119.8, 123.5, 128.8, 135.4, 136.9, 152.6, 168.1. HRMS-ESI (+): Calc. for $C_{22}H_{15}N_4O_6S_2$: 495.0433. Found: 495.0438 $[M+H]^+$.

2,2'-(α,α'-Xylene)bis(sulfanediyl)bis-(6-nitrobenzoxazole) (15f). Yield 81%; ^{1}H NMR (DMSO-*d*$_6$) δ 4.67 (s, 4H), 7.53 (s, 4H), 7.85 (d, 2H, *J* = 8.4 Hz), 8.27 (dd, 2H, *J* = 2.0 Hz, 8.4 Hz), 8.62 (d, 2H, *J* = 2.0 Hz); ^{13}C NMR (DMSO-*d*$_6$) δ 35.4, 106.9, 118.2, 121.0, 129.4, 135.9, 143.9, 146.6, 150.6, 170.0. HRMS-ESI (+): Calc. for $C_{22}H_{15}N_4O_6S_2$: 495.0433. Found: 495.0431 $[M+H]^+$.

2,2'-(α,α'-Xylene)bis(sulfanediyl)bis-(5-chlorobenzoxazole) (15g). Yield 49%; ^{1}H NMR (DMSO-d_6) δ4.60 (s, 4H), 7.36 (dd, 2H, J = 2.0 Hz, 8.8 Hz), 7.48 (s, 4H), 7.67 (d, 2H, J = 8.8 Hz), 7.76 (d, 2H, J = 2.0 Hz); ^{13}C NMR (DMSO-d_6) δ 35.2, 111.5, 118.1, 124.3, 129.0, 129.3, 136.0, 142.5, 150.1, 165.9. HRMS-ESI (+): Calc. for $C_{22}H_{15}N_2O_2S_2Cl_2$: 472.9952. Found: 472.9974 $[M+H]^+$.

2,2'-(α,α'-Xylene)bis(sulfanediyl)bis-(6-phenyl-5-cyano-4-oxopyrimidine) (16a). Yield 80%; ^{1}H NMR (DMSO-d_6) δ 4.26 (s, 4H), 7.31 (s, 4H), 7.44 (m, 6H), 7.77 (m, 4H); ^{13}C NMR (DMSO-d_6) δ 33.6, 88.8, 119.9, 127.8, 127.9, 128.6, 129.3, 137.2, 137.7, 166.8, 170.3, 171.5. HRMS-ESI (-): Calc. for $C_{30}H_{19}N_6O_2S_2$: 559.1011. Found: 559.0989 $[M-H]^-$.

2,2'-(α,α'-Xylene)bis(sulfanediyl)bis-(6-(3-tolyl)-5-cyano-4-oxopyrimidine) (16b). Yield 62%; ^{1}H NMR (DMSO-d_6) δ 2.35 (s, 6H), 4.24 (s, 4H), 7.31 (m, 8H), 7.54 (s, 4H); ^{13}C NMR (DMSO-d_6) δ 21.0, 33.6, 88.9, 120.1, 125.3, 127.9, 128.6, 128.8, 130.2, 137.2, 137.4, 137.8, 167.2, 170.5, 171.6. HRMS-ESI (-): Calc. for $C_{32}H_{23}N_6O_2S_2$: 587.1324. Found: 587.1348 $[M-H]^-$.

2,2'-(α,α'-Xylene)bis(sulfanediyl)bis-(6-(4-tolyl)-5-cyano-4-oxopyrimidine) (16c). Yield 80%; ^{1}H NMR (DMSO-d_6) δ 2.36 (s, 6H), 4.25 (s, 4H), 7.26 (d, 4H, J = 8.0 Hz), 7.32 (s, 4H), 7.68 (d, 4H, J = 8.0 Hz); ^{13}C NMR (DMSO-d_6) δ 21.0, 33.7, 88.6, 120.2, 128.1, 128.6, 128.9, 134.9, 137.4, 139.4, 166.9, 170.7, 171.7. HRMS-ESI (-): Calc. for $C_{32}H_{23}N_6O_2S_2$: 587.1324. Found: 587.1306 $[M-H]^-$.

2,2'-(α,α'-Xylene)bis(sulfanediyl)bis-(6-(4-ethylphenyl)-5-cyano-4-oxopyrimidine) (16d). Yield 96%; ^{1}H NMR (DMSO-d_6) δ 1.21 (t, 6H, J = 7.6 Hz), 2.65 (q, 4H, J = 7.6 Hz), 4.26 (s, 4H), 7.29 (d, 4H, J = 8.0 Hz), 7.32 (s, 4H), 7.70 (d, 4H, J =

8.0 Hz); ^{13}C NMR (DMSO-d_6) δ 15.5, 28.1, 33.7, 88.6, 120.3, 127.5, 128.2, 128.9, 135.2, 137.4, 145.6, 166.9, 170.7, 171.7. HRMS-ESI (-): Calc. for $C_{34}H_{27}N_6O_2S_2$: 615.1637. Found: 615.1613 $[M-H]^-$.

2,2'-(α,α'-Xylene)bis(sulfanediyl)bis-(6-(4-isopropylphenyl)-5-cyano-4-oxopyrimidine) (16e). Yield 87%; ^{1}H NMR (DMSO-d_6) δ 1.25 (d, 12H, J = 7.2 Hz), 2.98 (septet, 2H, J = 7.2 Hz), 4.52 (s, 4H), 7.36 (s, 4H), 7.38 (d, 4H, J = 8.4 Hz), 7.87 (d, 4H, J = 8.0 Hz); ^{13}C NMR (DMSO-d_6) δ 22.7, 32.7, 33.7, 91.8, 114.9, 125.8, 128.2, 128.4, 132.2, 135.3, 152.1, 161.1, 165.3, 166.4. HRMS-ESI (-): Calc. for $C_{36}H_{31}N_6O_2S_2$: 643.1950. Found: 643.1943 $[M-H]^-$.

2,2'-(α,α'-Xylene)bis(sulfanediyl)bis-(6-(4-methoxyphenyl)-5-cyano-4-oxopyrimidine) (16f). Yield 46%; ^{1}H NMR (DMSO-d_6) δ 3.81(s, 6H), 4.28 (s, 4H), 6.97 (d, 4H, J = 8.8 Hz), 7.30 (s, 4H), 7.82 (d, 4H, J = 8.8 Hz); ^{13}C NMR (DMSO-d_6) δ 33.7, 55.3, 88.2, 113.5, 120.4, 128.9, 129.8, 130.0, 137.4, 160.6, 166.3, 170.6, 171.4. HRMS-ESI (-): Calc. for $C_{32}H_{23}N_6O_4S_2$: 619.1222. Found: 619.1230 $[M-H]^-$.

2,2'-(α,α'-Xylene)bis(sulfanediyl)bis-(6-(4-bromophenyl)-5-cyano-4-oxopyrimidine) (16g). Yield 95%; ^{1}H NMR (DMSO-d_6) δ 4.25 (s, 4H), 7.31 (s, 4H), 7.67 (d, 4H, J = 8.4 Hz), 7.72 (d, 4H, J = 8.8 Hz); ^{13}C NMR (DMSO-d_6) δ 33.7, 88.9, 119.9, 123.3, 128.9, 130.2, 131.1, 136.8, 137.3, 165.9, 170.2, 171.8. HRMS-ESI (-): Calc. for $C_{30}H_{18}Br_2N_6O_2S_2$: 714.9221. Found: 714.9213 $[M-H]^-$.

2,2'-(α,α'-Xylene)bis(sulfanediyl)bis-(6-(biphenyl-4-yl)-5-cyano-4-oxopyrimidine) (16h). Yield 68%; ^{1}H NMR (DMSO-d_6) δ 4.28 (s, 4H), 7.35 (s, 4H), 7.40 (t, 2H, J = 7.2 Hz), 7.49 (t, 4H, J = 7.6 Hz), 7.75 (m, 8H), 7.88 (d, 4H, J = 8.4 Hz); ^{13}C NMR (DMSO-d_6) δ 33.7, 88.8, 120.3, 126.3, 126.8, 127.8, 128.7, 128.9, 129.0,

136.7, 137.4, 139.5, 141.3, 166.4, 170.4, 171.8. HRMS-ESI (-): Calc. for $C_{42}H_{27}N_6O_2S_2$: 711.1637. Found: 711.1661 $[M-H]^-$.

2,2'-(α,α'-Xylene)bis(sulfanediyl)bis-(6-(1-naphthyl)-5-cyano-4-oxopyrimidine) (16i). Yield 92%; ^{1}H NMR (CD_3OD) δ 4.37 (s, 4H), 7.32 (s, 4H), 7.44-7.57 (m, 8H), 7.74 (d, 2H, *J* = 8.0 Hz), 7.91 (d, 2H, *J* = 8.2 Hz), 7.96 (dd, 2H, *J* = 2.0 Hz, 7.0 Hz); ^{13}C NMR (CD_3OD) δ 35.7, 94.1, 119.1, 126.2, 126.5, 127.4, 127.8, 127.9, 129.5, 130.3, 130.9, 132.0, 135.2, 136.6, 138.5, 171.6, 174.0, 175.0. HRMS-ESI (-): Calc. for $C_{38}H_{23}N_6O_2S_2$: 659.1324. Found: 659.1343 $[M-H]^-$.

General procedure for the preparation of *S*-benzyl-2-thiouracils (17d, e, g-i). To a solution of the 2-thiouracil derivatives (**10d**, **e, g-i**, 2 mmol) and benzylchloride (253 mg, 2 mmol) in acetonitrile (10 mL) was added K_2CO_3 (829 mg, 6 mmol). The mixture was heated under reflux for 8 h and then cooled to room temperature. The liquid was removed on a rotavapor, and the residue was washed by H_2O (20 mL). Then the solid was dried in a vacuum oven at 40 ºC overnight to give **17d, e, g-i**.

***S*-Benzyl-5-cyano-6-(4-ethylphenyl)-2-thiouracil (17d).** Yield 28%; ^{1}H NMR (DMSO-d_6) δ 1.27 (t, 3H, *J* = 7.6 Hz), 2.71 (q, 2H, *J* = 7.6 Hz), 4.40 (s, 2H), 7.21 (m, 1H), 7.28 (m, 4H), 7.41 (d, 2H, *J* = 7.2 Hz), 7.74(d, 2H, *J* = 8.4 Hz); ^{13}C NMR (DMSO-d_6) δ 16.0, 29.8, 36.0, 90.6, 120.1, 128, 128.8, 129.2, 129.4, 129.8, 130.1, 136.0, 139.8, 148.2, 170.2, 174.9. HRMS-ESI (+): Calc. for $C_{20}H_{18}N_3OS$: 348.1171. Found: 348.1185 $[M+H]^+$.

***S*-Benzyl-5-cyano-6-(4-isopropylphenyl)-2-thiouracil (17e).** Yield 40%; ^{1}H NMR (DMSO-d_6) δ 1.23 (d, 6H, *J* = 6.8 Hz), 2.94 (septet, 1H, *J* = 6.8 Hz), 4.30 (s, 2H), 7.22 (t, 1H, *J* = 6.8 Hz), 7.31 (m, 4H), 7.40 (d, 2H, *J* = 7.2 Hz), 7.73 (d, 2H, *J* = 7.6 Hz);

^{13}C NMR (DMSO-d_6) δ 23.7, 33.3, 33.8, 88.7, 120.3, 126.0, 126.7, 128.2, 128.3, 128.8, 135.3, 139.0, 150.2, 166.8, 170.5, 171.5. HRMS-ESI (+): Calc. for $C_{21}H_{20}N_3OS$: 362.1327. Found: 362.1335 $[M+H]^+$.

***S*-Benzyl-5-cyano-6-(4-bromophenyl)-2-thiouracil (17g).** Yield 33%; ^{1}H NMR (DMSO-d_6) δ 4.27 (s, 2H), 7.22 (t, 1H, *J* = 7.2 Hz), 7.29 (t, 2H, *J* = 7.2 Hz), 7.39 (d, 2H, *J* = 7.2 Hz), 7.67 (d, 2H, *J* = 8.4 Hz), 7.71 (d, 2H, *J* = 8.4 Hz); ^{13}C NMR (DMSO-d_6) δ 33.8, 88.9,120.0, 123.2, 126.7, 128.3, 128.9, 130.2, 131.1, 136.9, 139.0 165.8, 170.1, 171.8. HRMS-ESI (+): Calc. for $C_{18}H_{13}N_3OSBr$: 397.9963. Found: 397.9950 $[M+H]^+$.

***S*-Benzyl-5-cyano-6-(biphenyl-4-yl)-2-thiouracil (17h).** Yield 37%; ^{1}H NMR (DMSO-d_6) δ 4.32 (s, 2H), 7.23 (t, 1H, *J* = 7.6 Hz), 7.31 (t, 2H, *J* = 7.6 Hz), 7.40 (m, 3H), 7.50 (t, 2H, *J* = 7.6 Hz), 7.74 (d, 2H, *J* = 8.0 Hz), 7.77 (d, 2H, *J* = 8.4 Hz), 7.90 (d, 2H, *J* = 8.0 Hz); ^{13}C NMR (DMSO-d_6) δ 33.8, 89.1, 126.4, 126.8, 126.8, 127.9, 128.3, 128.8, 128.9, 129.0, 136.6, 139.0, 139.4, 141.4, 166.4, 169.7, 171.3. HRMS-ESI (+): Calc. for $C_{24}H_{18}N_3OS$: 396.1171. Found: 396.1187 $[M+H]^+$.

***S*-Benzyl-5-cyano-6-(1-naphthyl)-2-thiouracil (17i).** Yield 43%; ^{1}H NMR (DMSO-d_6) δ 4.26 (s, 2H), 7.23 (t, 1H, *J* = 7.2 Hz), 7.29 (t, 2H, *J* = 7.2 Hz), 7.39 (d, 2H, *J* = 7.2 Hz), 7.55 (m, 5H), 7.78 (d, 1H, *J* = 8.0 Hz), 7.99 (t, 2H, *J* = 6.8 Hz); ^{13}C NMR (DMSO-d_6) δ 33.8, 92.4, 119.3, 125.2, 125.4, 126.0, 126.2, 126.4, 126.8, 128.2, 128.3, 128.9, 130.1, 133.1, 135.9, 138.9, 168.7, 167.6, 171.4. HRMS-ESI (+): Calc. for $C_{22}H_{16}N_3OS$: 370.1014. Found: 370.1015 $[M+H]^+$.

7.9.2. Biological evaluation

General in vitro biological methods: EcN68, the *N*-terminal fragment of SecA from *E. coli* without the C-terminal regulatory domain, and EcSecA, the full length SecA from *E. coli*, were over-expressed from pIMBB-8(Karamanou, Vrontou et al. 1999) and pT7-SecA,(Cabelli, Chen et al. 1988) respectively, and purified as described.[(Chen, Xu et al. 1996; Chen, Brown et al. 1998)] EcN68 was used for screening because it has higher intrinsic activity and is more sensitive to inhibitors.

All potential inhibitors were dissolved in 100% DMSO. The ATPase activity was determined by the release of phosphate (Pi) detected by malachite green as described(Lill, Dowhan et al. 1990) in a modified procedure(Maloney, Parks et al. 2000) and in the presence of 10% DMSO. Inhibitory effect was determined by the percentage of the remaining ATPase activity as compare to the controls without test compounds. Briefly, 50 µL reaction mixture was prepared so that it contained 2.25 µg N68 or 5 µg SecA, 2 mM ATP, 50 mM Tris-HCl (pH7.6), 20 mM KCl, 20 mM NH_4Cl, 1 mM DTT, and 2 mM $Mg(OAc)_2$. Reactions took place at 40 °C for 20 min (for N68) or 40 min (for SecA) then were stopped by adding 800 µL of malachite green and then 100 µL of 34% citric acid within 1 min. The mixtures were incubated at room temperature for 40 min and then the absorption at 660 nm was measured. All assays were done at least in triplicate, and the results were presented as bar graphs with standard error of the mean.

General in vivo biological methods: Log-phase growing cells (O.D. 600nm~ 0.5 to 1.0) were diluted to an absorbance of 0.05 at O.D. 600 nm, added with indicated compounds, and followed by culturing in an Eppendorf Thermomixer R (Brinkmann instru-

ments, Inc.) at 37 °C,1050 rpm for 10 to 12 hours. All cultures contain 5% DMSO with a final volume of 100 µl. All tested compounds were dissolved in 100% DMSO (Sigma).

Bacterial strain: NR698 (MC4100 *imp*4213)(Ruiz, Falcone et al. 2005) with increased outer membrane permeability. MC4100, an *Ecoli* K-12 wild-type strain (Casadaban 1976).

7.9.3. Computational method

Molecular simulation of ligand-SecA complexes. The 3D structures for these compounds were refined using the PM3 method in the MOPAC 7 program (Stewart 1990) and assigned with AM1-BCC partial charges (Jakalian, Bush et al. 2000; Jakalian, Jack et al. 2002; Tsai, Wang et al. 2008) by the QuACPAC program. All partial charges on the atoms of the homology model were derived from AMBER 8 parameters. Docking of the ligands into SecA around the active site (included residues Gly80, Mse81, Arg82, His83, Phe84, Gln87, Arg103, Thr104, Gly105, Glu106, Gly107, Lys108, Thr109, Leu110, Arg138, Asp209, Glu210, Arg509 and Gln578) was performed by using DOCK 5.4. (Moustakas, Lang et al. 2006). After docking, MD simulations were conducted with the ligand-receptor complexes following similar procedures we reported before (Li and Wang 2006; Li and Wang 2007; Li, Ni et al. 2008; Zheng, Kaur et al. 2008). In brief, the docked complexes were solvated by using the TIP3P water model (Jorgensen, Chandrasekhar et al. 1983), subjected to 500-steps of molecular mechanics minimization and molecular dynamics simulations at 300 K for 1.0 ns using the SANDER module in the AMBER 8 program (Case, Cheatham et al. 2005). The resulting structures were then analyzed using PyMOL 1.0, (DeLano 2006) HBPLUS 3.06 (McDonald and Thornton 1994) and Ligplot 4.22 (Wallace, Laskowski et al. 1995) to identify specific contacts be-

tween ligands and SecA. During the computation, molecular docking (DOCK 5.4), binding analysis (HBPLUS 3.06 and Ligplot 4.22) and visualization (PyMOL 1.0) were carried out on a Xeon-based Linux workstation. Molecular mechanics calculations and molecular dynamics simulations (AMBER 8) were performed on URSA, a 160-processor computer based on the Power5+ processor and IBM's P series architecture.

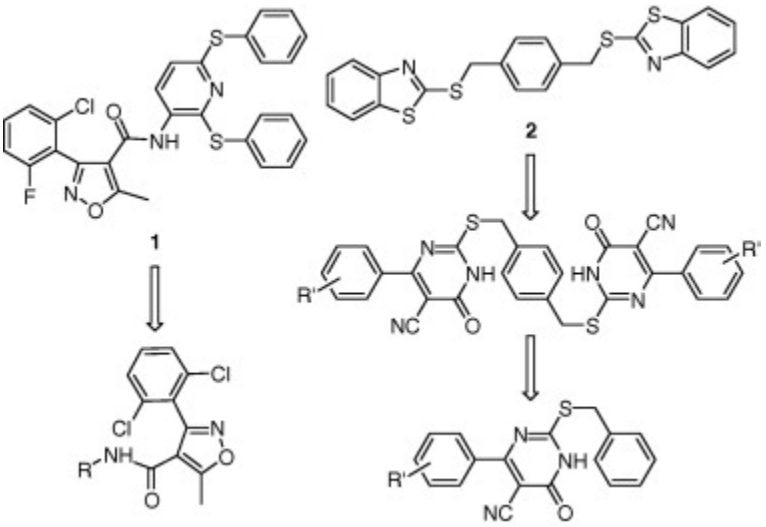

Figure 7.7. Two hit compounds and their derivatives.

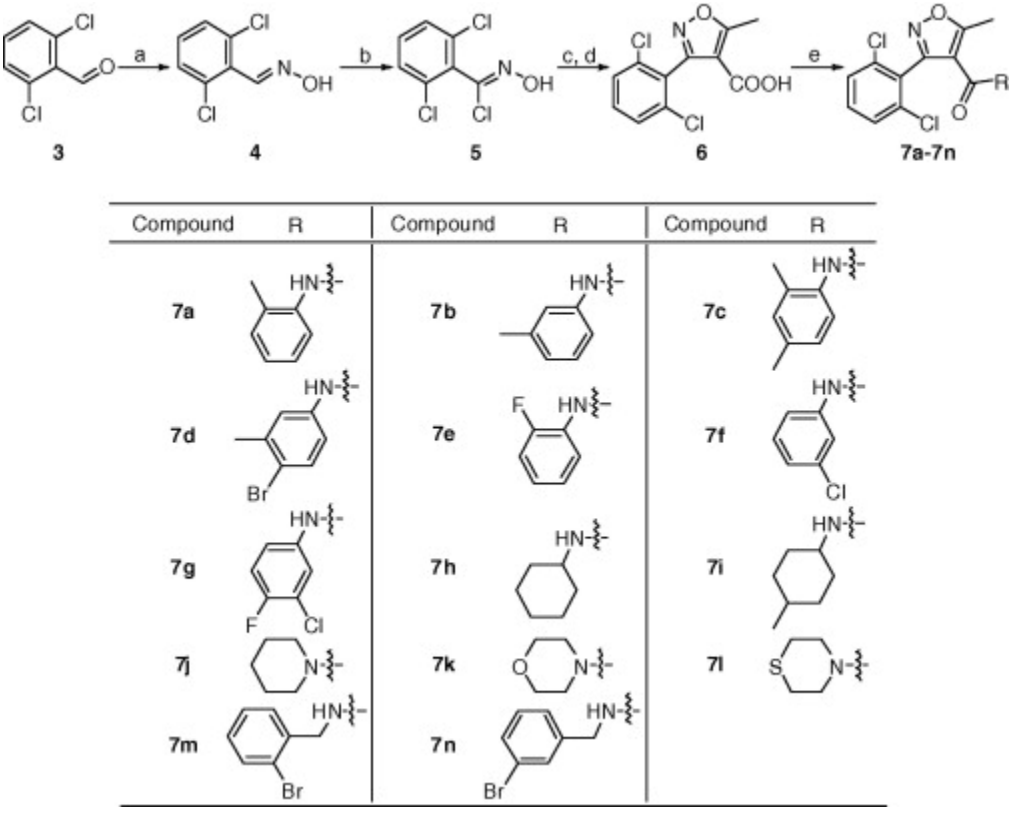

Scheme 1. Synthesis of isoxazole carboxamides 7a–n. Reagents and conditions: (a) HONH2•HCl, NaOH, EtOH, H2O, reflux; (b) NCS, DMF; (c) ethyl acetoacetate, MeO-Na, THF; (d) NaOH, EtOH, H2O; (e) EDCI, HOBt, DMAP, DMF.

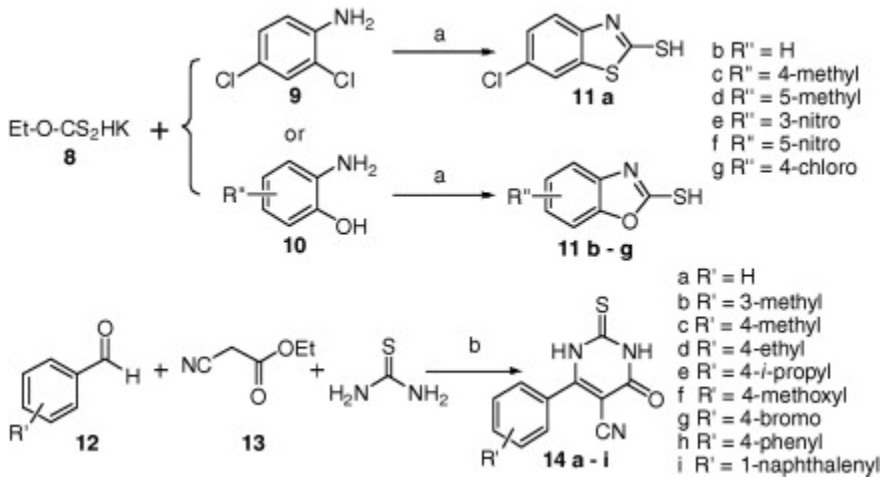

Scheme 2. Synthesis of compounds 11a–g and 14a–i. Reagents: (a) EtOH, reflux; (b) piperidine, EtOH, reflux.

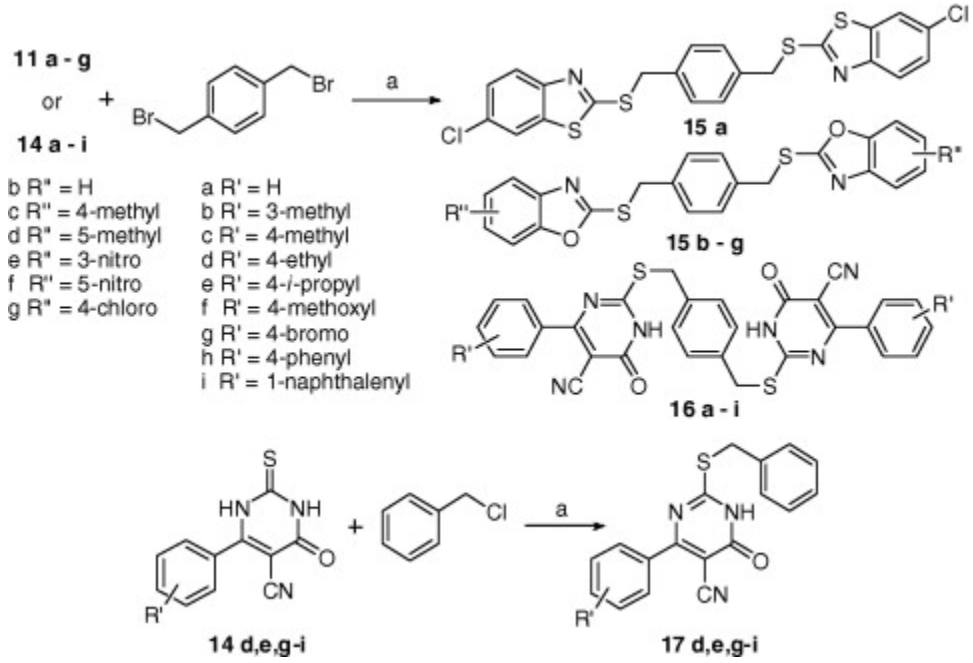

Scheme 3. Synthesis of compounds 15a–g, 16a–i and 17d,e,g–i. Reagents: (a) K2CO3, CH3CN, reflux.

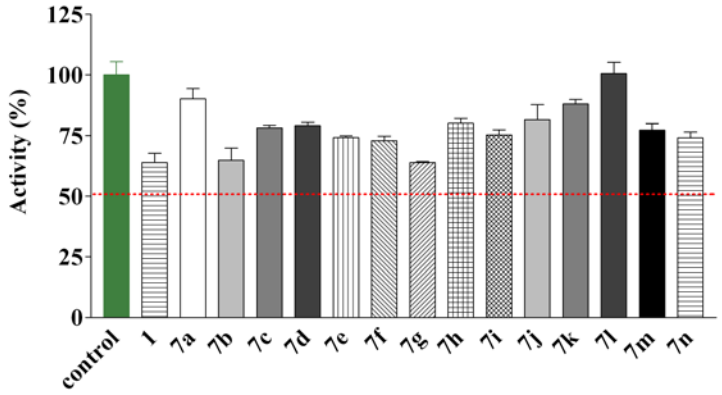

Figure 7.8. Inhibitory effect of compounds 1 and 7a-n at 100 µM against EcN68 Sec A.

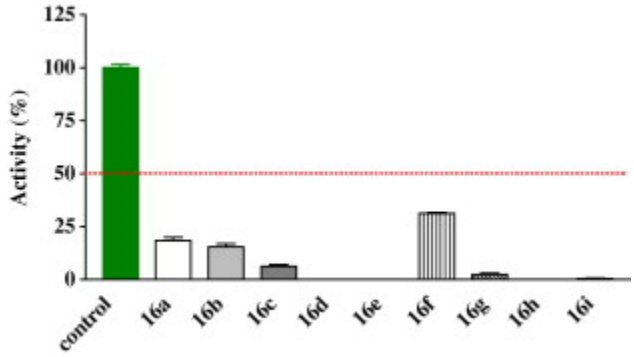

Figure 7.9. Inhibitory effect of compounds 16a–i at 30 µM against EcN68 Sec A

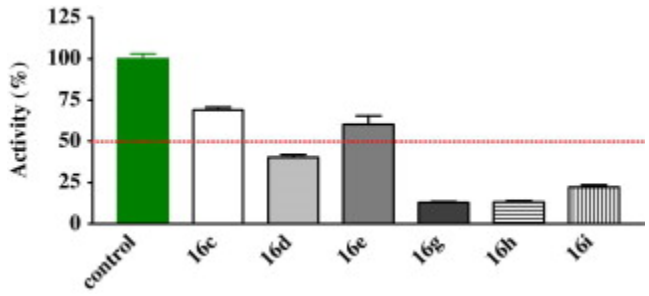

Figure 7.10. Inhibitory effect of compounds 16c–e,g–i at 5 µM against EcN68 Sec A.

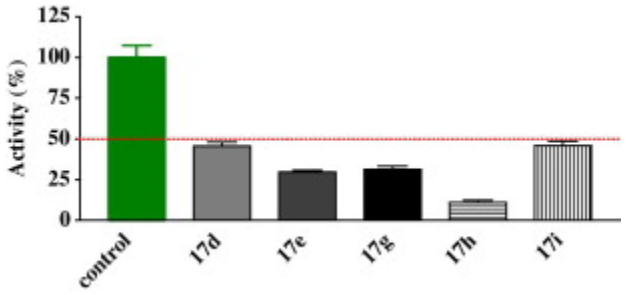

Figure 7.11. Inhibitory effect of compounds 17d,e,g–i at 30 μM against EcN68 Sec A.

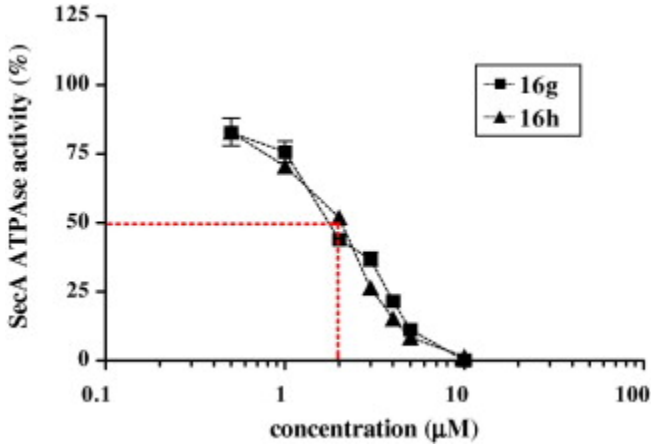

Figure 7.12. The inhibitory curves of the two most potent compounds, 16g and 16h, against EcN68 Sec A.

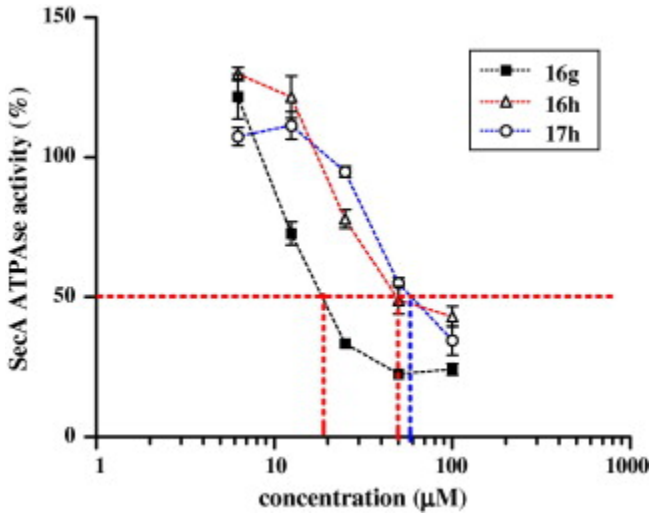

Figure 7.13. The inhibitory curves of 16g,h and 17h against EcSecA.

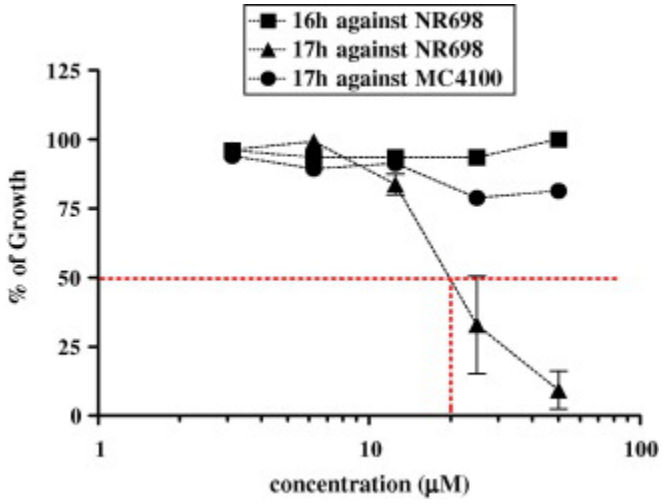

Figure 7.14. The inhibitory curves of 16g,h and 17h against bacterial growth.

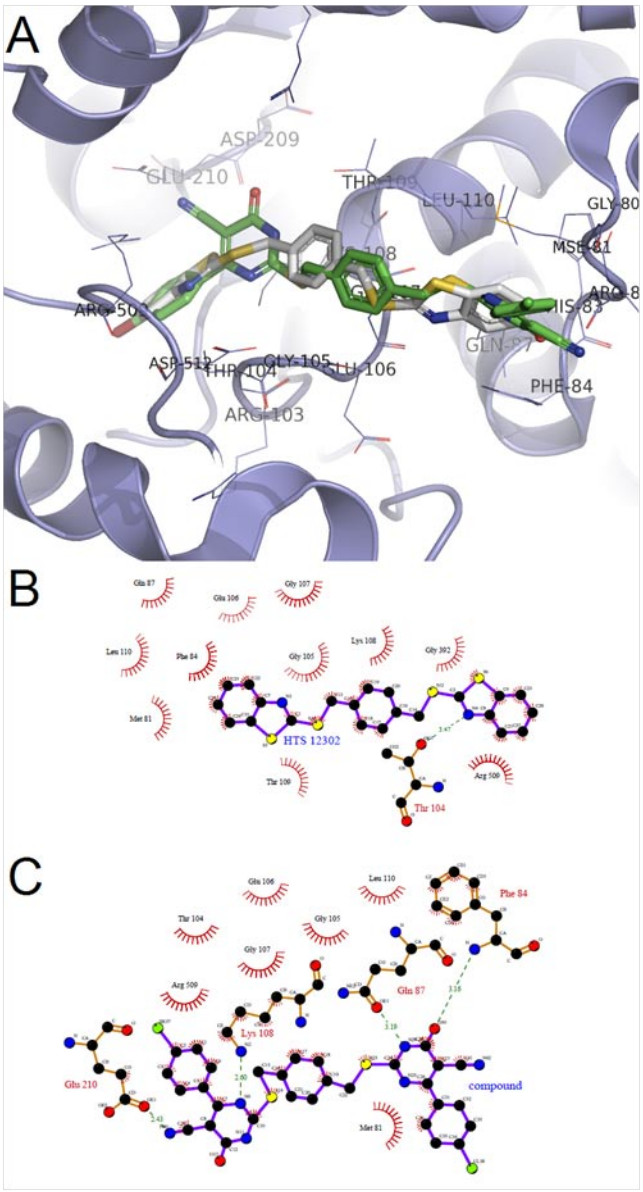

Figure 7.15. (A) The proposed docking conformation of HTS-12302 (white sticks) and compound **16g** (green sticks) around SecA ATP-site; (B) The proposed schematic interactions of HTS-12302 with SecA; (C) The proposed schematic interactions of compound **16g** with SecA.